

Vegard Huse

Analysis and design of the SEVAN FPSO against abnormal ice actions

Master's Thesis

Supervisor Professor Jørgen Amdahl

Trondheim, June 2010

Norwegian University of Science and Technology

Department of Marine Technology



for

Stud. Techn. Vegard Huse

Analysis and design of the SEVAN FPSO against abnormal ice actions

Analyse og dimensjonering SEVAN FPSO mot ekstreme islaster

As the exploration and exploitation for hydrocarbons move to arctic waters severe ice actions are to be expected. Design of ships for arctic conditions is fairly well established; ships are normally designed for ice loads with a few years return period. Little plastic deformation is allowed. Hence, the ships structures are typically designed on the basis of linear elastic or limit plastic analysis with moderate nonlinear material behaviour.

For offshore structures it is common to perform checks of environmental actions in the ultimate limit state format and the accidental limit state format. The first criterion is typically related to ice actions with a return period of 100 years, the second with return periods of 10,000 years. In the new code ISO/CD 19906: Petroleum and natural gas industries — Arctic offshore structures, which is under preparation, the two checks are denoted Extreme Level Ice Event (ELIE) and Abnormal Level Ice Event (ALIE), respectively. In the ALS/ALIE checks it is accepted that large permanent deformations may develop, but penetration of cargo tanks leading to oil spill should not take place. Global integrity should also be maintained.

By contrast to ULS/ELIE checks, design methods for ALS/ALIE are less well established. The purpose of this work is to contribute to the development of improved design methods for ALS/ALIE. The approach adopted will be applied to assessment and design of the conical side shell structure of the SEVAN FPSO.

The work should comprise the following tasks:

- 1) Calculate characteristic local and global ELIE and ALIE ice actions on the buoy for level ice and ice ridges. Local actions for design of plates, stiffeners and stringers will depend on the layout of the structure and should be reflected in the calculations. The effect of cone angle may be included. Discuss how the ice actions should be applied in nonlinear finite element analysis (NLFEA)
- 2) Perform simple estimates of local scantlings (plates, stiffeners, stringers) based on simple elastic or limit plastic analysis. Determine the optimum scantlings with respect to weight taking into account fabrication costs and any fabrication limitations.
- 3) Select a structural layout of the conical part for nonlinear NLFEA. Several FE models may be made, ranging from local models to large substructure models. The models may be

made parametric facilitating easy change of scantlings. Analysis shall be carried out through small deformations (ELIE) to large plastic deformations (ALIE). Acceptable strain levels for both design events shall be discussed, including the influence of mesh size. The analyses shall conclude on required scantlings with respect to ELIE/ALIE for level ice/ice ridges

- 4) Investigate whether integrated analysis of ice/structure is possible through continuum mechanics modelling in ice. Reference is here made to the work of PhD student Zhenhui Liu.
- 5) Perform assessment of potential impacts from ice berg of various sizes. First the likely size and drift velocity of various ice berg classes shall be established. Investigate also whether platform motion may be significant. The ice berg impact may be split into external and internal mechanics. The external mechanics provides information of the required kinetic energy to be distributed as strain energy. From this evaluation the critical impact events shall be identified and the deformation and energy dissipation in the hull shall be investigated by means of NLFEA. It shall be evaluated whether implicit or explicit methods are to be used.
- 6) On the basis of the experience obtained from the investigation develop guidelines for when ELIE or ALIE will govern the design.
- 7) Conclusions and recommendations for further work

Literature studies of specific topics relevant to the thesis work may be included.

The work scope may prove to be larger than initially anticipated. Subject to approval from the supervisors, topics may be deleted from the list above or reduced in extent.

In the thesis the candidate shall present his personal contribution to the resolution of problems within the scope of the thesis work.

Theories and conclusions should be based on mathematical derivations and/or logic reasoning identifying the various steps in the deduction.

The candidate should utilise the existing possibilities for obtaining relevant literature.

Thesis format

The thesis should be organised in a rational manner to give a clear exposition of results, assessments, and conclusions. The text should be brief and to the point, with a clear language. Telegraphic language should be avoided.

The thesis shall contain the following elements: A text defining the scope, preface, list of contents, summary, main body of thesis, conclusions with recommendations for further work, list of symbols and acronyms, references and (optional) appendices. All figures, tables and equations shall be numerated.

The supervisors may require that the candidate, in an early stage of the work, presents a written plan for the completion of the work. The plan should include a budget for the use of computer and laboratory resources which will be charged to the department. Overruns shall be reported to the supervisors.

The original contribution of the candidate and material taken from other sources shall be clearly defined. Work from other sources shall be properly referenced using an acknowledged referencing system.

The report shall be submitted in two copies:

- Signed by the candidate
- The text defining the scope included
- In bound volume(s)
- Drawings and/or computer prints which cannot be bound should be organised in a separate folder.

Thesis supervisor

Prof. Jørgen Amdahl

Contact person at SEVAN Marine

Ragnar Thunes\Kåre Syvertsen

Trondheim, August 24, 2009

Jørgen Amdahl

Preface

This master thesis is a part of the master graduate program at the Department of Marine Technology at NTNU in Trondheim. The work has been performed at the Marine Technology Centre in Trondheim. The aim for the thesis has been to study ice actions in accordance to ELIE and ALIE, and structural capacity through non-linear finite element analysis.

I would like to thank my supervisor Professor Jørgen Amdahl at NTNU for cooperative guidance during my work. I would also like to thank Ragnar Thuenes and Kåre Syrvertsen, Sevan Marine for information with regards to the structural drawings of the Sevan FPU-ICE.

The scope of the project was larger than I had anticipated. Especially modeling has showed to be time consuming due to the circular geometry. The onset of proper boundary conditions of the structure has showed too be difficult. The different subjects have been carried out in best possible way within the time limit.

Abstract

As the oil price is relative high, oil companies continue their quest for oil in new areas where it was supposed impossible earlier. 25 % of the world petroleum reserves are assumed to be in Arctic areas. In these areas ice contribute to significant engineering challenges. Ice conditions, emergency response, winterization and extreme low temperatures are some of the challenges that have to be address for design and operation purpose.

Ice is an interesting material for an engineer. The knowledge of ice mechanics and physics is essential for understanding how ice forces are developed and acts. The agreement in estimating of forces and development of ice loads have been over time been evaluated for the writing of new structural code. Structural layout proofs to be a significant factor in how ice is managed and therefore in reducing ice actions. However studies have showed that prediction of ice actions is hard to establish and therefore it is difficult to establish proper loading cases.

For designing a FPSO in the arctic waters, the classification criteria for floating units need to be complied with. The DNV rules for offshore structure refer to the class rules for ship with additional ice strengthening class. The ISO (International Organization for Standardization) the world's largest developer and publisher of International Standards have issued a draft for a design code for Arctic offshore structures. These two rules and codes have been compared in connection with local structural arrangement.

For arctic structures, two design checks ELIE and ALIE are required. These design checks are less established. ELIE ice checks have a return period of one hundred year (10^{-2}) and ALIE one thousand year (10^{-4}). The SEVAN-FPU ice is designed for handling level ice up to 3 m according the DNV Polar 30 Class Notation. Structures are according to the codes required to withstand the ice actions from ELIE within the elastic region. ALIE action will involve plastic damage, but the requirement is to maintain structural integrity to survive a ULIE check. The master thesis purpose is to determine ELIE and ALIE. The ELIE and ALIE are clearly depended on local field data which makes it a challenge in estimations.

The ELIE design load for the Sevan FPU-ice is based on a pressure-area equation for massive ice feature. The pressure-area equation is based on empirical data measurement from several field programs. The load area for a plate design is assumed to be the whole plate area, while for the stiffener design 80% of the plate height times four stiffener spacing. The ELIE pressure is respectively 5.11 MPa and 2.37 MPa.

For arctic structures, iceberg is the governing factor for ALIE. Designing for an impact of a large iceberg in 100 or 10 000 years storm may be impossible due to the massive energy involved. Sevan FPU-ice is designed with possibility of disconnecting. This may reduced the ALIE load, however the possibility of failure in disconnecting should be included in ALIE. In estimation of iceberg impact, kinetic energy is the load applied for calculations. Structural resistance for impact is measured in energy dissipated in strain before fracture. The plastic strain gives the dominating dissipated energy and elastic strain is in a small magnitude. By equating kinetic energy applied and strain energy dissipated before fracture can be seen as what the structure can withstand.

Analysis and design of the Sevan FPSO against abnormal ice actions

ABAQUS standard has been applied for analyzing different structural layout with the intentional structural layout for SEVAN- FPU-ice as a basis. A non linear finite element analysis is preformed to investigate structural capacity and the energy dissipated in plastic strain in order to check for ELIE and ALIE. The model has been created using the ABAQUS CAE.

The ELIE design loads for plate and stiffener design are applied for the ABAQUS for the intentional structural layout. Both plate and stiffener design check was applied in the elastic region.

Six different models were made with different stiffener profile. Plate and stiffener spacing were hold constant with the structural layout given from Sevan. For finding the ultimate strength of the, a plate patch load was applied with three different load intensity. The load intensity was found in the using the same pressure area curve as for the ELIE design load. The loads were scaled up to an assumed strain level beyond critical strain. The result showed that a T-bar stiffener withstands the pressure loads significant better. The results from the analysis should be handled with care. In particular the boundary conditions should be evaluated further. The results should be verified by more extensive use of finite element programs.

Table of Content

1	Introduction.....	1
2	ICE and the Arctic environment	2
2.1	Artic areas.....	2
2.2	Ice properties	3
2.2.1	Compressive strength.....	3
2.2.2	The tensile and flexural strength.....	3
2.2.3	Ice failure modes	3
2.3	Ice interactions with sloping structures	5
2.4	Limiting mechanisms.....	5
2.5	Ice types.....	6
2.5.1	First-year ice	6
2.5.2	Multi-year ice	6
2.6	Level ice	6
2.7	Ice ridges.....	7
2.8	Iceberg.....	7
2.9	The Barent Sea	8
2.9.1	ISO 19906 description of the Barent sea.....	8
3	Sevan FPU-ICE.....	10
4	Ice loads.....	11
4.1	Prediction study.....	11
5	Full scale measurement.....	13
6	DNV Rules and standards	15
6.1	DNV Offshore codes	15
6.2	Ice Class rules	15
6.3	Design loads and load area.....	15
6.4	Structural requirements	17
6.4.1	Plate thickness.....	18
6.5	Transverse Stiffener	19
6.6	Conclusion	20

Analysis and design of the Sevan FPSO against abnormal ice actions

7	Limit state design method.....	21
7.1	Ultimate limit state.....	21
7.2	Accidental limit state.....	22
7.3	SLS- Serviceability limit states	22
7.4	FLS- Fatigue limit states.....	23
7.5	Representative values	23
7.6	Ice action scenarios	23
8	Local Ice Actions	25
8.1	Localized pressure due to ice crushing.....	25
8.2	Local design ISO 19906.....	27
8.2.1	Local actions from thin first-year ice.....	28
8.2.2	Massive ice features.....	30
8.3	Estimates of ice loads	31
8.3.1	Plate design	31
8.3.2	Stiffener design.....	31
8.3.3	Impact pressures from glacial ice.....	32
9	Global Loads	33
9.1	Global model test of the SEVAN FPU-ice.....	33
9.1.1	Test set-up.....	33
9.1.2	Test results	34
9.1.3	Managed ice	34
9.1.4	Results	35
9.2	Global loading area.....	35
10	Non linear finite element of ice actions	36
10.1	Ice in finite element program.....	36
10.2	Isotropic Failure Criterion.....	36
10.3	Anisotropic Failure Criterion	36
10.4	Transformation of state due to cracking and crushing	37
10.5	Modeling ice	37
10.6	Friction model	37
10.7	Test analysis.....	37
10.8	Ice ridges in finite element simulation	38

10.9	Ice ridges simulation results.....	39
10.10	Discussion.....	41
11	Methods for large displacement and plastic analysis.....	42
11.1	Strain hardening.....	42
11.2	Plastic moment and moment capacity.....	42
11.3	Mechanism method for beams.....	45
	Analogous method for a fixed ended beam with uniform load gives.....	46
11.4	Membrane forces to a beam.....	46
11.5	Plastic plate capacity.....	48
12	IACS Rules for polar ship.....	48
12.1	Comparing plastic resistance - weight.....	49
12.2	Welding cost.....	50
12.3	Strain level.....	50
13	Collisions.....	52
13.1	Design principles.....	52
13.2	Analysis of collision.....	52
13.2.1	Kinetic energy from iceberg.....	53
13.2.2	Senario of collision.....	53
13.2.3	Velocity and added mass.....	53
13.2.4	Glancing.....	54
13.2.5	Lateral collision.....	54
13.3	Structure-ice collision model.....	55
13.4	Discussion.....	57
14	Finite element method.....	59
14.1	Shell elements.....	59
14.2	General purpose elements.....	59
14.3	Thin plate theory.....	60
14.4	Thick plate theory.....	60
15	Non linear theory.....	61
15.1	Geometrical nonlinearity.....	61
15.2	Non linear material.....	62
15.3	Solution methods.....	62

Analysis and design of the Sevan FPSO against abnormal ice actions

15.3.1	Incremental method, Euler-Cauchy.....	63
15.3.2	Newton-Raphson method	63
15.4	Combined methods	64
15.4.1	Arc-length method	64
15.5	Direct integration methods	65
15.5.1	ABAQUS/Explicit	65
15.6	Numerical integration	66
15.6.1	Full integration	66
15.6.2	Reduced integration	66
15.7	Imperfections	67
15.8	Fracture	67
15.9	Implementing in fracture FEM	68
15.10	Ductile fracture.....	68
16	Modell	69
16.1	Modell 1.....	69
16.2	Various models	70
16.3	Material	71
17	ABAQUS Analysis	72
17.1	Abaqus parameters	72
17.1.1	Step.....	72
17.1.2	Elements applied	72
17.1.3	S4R.....	72
17.1.4	SR8.....	72
17.1.5	Mesh.....	72
17.2	S8R.....	74
17.2.1	Boundary conditions.....	74
17.3	Load conditions	77
17.3.2	Load case 3	Feil! Bokmerke er ikke definert.
17.3.3	Load case 4	79
17.4	Plastic strain energy dissipated	83
17.5	External Energy for the whole model.....	84
18	Conclusion and recommendations for further work.....	85

Bibliografi 86

Analysis and design of the Sevan FPSO against abnormal ice actions

s	[mm]	Stiffener spacing
l	[mm]	Plate length
t	[mm]	Plate thickness
h_w	[mm]	Height of stiffener web
t_w	[mm]	Web thickness
b_r	[mm]	Flange width
t_f	[mm]	Flange thickness
h_s	[mm]	Stringer height
t_{sw}	[mm]	Stringer web thickness
F_h	[N]	Horizontal ice force
N	[N]	Normal ice force
μ	[-]	coefficient of kinetic friction
α	[deg]	Inclination angle between structure and ice
F_v	[N]	Vertical ice force
ξ	[-]	Ratio of horizontal ice force and vertical ice force
H_s	[m]	Sail height of an ice ridge
θ_k	[deg]	Keel angel of ice ridge
H_k	[m]	Keel depth of an ice ridge
h_c	[m]	Thickness of consolidated layer
h_k	[m]	Distance between bottoms of the consolidated layer and the keel
E_{kin}	[J]	Kinetic energy
m_1	[kg]	Mass of an ice berg
m_1^a	[kg]	Hydrodynamic mass of an ice berg
v_1	[m/s]	Velocity of an ice berg
a_d	[m]	Load height of ice actions
W_L	[m]	Load width of ice actions
h_{ice}	[m]	Ice thickness
h_{incl}	[m]	Load height incline ice actions
h_{lc}	[m]	Load height incline ice actions due to ice geometry
F_L	[N]	Ice actions from thin first year ice
p_F	[MPa]	Full thickness local ice pressure
h	[m]	Ice thickness
p_L	[MPa]	Local pressure due to ice thickness
γ_l	[-]	Load coefficient

Analysis and design of the Sevan FPSO against abnormal ice actions

A	$[m^2]$	Area
γ_p	[-]	Permanent load factor
x_p	[-]	Permanent load
γ_v	[-]	Variable load factor
x_v	[-]	Variable load
γ_e	[-]	Environmental load factor
x_e	[-]	Environmental load
γ_c	[-]	Resistance
γ_m	[-]	Material load factor
ε	[-]	Strain
ε_y	[-]	Yield strain
σ	[MPa]	Stress
σ_y	[MPa]	Yield stress
y_e	[mm]	Height to elastic neutral axis
y_p	[mm]	Height to plastic neural axis
y'	[mm]	Height to plastic moment
Z	$[mm^3]$	Plastic section modulus
M_p	[Nmm]	Plastic moment
P	[N]	Force
W	$[mm^3]$	Elastic section modulus
I_e	$[mm^4]$	Elastic moment of inertia
α	[-]	Shape factor
M_y	[Nmm]	Elastic moment
E	[MPa]	Young module
P_c	[N]	Critical load
q_c	[N/m]	Critical uniform load
N	[N]	Axial force
θ	[rad]	Rotation
w	[mm]	Deflection
ε_{cr}	[-]	Critical strain
S_{ice}	$[N/mm^2]$	Nominal ice strength
h_{ice}	[m]	Nominal ice thickness
p_0	$[kN/m^2]$	Ice pressure load DNV
F_A	[-]	Correction factor

Analysis and design of the Sevan FPSO against abnormal ice actions

k_w	[-]	Influence factor for narrow strip load
k_a	[-]	Influence factor for small aspect ratio
t_k	[mm]	Corrosion addition
r_c	[MPa]	Collapse resistance for a plate
f_y	[MPa]	Yield strength
α	[-]	Plate aspect factor
r	[MPa]	Collapse resistance for a plate
D_{cr}	[-]	Ductile fracture criteria
ε_{eq}^{th}	[-]	Threshold strain
ε_{eq}^f	[-]	Effective fracture strain
$\frac{\sigma_H}{\sigma_{eq}}$	[-]	Hydrostatic stress-equivalent stress ratio, called triaxiality
S,Mises	[MPa]	Von Mises Stress
PEEQ	[-]	Plastic equivalent compression strain

1 Introduction

The cold and severe Arctic climate is expected to be a major challenge in development of hydrocarbons in Arctic areas. 25 % of the worlds remaining resources are expected to be located in Arctic areas. Recently the Shtockman oil field has been approved for field development with a FPSO solution and Statoil applied for seismic activity at the coast of Greenland. Arctic areas are covered with ice in large parts of the year, it is therefore necessary to design both ships and platforms to withstand the loading from interactions. The importance of design checks for ULIE/ULS, ALIE/ALS and classifications rules are important not only for safety of personnel and structure, but also for the damage that an oilspill may cause the vulnerable wildlife and environment. The recent accident in the Gulf of Mexico is a reminder of the risk that lies in offshore operations.

The first part of this thesis contains a literature study of arctic areas, ice. The understanding of ice properties and mechanics, are essential in order to determine ice actions.

The second part focuses on classification rules of the DNV and the ISO 19906 for offshore arctic structures. A FPSO are classified as an offshore structure and therefore under the Offshore rules and guidelines. The local strength requirement in the offshore rules refers to Pt 5 Ch. 1 Sec4 "Vessels for arctic and Ice Breaking Service".

For a FPSO, it is common to perform checks of environmental actions in the ultimate limit state format and the accidental limit state format. The Extreme Level Ice Events (ELIE)/ULS criterion is typically related to ice actions with a return period of 100 years, the Abnormal Level Ice Event/ALS with return periods of 10,000 years. In the new code ISO/CD 19906: Petroleum and natural gas industries — Arctic offshore structures, which is under preparation. In the ALS/ALIE checks it is accepted that large permanent deformations may develop, but penetration of cargo tanks leading to oil spill should not take place. Global integrity should also be maintained.

The third part consists of a non linear FEM analyses. Some general nonlinear FEM theory is presented. ABAQUS is used both for the modelling and analysis. For the modelling ABAQUS/CAE, is used and for the analysis ABAQUS/Standard is used. Ice actions are simulated by pressure loads and the focus has been on the structural resistance of the structure.

2 ICE and the Arctic environment

2.1 Arctic areas

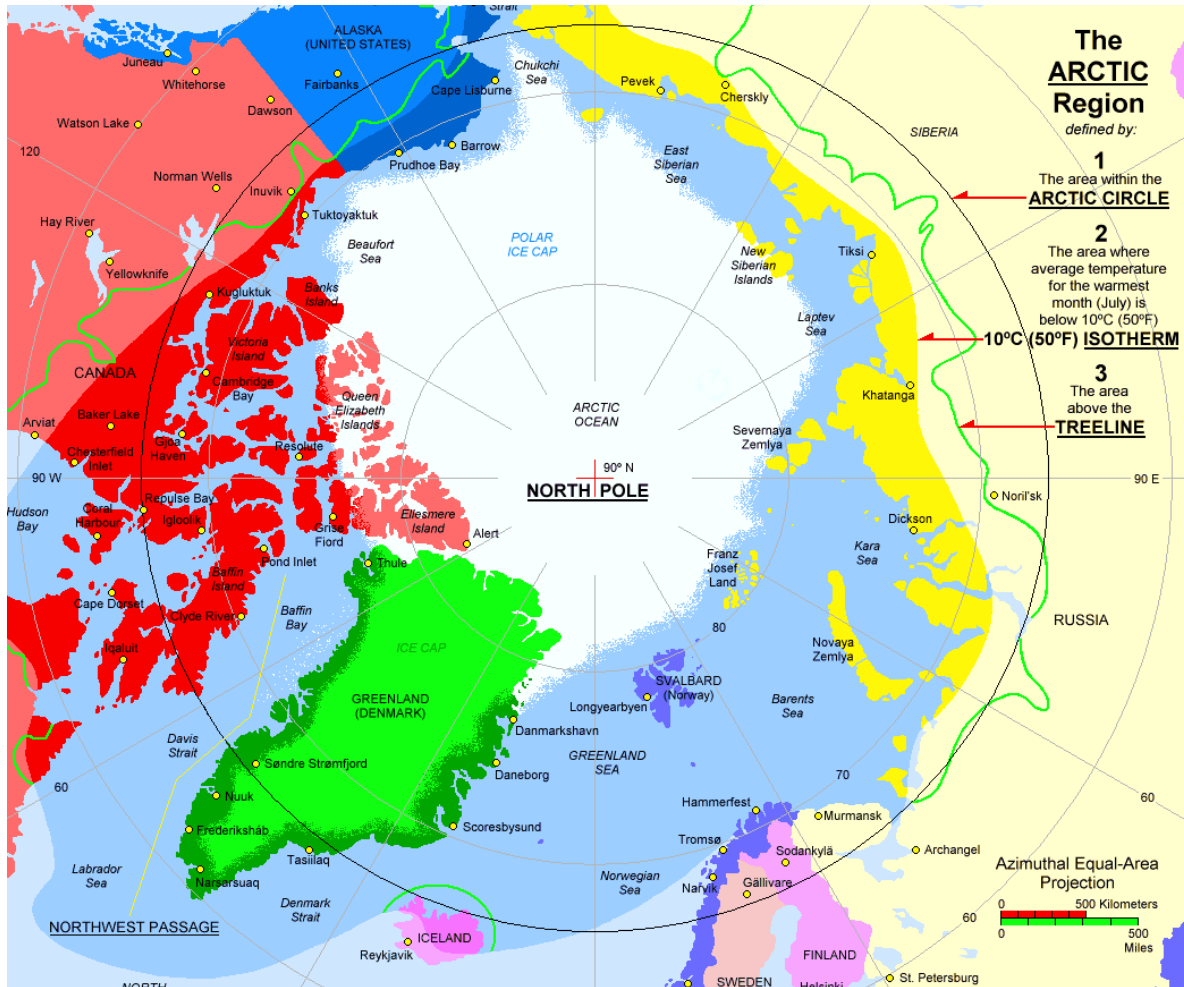


Figure 2-1, The Arctic area (www.athropolis.com)

The definition of Arctic areas may vary from the Arctic Circle, sea ice cover, 10 degrees isotherm in July and the tree line. In these areas, national and international companies and research institute believes that 25 % of the world's oil and gas resources are located. Ice is also an engineering issue in other areas below the Arctic Circle. The Caspian Sea and Bohai Bay have ice cover during winter season. The New Foundland coast experience ice and ice berg drifting from the arctic area during spring and summer season. For a design view, the most appropriate definition of Arctic areas may therefore be ice occurrence. The harsh and cold environment has earlier made these areas off limit due to restrictions. Ice actions, effect of low temperature and the lack of infrastructure are challenges the offshore industry has to overcome with a significant low risk before entering ice infested waters.

2.2 Ice properties

The properties and mechanics vary a lot depending on environmental conditions. Sea ice is in general an inhomogeneous, anisotropic and non-linear viscous material. This makes ice to an interesting material from an engineering point of view. The main properties for ice properties are:

- Compressive strength
- Tensile strength
- Fracture toughness
- Friction and adhesion
- Shear strength and cohesion of fragmented ice
- Elastic modulus
- Density

The main parameters that affect the mechanical behavior of ice:

- The temperature, T
- The porosity, η
- The grain size, d
- The loading rate
- The salinity

In general the ice becomes weaker (lower strength) and softer (lower E) with increasing T , η and d . The temperature T and the salinity govern the brine volume and therefore the porosity η . The strength increase with increasing strain rate until brittle fracture takes over.

2.2.1 Compressive strength

The compressive strength of sea ice depends on the main parameters above. The most common measurement of compressive strength is the uniaxial strength. The uniaxial strength is used for theoretical calculations on marine structures. Exposed to uniaxial strength, the ice goes through a transition from ductile to a brittle mode of failure. The uniaxial compressive strength has its maximum at a strain rate of approximately $\dot{\epsilon} = 10^{-3} \text{ sec}^{-1}$. The horizontal and vertical compressive strength ranges of (0.5-5MPa) and (0.5-10MPa).

2.2.2 Tensile and flexural strength

During flexural failure of ice, the material fails in bending. By using the assumptions of beam theory, an ice sheet will both have tensile and compressive stress. The flexural strength is defined as the extreme fibers stress in tension. The flexural strength of sea ice depends on the parameters above. The tensile strength in the growth (vertical) direction of columnar ice is about twice as high as in the horizontal direction. For sea ice flexural strength often range of 0.3-0.5MPa for winter season and 0.2MPa for warmer seasons.

2.2.3 Ice failure modes

The way ice failure against structures has a significant effect on the magnitude of the ice actions. The failure modes for sea ice are creep, crushing, flexure and shear. Failure modes depends on strength level,

stress distribution, ice velocity and structure shape. Different modes of ice failure can occur on the same structure type depending on ice thickness, velocity, the ice feature size.

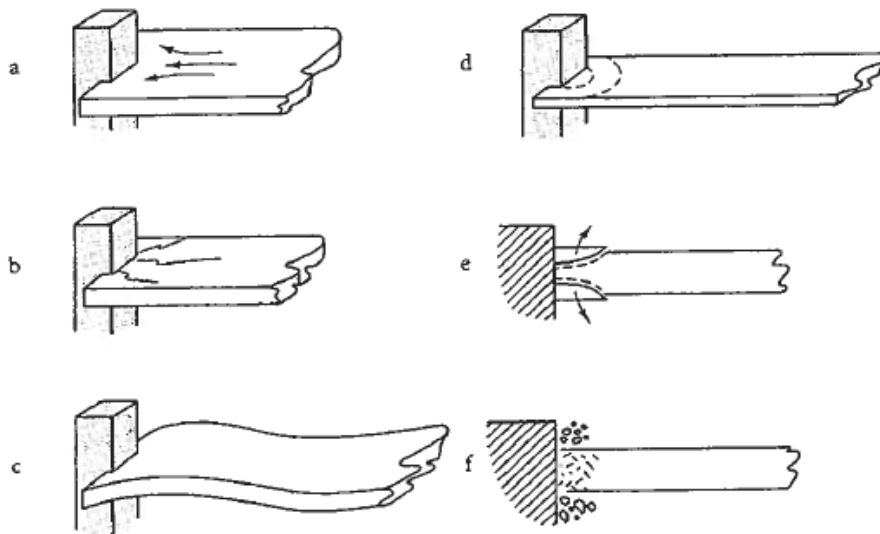


Figure 2-2, Ice failure modes. Figure 5.1.2 (S.Løset, 2006)

- a) Creep - Develops at very low indentation rate at speeds below 1-3mm/s when ice yields. The deformation develops continuously and no cracks form in the ice. Relevant for narrow structure.
- b) Radial cracks- Associated with tensile failure. For rectangular structure, cracks radiate from structures corner.
- c) Buckling - Characteristic for thin ice and wide structures. This type of failure is often connected with radial or circumferential crack formation.
- d) Circumferential cracks - May form as a result of elastic buckling or due to an out-of-plane bending moment caused by eccentric action conditions.
- e) Spalling formation- Out-of-plane horizontal cracks which grow away from the contact zone divide the ice into layers. The higher the velocity the smaller is their length.
- f) Crushing- At high rates, ice crushes in a brittle manner against both wide and narrow structures. The ice escapes as pulverized ice upwards and downwards.

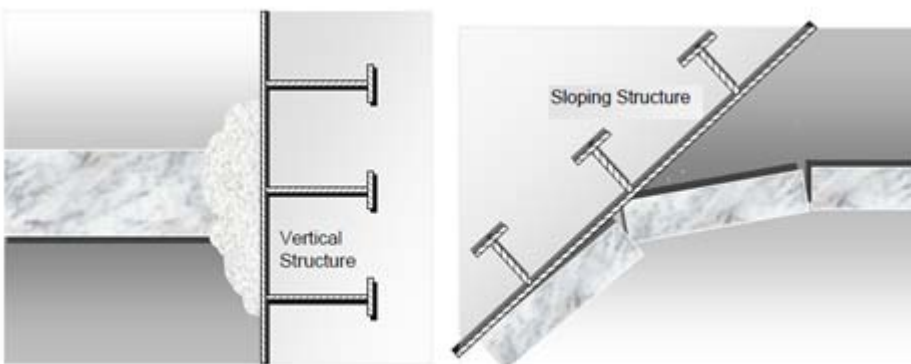


Figure 2-3, Failure modes, Figure A.8-4 (Internastional, 2007)

2.3 Ice interactions with sloping structures

Ice interaction with sloping structures will mainly fail in circumferential and radial cracking patterns. Usually these failures appear after the other. Early formations of circumferential cracks are typical for wide structures and radial cracking patterns often occur for narrow structures first. The maximal action depends on which failures which occur first.

Slope ice-breaking surfaces can also reduce ice actions from ice ridges. Slope structures have been investigated in several field programs. Level ice impact with a sloping face will fail in flexures as it rides up or down from the face of the structure. The resulting ice actions will generate a vertical and a horizontal force.

In a down breaking slope, the vertical force will be working upward

$$F_H = N \sin \alpha + \mu \cos \alpha$$

Equation 2-1

$$F_v = N \cos \alpha - \mu N \sin \alpha$$

Equation 2-2

Where N is the component normal to the structure surface, α is the inclination angle of the structure and μ is the coefficient of kinetic friction between the ice and structure surface. The subscript v and H is respectively vertical and horizontal direction.

$$F_v = \frac{F_H}{\xi}, \text{ where } \xi = \frac{\sin \alpha + \mu \cos \alpha}{\cos \alpha - \mu \sin \alpha}$$

Equation 2-3

2.4 Limiting mechanisms

There are three basic mechanisms by which ice loads can be exerted on a structure

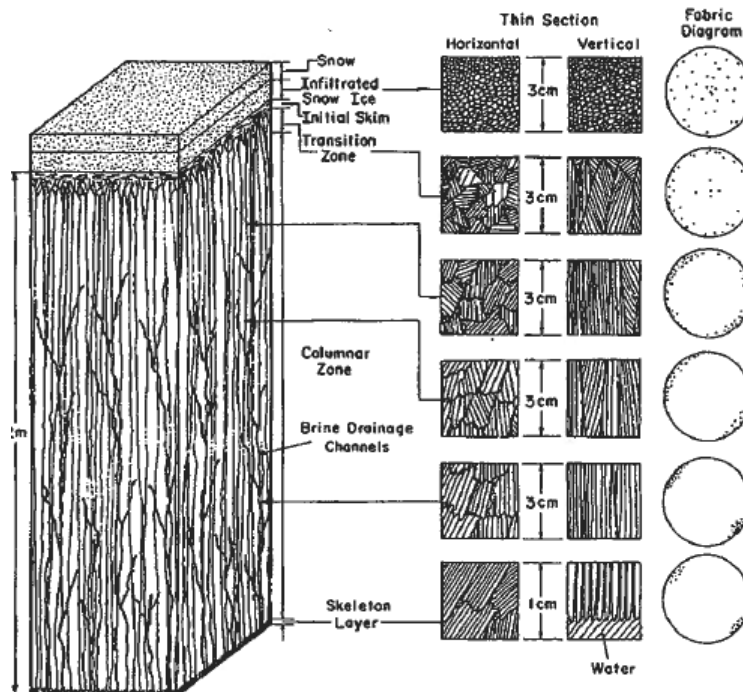
- Limiting stress - the maximum load for an event is governed by the failure of the ice immediately adjacent to the structure. Limit-stress actions include direct ice failure against the structure, ice failure within rubble lodged against the structure, floe buckling or floe. The ice strength depends on the physical properties and the failure mode of the ice. Limiting stress mechanism very often controls the maximum action.
- Limit energy (momentum) - when the kinetic energy of the ice feature is insufficient for the structure to penetrate significantly into ice. Most often this scenario can be seen during ridge or iceberg actions.
- Limiting force – develops if a strong ice field is brought to rest in front of a wide structure and transmits actions exerted by the surrounding ice features, wind and currents.

2.5 Ice types

Ice can be categorized into several types. With regards to structure analysis of ALIE, Ice berg will be of interest. Icebergs are a major concern for structures operating in the Arctic and will in many cases give the design load with regards to ALIE.

2.5.1 First-year ice

Sea water freezes at approximately -1.9° depending on the seawater brine content. The first type of ice which forms on water is primary ice. Below the layer of primary ice is the transition zone. In the transition zone, brine content is extracted as time goes. Above the layer of primary ice, there is a layer of superimposed ice. Snowcover on the top of the ice and contribute a lot to the frictional force.



2-4, First-year ice (actions from ice on arctic offshore and costal structure (3.1.2) (S.Løset, 2006)

2.5.2 Multi-year ice

Second year ice is defined as ice that have survived the summer season. Multi-year year ice is ice which has survived at least two summer season. The distinction between second year ice and multi-year ice is often so difficult that both terms are referred to as multi-year ice. The porosity decrease as the brine content decrease, hence an increase in ice strength.

2.6 Level ice

There are different types of level ice. Fast ice is ice that is frozen along the coast, and may contain large floes. Pack ice is drift ice created on the surface and subsequently packed together. If the floes in fast ice are small, the ice is quite similar to pack ice. Level ice may consist of first year ice and multi-year ice.

2.7 Ice ridges

Ridges are featured which is formed under pressure or shear processes in the ice cover and exist in most high-latitude ice-infested waters. Ridges are formed when several ice sheets drift together and for a ridge. An ice ridge has in general curvilinear features, but can be found as straight lines. Multi-years ridges are ridges consisting of ice that have survived the summer season and first years ice, and first-years ridges from ice less than one year. The porosity decrease as the age increase, hence the increase in strength.

In general, ridges show a wide range of shapes and sizes. Keel depths up to 50 m and sails up to 12.8 m have been measured. Ridge keels deeper than 30 m are very infrequently indeed.

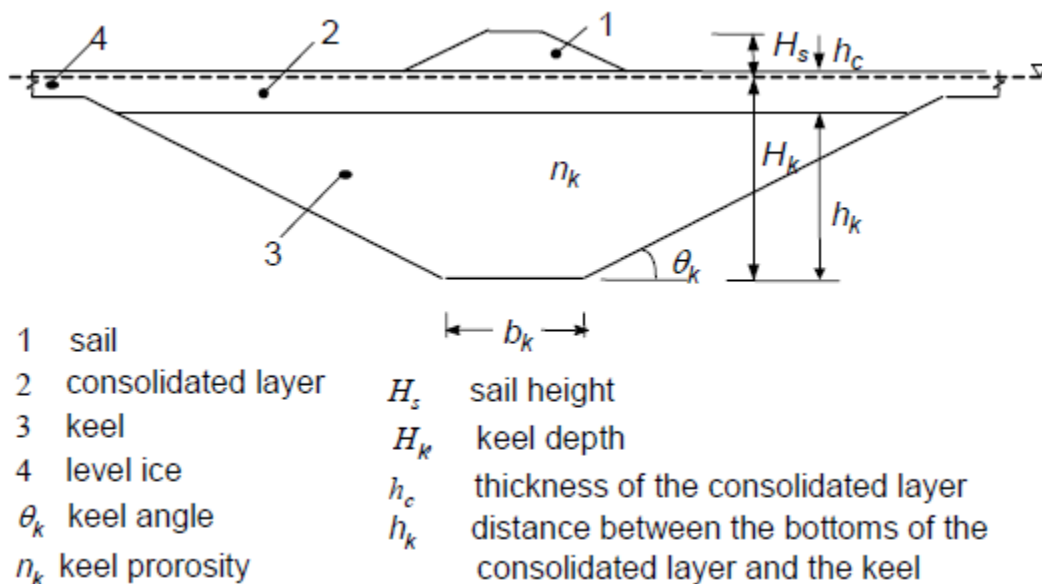


Figure 2-5, Ice ridge geometry, Figure A.8-12 (Internastional, 2007)

2.8 Iceberg

In Arctic areas, icebergs calving from glacier are found. These icebergs can be as large as several hundreds of tons. Iceberg can be classified by size:

- Ice island: A large piece of floating ice that has broken away from the Arctic ice shelf, extends about 5 m above sea level, is 30-50 m thick and has a few thousand square meter to 500km² or more
- Iceberg: A massive piece of glacial ice that broken away from the glacier, is afloat or aground, and is cresting more than 5 m above sea level
- Bergy bit: A large piece floating glacier ice, showing 1-5 m above sea level. Normally 100-300m²

- Growler A piece of floating glacier ice, often transparent but appearing green, extending less than 1 m above sea level. Normally 20m²

The icebergs consist of snow which is gradually compressed over many hundreds of years. The strength of icebergs consisting of glacier ice is therefore very high.

2.9 The Barent Sea

The Sevan FPU-ICE was originally design for the Shtockman oil field in the Barent Sea. Recently, Norway and Russia come to agreement over the borderline dividing the Barent Sea, making the exploration for oil of interest. The progress of the Shtockman field may also lead to additional field development as the new oil filed may take advantage of the synergy effect of the construction of infrastructure. To be able to predict ice loads for the Sevan FPU-ICE, the Barent Sea have been investigated.

2.9.1 ISO 19906 description of the Barent sea

The Barent Sea is a marginal sea bordering on the Arctic Ocean in the north, the Greenland and the Norwegian Seas in the west, the Kara Sea in the east and the coast of the Kola Peninsula in the south. The Barents seas depths from 600 m at the deepest in the central part to depths less of 100 m in the southeast and near the coast of Svalbard Archipelago.

Barents Sea	Characteristic
Area	1 424 00 km ²
Water volume	316 000 km ³
Average depth	222 m
Deepest depth	600 m

Table 2-1, Barent Sea Numbers

The Barent Sea is often divided into three regions; Western, North-eastern and South-eastern.

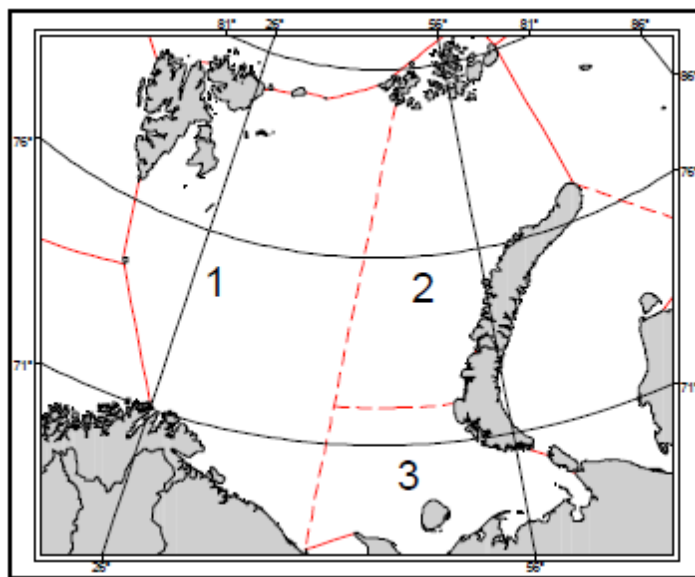


Figure 2-6, Map over Barent Sea, Figure B.16.1 (Internastional, 2007)

The Barent Sea is never completely ice-covered. During March to April, sea ice usually over 55-60% of the surface area. The ice cover can be a combination of multi-year ice up to about 3 m. The first year ice is generally less than 1.5 m. Multi-year ice spreads in a narrow zone along the eastern shores of the Svalbard Archipelago and Franz Josef and predominantly in spring. During maximum ice cover, the fraction of multi-year averages 10 %, while the fraction of young ice is around 15 %.

The Barent seas contain icebergs from the glacier of Svalbard, Franz Josef Land and Novaya Zemlya. The drift of these icebergs can move large distances during their life span. The drift is influence, by prevailing wind and ocean currents.

The tides in the Barent Sea are regular semi-diurnal in the western and southern area, leading to surface oscillations of 2.2 to 3.7 m.

Table B.16-3 – Barents Sea sea-ice conditions

	Parameter	Western Region		Northeastern Region		Pechora Sea	
		Average Annual Value	Range of Annual Values	Average Annual Value	Range of Annual Values	Average Annual Value	Range of Annual Values
Sea ice							
Occurrence	First ice	All year (North area)	All year (North area)	All year	All year	25 October	20 October to 5 Nov
	Last ice	All year (North area)	All year (North area)	All year	All year	5 July	25 June to 15 July
Level ice (first-year)	Landfast ice thickness (m)	1,4	1,3 to 1,5	1,5	1,4 to 1,6	1,0	0,9 to 1,1
	Floe thickness (m)	1,3	1,2 to 1,4	1,4	1,3 to 1,5	0,8	0,7 to 0,9
Rafted ice	Rafted ice thickness (m)	0,4	0,3 to 0,5	0,4	0,3 to 0,5	0,4	0,8 to 1,0
Rubble fields	Sail height (m)	-	-	-	-	-	-
	Length (m)	-	-	-	-	-	-
Ridges (first-year)	Sail height (m)	4,7	4,5 to 5,0	4,2	4,0 to 4,5	3,5	3,0 to 4,0
	Keel depth (m)	17,5	15,0 to 20,0	15,0	14,0 to 16,0	16,0	15,0 to 18,0
Stamukhi	Water depth range (m)	< 20	< 20	< 20	< 20	< 15	< 20
	Sail height (m)	3 to 5	8 to 10	3 to 5	8 to 10	3 to 5	10 to 11
Level Ice (Second and Multi- Year)	Landfast Ice Thickness (m)	2,5	2,2 to 2,8	2,5	2,2 to 2,8	No	No
	Floe Thickness (m)	2,7	2,5 to 3,0	2,8	2,5 to 3,0	No	No
Ridges (Second and Multi- Year)	Sail Height (m)	-	-	-	-	No	No
	Keel Depth (m)	-	-	-	-	No	No
Rubble Fields (second/Multi-year)	Av. Sail Height (m)	-	-	-	-	No	No
	Length (m)	-	-	-	-	No	No
Ice movement	Speed in nearshore (m/s)	0,5	0,4 to 0,6	-	-	0,7	0,6 to 0,8
	Speed in offshore (m/s)	0,6	0,5 to 0,7	0,5	0,4 to 0,6	-	-
Icebergs							
Size	Mass (tonnes)	Up to 6 000 000		Up to 4 000 000			
Frequency	Months Present	Jan to Jun		All Year		Infrequent Occurrence	Infrequent Occurrence
	Number per Year	10 to 40					
	Maximum Number per Month	30					

Figure 2-7, ISO 19906 Barent sea ice conditions, Table B.16-3 (Internastional, 2007) (G.W.Timeco, 2006)

3 Sevan FPU-ICE

Sevan FPU-Ice is a floating production and storage for hydrocarbons, built for operations in ice-infested area. The concept of Sevan is to have a cylinder shaped form hull moored to the seabed. The Sevan FPU-ICE is designed with basis with traditional Sevan hull, but modified with a downward sloping cone in the water line. When operating in ice condition, the draft of the Sevan FPU-ICE is 26 m. The inclined conical side of the hull will bend the ice down and break it. The broken ice will be pushed down and to the side during ice drifting towards the hull. Both theoretical analysis and model tests in ice have been executed to prove the theory. In ice draft mode the displacement of the buoy is 165 820 mT. Sevan FPU-ice is also design for open water condition. The draft is then reduced to a 15 m.

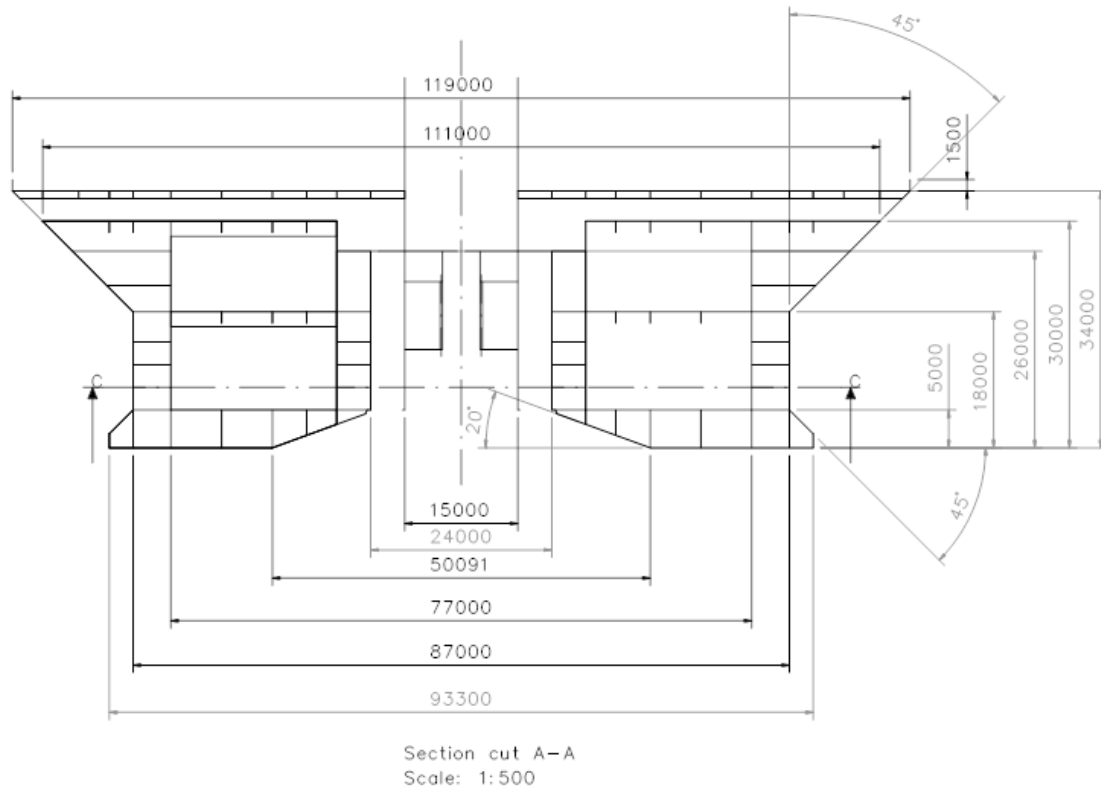


Figure 3-1, Section cut of the Sevan FPU-ICE

4 Ice loads

Design of offshore structures in Arctic waters is depended on both local and global loads. These loading are in contact forces transmitted to the structure by interactions with ice floes, ice ridges or icebergs. The prediction of ice forces on structure relies on an understanding of ice mechanics as well as knowledge of interactions between ice and structure. Predicting ice loads are in general difficult. Ice is a material that may change properties from one region to another. A full scale measurement test in one region may give different results in another area. The structure shape is also essential in establishing.

In a design aspect, result from similar project, model testing and numerical methods may give an estimate on local loads and global loads. This chapter describes how ice predictions may vary and result of similar model testing and full scale measurement.

4.1 Prediction study

A study in 2006 (G.W.Timeco, 2006) was preformed to investigate the general level of agreement of predicting ice loads from various international experts. The structure interactions scenarios investigated by 21 leading international experts on this field.

- Structural configuration 1: Cylinder-shaped structure of a 100 m diameter.
- Structural configuration 2: Conical-shaped structure with a width of 50 m in the waterline.
- Ice condition 1: First-year ice, an ice sheet of thickness 1.5 m velocity of 0.05 ms^{-1} .
- Ice condition 2: 1 km long first year ridge with a sail of 2.5 m embedded in 1.5m thick ice sheet. The event takes place in mid January with an ice temperature -20°C . Incoming velocity is 0.1ms^{-1}
- Ice condition 3: Multi-year floe, a 1 km in diameter floe with a velocity of 0.5 ms^{-1} . The floe thickness is 6 m and the average temperature is -5°C

The 21 predictors were asked to provide their estimate of the 100-year load for four scenarios as shown in table 4-1. The methods used by the different predictors various methods as codes, full scale measurements and numerical methods.

Scenario	Structure	
1	Vertical	1 - Level Ice
2	Vertical	2 - Ridge
3	Vertical	3 - Multi-year Floe
4	Conical	1 - Level Ice

Table 4-1, Different ice prediction scenarios

Predictor	Scenario			
	1	2	3	4
1	150	175	100	18
2	210	605	660	60
3	199	No prediciton	125	No prediciton
4	200	270	210	25
5	190	270	No prediciton	50
6	250	430	700	28
7	127	185	201	73
8	190	310	400	60
9	120	172	630	21
10	160	250	450	18
11	164	164	210	23
12	225	450	375	15
13	265	190	360	80
14	300	190	No prediciton	31
15	210	265	460	55
16	150	120	350	140
17	193	311	634	12
18	210	289	323	16
19	220	200	300	No prediciton
Average	196	269	382	43
SD	46	122	188	33

Figure 4-1, Results of ice loads predictions, Table 3 (G.W.Timeco, 2006)

Figure 4-1 shows an overview of load predictions for all scenarios. Scenario 2 is for first year ridges which is often used as design criteria and is therefore of interest for load predictions. The results vary from a low value of 120 MN to a five times higher value 605 MN. The study is a show that predictions of ice load vary and that ice actions is a scientific field that need more research in order to get more accurate results. For the Sevan design point of view, comparing scenario 1 and scenario 4 shows how failure modes affect the load. Scenario 1 have a 100 m wide cylindrical structure, while at scenario 4 it is a 50 m wide conical structure. By comparing the result, the conical structure had significant lower global loading in spite of the fact that the loading area in scenario 1 had twice the size.

5 Full scale measurement

The Kulluk was a ice reinforced drillship designed as a conical drilling unit. The Kulluk were used for drilling operations in the intermediate to deeper water of the Beaufort Sea from the mid 1970s to the early 1990s. The main purpose for the for reinforce Kulluk was to extend the open water season, by beginning drilling operations in the spring break up period and continuing until early winter. The experience made by the Kulluk provides source data for most consideration related to moored vessel station keeping operating in various pack ice conditions. (Ltd., July 2000)

In terms of dimension, Kulluk had a waterline diameter of 70m and a deck diameter of 80m. The operating draft was 11.5m and a displacement of 28.000 tones. The Kulluk design is very similar to the Sevan FPU-Ice with a downward sloping circular hull which failed the oncoming ice in flexural bending. Kulluk had a radically symmetric mooring system combined with the circular shape which provided capacity to resist ice and water from any directions. The mooring system consisted of 12, 3½ inch steel wire mooring lines, each with a capacity of 520 tonnes breaking strength. The lines were equipped with equipment to permit quick disconnections.

The Kulluk was designed to tolerate global loads of 750 tonnes in a drilling mode within an offset of 5% of water depth, with maximum individual line tension of 260 tonnes. In survival mode global load of more than 1000 tonnes, with riser disconnected and offset of 10% of water depth and 75% of the breaking strength.

Ice management was an important factor in enhancing the Kulluk's stationkeeping. Normally oncoming pack ice cover was managed into smaller bit by 2 or 4 icebreakers, to guarantee availability in sensible station keeping operations due to drilling. In the Beaufort Sea where the Kulluk operated, ridges and rubbles

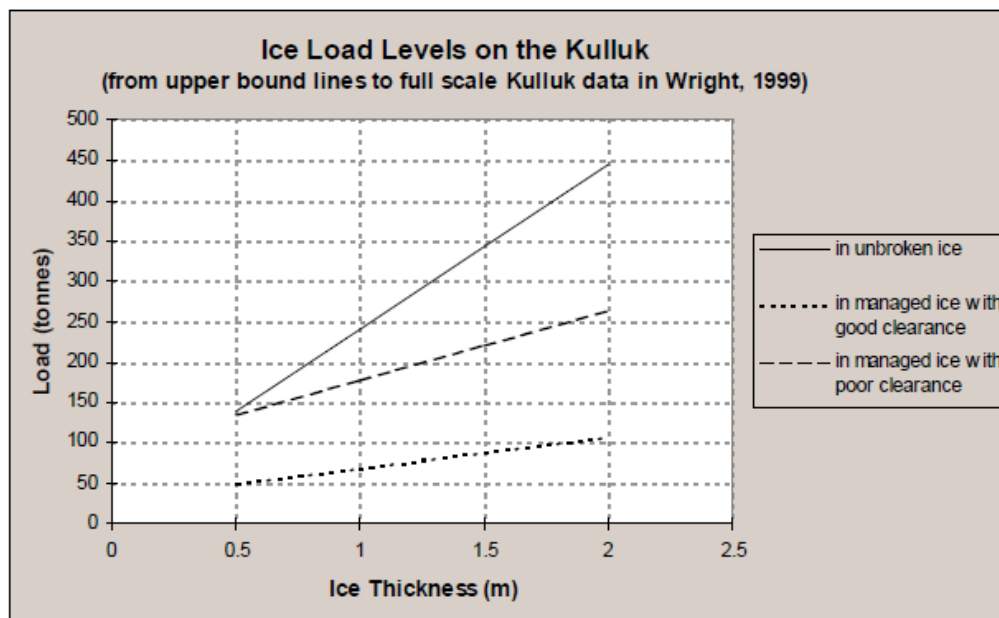


Figure 5-1, Kulluk ice load level-ice thickness, Table 6.1 (Ltd., July 2000)

Analysis and design of the Sevan FPSO against abnormal ice actions

As the figure 5-1 above show how the loads increase with an increase in ice thickness. It also shows how ice management reduces the global load level significantly.

There is a great similarity between the Sevan FPU-ice and the Kulluk drilling vessel. Measurement from the Kulluk vessel in both local and global ice action may be used in determination in similar ice action. The Kulluk was recently acquired by Shell for further activities in Alaska. (G.W.Timco, February 2009)

6 DNV Rules and standards

DNV is a classification company which ensures the quality of the structure in a rules and standards. For the Sevan FPU both offshore standards and ship rules apply. The DNV rules are based on principle of elastic strains. Sevan FPU-ice is pr definition an offshore structure and will therefore be legislated in term of DNV class by the DNV Offshore Codes.

6.1 DNV Offshore codes

The DNV offshore codes are standards developed for offshore structures. The offshore codes consist of a three level hierarchy of documents;

- Offshore Service specifications (OSS): Provide principles and procedures of DNV classification, certification, verification and consulting services.
- Offshore Standards (OS): Provides technical provision and acceptance criteria for general use by the offshore industry well as the technical basis for DNV offshore service.
- Recommended Practice (RP): Provides proven technology and sound engineering practice as well as guidance for the higher level OSS and OS.

The Sevan FPU-Ice DNV-OSS-102 rules for Classification of Floating Production, Storage and Loading Units refers in the rules regarding ice loading and structural requirement to the ice classes rules DNV Pt5Ch1Sec3 and 4.

6.2 Ice Class rules

The DNV ice class rules are divided into two categories;

- Pt .5 Ch.1Sec.3 Ice Strengthening for the Northern Baltic
- Pt.5 Ch.1 Sec4. Vessels for Arctic and Ice Breaking Service

The Pt .5 Ch.1Sec.3 rules are for merchant vessels sailing in ice with ice breaker support. The DNV 1A* class notation have a design ice thickness of 0.1m.

The Pt.5 Ch.1 Sec4 are rules for ships designed ice breaking in ice infested areas, and are therefore most appropriate for the Sevan FPU-ICE. Vessels intended for ice breaking as their main purpose may be given Icebreaker ICE or Icebreaker POLAR notation. For vessels built for another purpose, while intended for operating in areas where icebreaking is necessary, may have additional class notation ICE or POLAR.

Vessels with the class notation Icebreaker, and other POLAR class vessels are expected to encounter pressure ridges and other ice features of significantly greater thickness than the average thicknesses specified in figure 6-1. The Sevan FPU-ice is design with regards to the class notation Polar 30.

6.3 Design loads and load area

The ice impact force on the bow is found from energy calculations. The local ice pressure is directly proportional with the selected crushing strength multiplied be a weighting factor F_A for different sections of the hull. The bow area is used due to have the most conservative predictions on design loads. The Sevan FPU-Ice is a cylinder shape structure design to encounter ice and waves from all angles. Therefore is the structure pressure equal to bow pressure.

$$p_o = 1000F_A\sigma_{ice} \left[\frac{kN}{m^2} \right]$$

Equation 6-1

σ_{ice} is determined in table A in the rules and F_A is a correction factor for reinforced area in questions. For an icebreaker bow, the F_A factor is 1.0.

Pt.5 Ch.1 Sec.4 A

Table A1 Ice conditions					
Class notation	Type of ice encountered	Nominal ice strength $s_{ice} (N/mm^2)$	Nominal ice thickness $h_{ice} (m)$	Limiting impact conditions	
ICE-05 ICE-10 ICE-15	Winter ice with pressure ridges	4.2 5.6 7.0	0.5 1.0 1.5	No ramming anticipated	
POLAR-10 POLAR-20 POLAR-30	Winter ice with pressure ridges and multi-year ice-floes and glacial ice inclusions	7.0 8.5 10.0	1.0 2.0 3.0	Occasional ramming	
Icebreaker	As above	As above	As above	Repeated ramming	

Figure 6-1, Class notations and ice pressure, Table A1 (DNV, 2009)

For a vessel with class notation Polar-30 the maximum design ice pressure is 6.835 [MPa]. The pressure is based on the ice crushing strength and do not take failure mode in contemplation.

$$p = F_b p_o \left[\frac{kN}{m^2} \right]$$

Equation 6-2

$$F_B = \frac{0.58}{(A_c)^{0.5}} \text{ for } A_c \leq 1.0 \text{ m}^2$$

Equation 6-3

$$F_B = \frac{0.58}{(A_c)^{0.15}} \text{ for } A_c > 1.0 \text{ m}^2$$

Equation 6-4

$$A_c = h_0 w$$

Equation 6-5

$h_0 = 0.8h_{ICE}$ for stem area and l for maximum for non longitudinal frames and w is the critical width of contact area in m . For non longitudinal frames is $w = s$. The load area is according to DNV 1.44 m^2 and a design pressure of 5.49 MPa

The design pressure decreases with increase stiffener spacing.

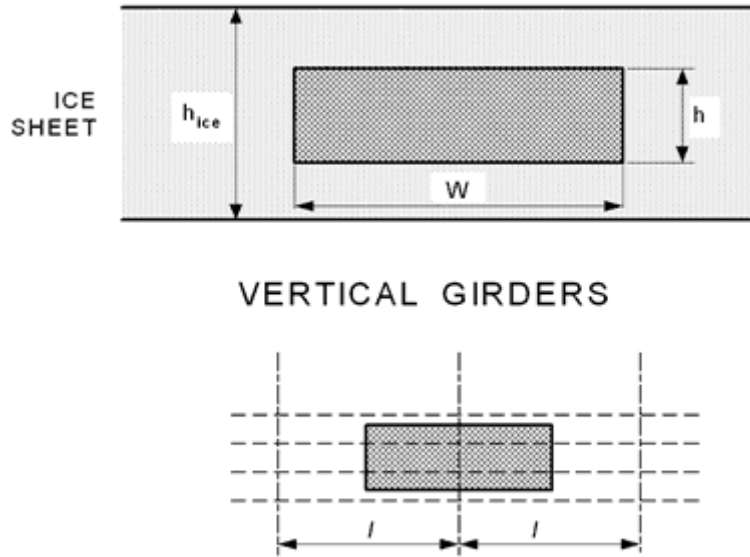


Figure 6-2, DNV Design Contact Area, Fig 4 (DNV, 2009)

6.4 Structural requirements

The DNV structural requirements are based on linear elastic theory. The standard design limit state used is Von Mises equivalent stress criteria. The Von Mises stress is the most commonly used and is based on the strain energy in the material. Von Mises stress gives reasonable agreement with empirical test results. The reference stress is often taken as the yield point for the material, i.e. first yield criterion has been applied.

$$\sigma_j = \sqrt{\sigma_1^2 + \sigma_2^2 + \sigma_3^2 - \sigma_1\sigma_2 - \sigma_2\sigma_3 - \sigma_1\sigma_3}$$

Equation 6-6

Where $\sigma_1, \sigma_2, \sigma_3$ are bending stresses in 1, 2 and 3 direction. For linear theory, σ_3 is equal to 0 and the equation 6-6 is reduced to:

$$\sigma_j = \sqrt{\sigma_1^2 + \sigma_2^2 - \sigma_1\sigma_2}$$

Equation 6-7

Von Mises stress criterion is often plotted as an ellipse as shown in figure 6-3 where combination of σ_1 and σ_2 the ellipse will cause yield.

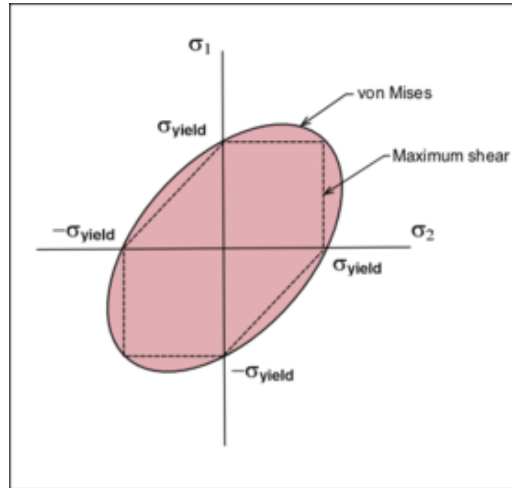


Figure 6-3, Von Mises

6.4.1 Plate thickness

The thickness of the plating exposed to patch load is generally not to be less than:

$$t = 23k_a \frac{s^{0.75}}{h_0^{0.25}} \sqrt{\frac{k_w p_0}{m_p \sigma_f}} + t_k$$

Equation 6-8

$$k_a = 1.1 - 0.25 \frac{s}{l}; k_a \in [0.85 - 1.0]$$

Equation 6-9

$$k_w = 1.3 - \frac{4.2}{(a/s + 1.8)^2}; k_w \in [0.85 - 1.0]$$

Equation 6-10

k_a is the aspect ratio factor for a plate field, and the k_w is the influence factor for narrow strip of load (perpendicular to s). a is for transversely stiffened panel h_0 . The bending moment factor m_p is 2.68 from Table F1 in the DNV Rules. t_k is the corrosion addition given in B500 in the DNV rules.

The thickness requirement may be used in a reversal way to find the plate resistance at a given thickness when the corrosion factor is neglected.

$$r = p_0 = \left(\frac{h_0^{0.25} t}{23 \cdot k_a s^{0.75}} \right)^2 \cdot \frac{m_p \sigma_f}{k_w}$$

Equation 6-11

For the given dimension of the Sevan FPU-ice, the resistance of the plate is 10.86 MPa

6.5 Transverse Stiffener

The DNV rule classifies stiffeners into longitudinal stiffener and other stiffener. The SEVAN FPU-ICE is a transverse stiffener. Section F 400 in the DNV rules will apply for transverse stiffener.

The web sectional area is set by:

$$A_w = \frac{5.8k_s(h_0s)^{1-\alpha}(1-0.5s)p_0}{\tau l \sin(\beta)} + A_k$$

Equation 6-12

$$k_s = 1 + 0.5 \frac{(C_1 + 0.5h_0)^3}{l^3} - 1.5 \frac{(C_1 + 0.5h_0)^2}{l^2}$$

Equation 6-13

k_s and α is a correction factor, C_1 is the arm length of bracket in m, β is the angel of web with shell plating.

The web thickness requirement is:

$$t_w = 1.5 \left(\frac{p_0}{\sigma_f \sin \beta} \right)^{0.67} \left(\frac{h_w s}{t_s} \right)^{0.33} + t_k$$

Equation 6-14

Section modulus requirement is:

$$Z = \frac{520l^2 s^{1-\alpha} p_0 w_k}{m_e \sigma h_0^\alpha \sin \beta}$$

Equation 6-15

h_0 is the value of h and s whichever smallest. h_w is the stiffener web height. $\tau = 0.45\sigma_f$ where σ_f is the yield strength of the steel used.

6.6 Conclusion

With regards to local design, plate thickness, stiffener spacing and the steel quality is the main parameter. The pressure increase as the stiffener spacing decreases. An increase in the plate thickness causes an increase in the plate capacity. An increase in the stiffener spacing leads decrease in plate capacity. A major concern in choosing the right ratio of stiffener spacing plate thickness is weight and the assembly cost. Weight is especially important with regards to the deck load and storage capacity as well as cost of steel.

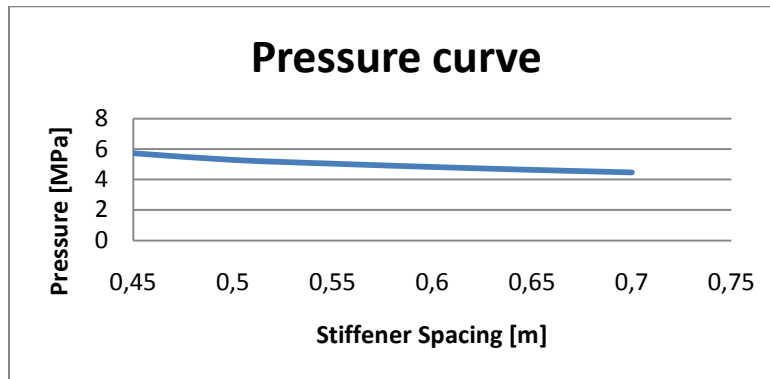


Figure 6-4, Pressure depending on stiffener spacing

7 Limit state design method

The Principle Standard design of offshore structures is ISO 19900 Petroleum and Natural Gas Industries - General Requirement for Offshore Structures. On the Norwegian shelf the NORSOK standard is still referred to.

The term limit state refers to a state of the structure where the structure or a part of the structure no longer fulfils the requirements ensuring that the structure or a part performs according to the design specifications. A limit state is controlled by the following equations (Norway)

$$\gamma_p x_p + \gamma_v x_v + \gamma_e x_e \leq \frac{\gamma_c}{\gamma_m}$$

Equation 7-1

The limit state design requirements critical and the quantitative reliability targets shall be achieved or proven better because exceedance of these limit states can directly result in human, environmental or asset loss.

x_p , x_v and x_e is respectively permanent, variable and characteristic environmental loads. γ_p , γ_v , γ_e and γ_m are partial safety factors ensuring adequate margin between the characteristic limit state response and corresponding limit state capacity.

Limit states are divided into the following four categories:

- ULS that generally correspond to resistance to extreme applied actions;
- SLS that correspond to criteria governing normal function use;
- FLS that correspond to the accumulated effect of repetitive actions;
- ALS that correspond to accidental events and abnormal environmental events;

7.1 Ultimate limit state

Ultimate limit state is important regarding structural safety. By this control it shall be ensured that all foreseen actions (loads) can be resisted with an adequate margin. When applying the ultimate state it is usually applied on a component basis. The characteristic values for the various loads correspond to an annual exceedance probability of 10^{-2} . The ultimate limit state is typically checked for two different scenarios; a) The case when the permanent load and the variable actions are governing, B) The case when the environmental load is governing. The ULS requirement for ice is referred to as ELIE (extreme level ice event). The material factor γ_m for ULS is according to the Norsok N-004 1.15 unless noted otherwise.

Actions combination	Permanent actions	Variable Actions	Environmental actions
a	1.3	1.3	0.7
b	1.0	1.0	1.3

7-1, Tabell 1 Norsok N-001

7.2 Accidental limit state

ALS (Accidental (abnormal) limit state) is a criterion to ensure that the structure to a given accidental scenario does not lead to a complete loss of integrity of the structure, but have sufficient reserve strength, displacement or energy dissipation capacity to sustain large actions and other effects. Typical accidental actions are

- Impact from ships collisions
- Impact from dropped objects
- Fire
- Explosion
- Sea state with return period 10 000 years

The accidental damage limited state is to be checked at two levels; a) Survive a accidental action with return period of 10^{-4} , b) demonstrate that the structure in a damage situation can survive environmental loads corresponding to an annual exceedance probability of 10^{-2} .

ALS for ice actions defined as abnormal-level ice event (ALIE). According to ISO 19906 should both local and global actions be considered. To ensure ALIE design check, non linear analysis may be used. Structural components are allowed to behave plastically.

Iceberg and ice island impact events with an annual probability of occurrence between 10^{-4} and 10^{-5} , and with an exceedance not greater than 10^{-2}

As the figure shows, the ALS loads is substantially bigger

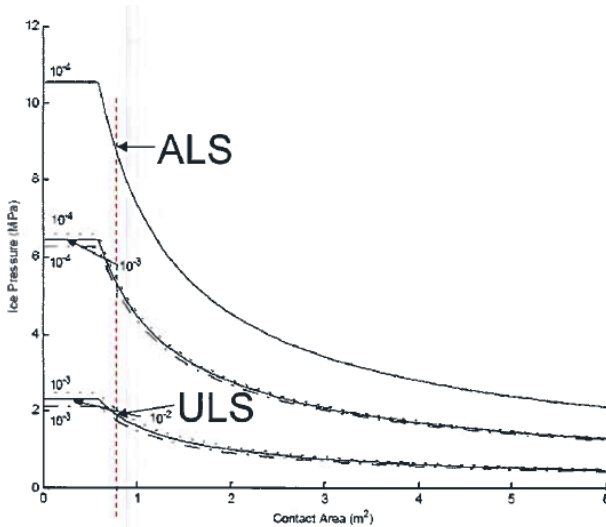


Figure 7-1, ALS and ULS loads for ice pressure(Amdahl P. j., 2003)

7.3 SLS- Serviceability limit states

Exceedance of SLS results in loss of capability of a structure to perform adequately under normal use. The setting of SLS reliability targets is generally the owner's responsibility, except for considerations that could lead to long term-structural degradation such as corrosion of reinforcement in concrete. SLS for ice actions is SLIE, Serviceability-level ice event.

7.4 FLS- Fatigue limit states

Exceedance of FLS of offshore structures results from cumulative damage due to repeated actions. All actions over the design service life shall be considered. For ice actions, cyclic variations are generally associated with compressive and flexural ice failure.

7.5 Representative values

As stated in the ISO 19906(Internastional, 2007) the annual probability for exceeding ELIE and ALIE is 10^{-2} and 10^{-4} . The ISO 19906 has stated two methods for estimating the ice actions.

- Probabilistic methods
- Deterministic methods

Probabilistic approach demands sufficient site specific data associated with the particular interaction scenario. In cases with absence of sufficient data, deterministic method is preferred. For both of these methods, the ice action Z is a function of n contributing parameters, X_i , $Z=Z(x_1, \dots)$

The relationship between the action Z and the contributing parameters X_i , does not have to be analytical expression. The contributing parameters X_i could consist of several relationships for mechanisms acting simultaneously against the structure, ice thickness and, interacting width and ice crushing

Z is typically global horizontal action in, however it could be an overturning moment, vertical action or a local action.

7.6 Ice action scenarios

Design actions reflect on relevant ice scenario, limiting mechanisms and ice failure modes for the geographical location of the structure. The structural configuration and the relevant operational scenarios should include physical ice management, maneuvering of the installation and disconnection.

Ice scenarios that may be applicable;

- First year ice feature,(level ice, land fast ice, floes, ridges, rubble fields, and refloated stamukhi
- Multi-year ice features (level ice, floes, ridges, rubble or hummocks fields)
- Icebergs
- Ice islands

Subsidiary conditions that can act in combination with feature or can influence the nature of the interaction include:

- Seasonality
- Ocean currents including tidal effect;
- Wind
- Waves
- Water depth

8 Local Ice Actions

Over the last decades much has been learned about problems of local ice pressure on ships and offshore structure. Ships such as icebreakers and offshore structures such as lighthouse and drilling vessels have been instrumented to facilitate the direct measurement of local ice pressure. On the basis of these measurements, most of the derivations of local pressure vs. load area are made. It has been found that the effective local pressure decreases as the size of the loaded area increases. This has an important implication for the design of hull structure since only smaller, local areas have to withstand the higher pressures and the larger areas can be designed for significant lower pressures. (M.E Johnston, 1998)

Local actions shall according to the ISO 19906 be based on relevant full-scale or established theoretical methods. The variations in ice properties due to geographical differences shall be investigated.

Local actions shall be considered for all parts of the structure contributing to its overall integrity and stability. For steel structures as the Sevan FPU-ice, local actions shall apply for sheet piling, plates stiffeners, frames and bulkheads. Design contact areas shall be considered on the local structural configuration, including frame spacing, plate thickness and appendage dimensions. The size and placement of the local contact areas shall be selected to ensure that the most critical cases are addressed.

8.1 Localized pressure due to ice crushing

Ice crushing is a failure mode that frequently occurs with vertical structures and over local area on sloping structures (M.E Johnston, 1998). During ice crushing, the interaction zone may be characterized by critical zones where intense pressure occurs over a short period of time. The critical zones are found to be approximately 0.10m^2 in area and may exert forces ranging from 0.1-4 MN. With an area of 0.10m^2 , a force of 4 MN is equivalent to a pressure of 40 MPa. Various loading data, ranging from laboratory tests and full scale ice-structure interactions indicates decreasing pressure with increasing area. Power law equations have been introduced to correlate loading areas and pressure during ice crushing.

$$P = Ca^n$$

Equation 8-1

Where a is the contact area, and C and n is constants. The constant is established by fitting a curve through the scatter of pressure-area data. n is a usually value between -0.7 and -0.3. By fitting a single curve, it does not consider partial fits within certain data ranges and does not account for area within an area.

Area of ice does not fail simultaneously at a single peak pressure. The overall applied load reflects the average of numerous, small zones which do not necessarily have equivalent peak stresses. The crushing process results in three different regions of pressure;

- Recently spalled ice
- Regions of background pressure
- Critical zones

During ice crushing, most of the applied load is concentrated in the critical zones. These critical zones are characterized by high stresses, potentially of excess of 40 MPa. The distribution of pressure within the critical zone is dependent upon the geometry of the layer of crushed ice that exists between the critical zone and structure.

In the paper, four analyses considered several types of interactions, each having different areas of instrumentations and confining stresses where presented. Hobson's Choice indentation test, ramming trials Louis S. St Laurent Ship and Kigoriak and Case study of the Molikpaq offshore structure. The main purpose with these full scale trials data was to establish estimates of pressure, size, force and spatial density of critical zones.

The Critical zones were shown to be highly variable in space and in time. If the mean critical zone force from the Louis S. St Laurent data set is accepted as a valid basis for interpreting data from the Kigoriak and Molikpaq, the size of critical zones are quite similar (0.10m^2) for interactions scenarios, despite the effect of contact area, confining stress and ice type. Data from various interactions indicates an average pressure of 7 MPa for small areas (0.045m^2) and a representative average pressure of 0.5-1 MPa for areas between 1 m^2 and 162 m^2 .

Confining stress is largely a function of the distance to the nearest free surface. This is in most rules and design criteria expressed in terms of aspect ratio. For the types of aspect ratio examined, average pressure substantially decreases as contact area exceeds $2\text{-}3\text{m}^2$. This is important for design criteria regarding local pressure. For instance a small local area of extreme pressure may be considered randomly generated point loads that, after exceed a certain contact area, decrease in influence due to increasing regions of background pressure.

8.2 Local design ISO 19906

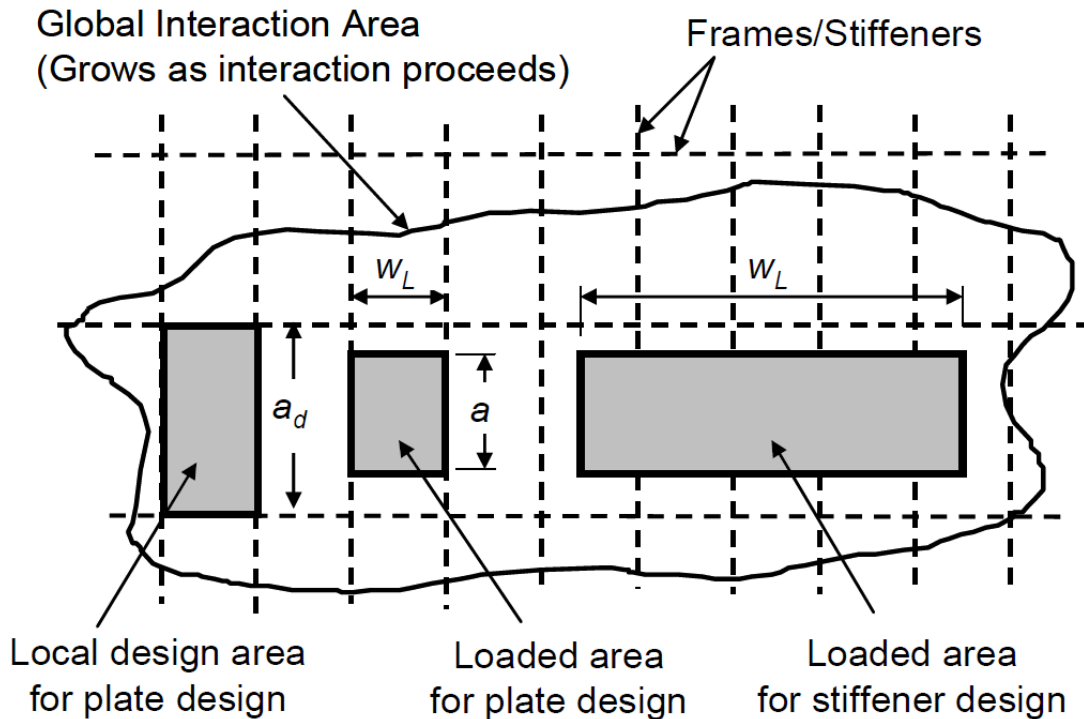


Figure 8-1, Definition of loaded areas for local actions, Figure A.8-16 (International, 2007)

When calculating the local load the proper load area is the challenge. The ISO 19906 has made suggestions to estimate the load area and loads. Local pressures should be used in design of shell or stiffening element as figure 8-1, Ice interactions can produce pressure constant over an area A , where

$$A = a * w_L$$

Equation 8-2

a is the height and w_L is the width. There is not stated in the ISO 19906 code the use of w_L , a and a_d other than the figure. However ISO 199906 states that maximum action effect usually occur when the height a of the loaded area equals the height of the local design area a_d .

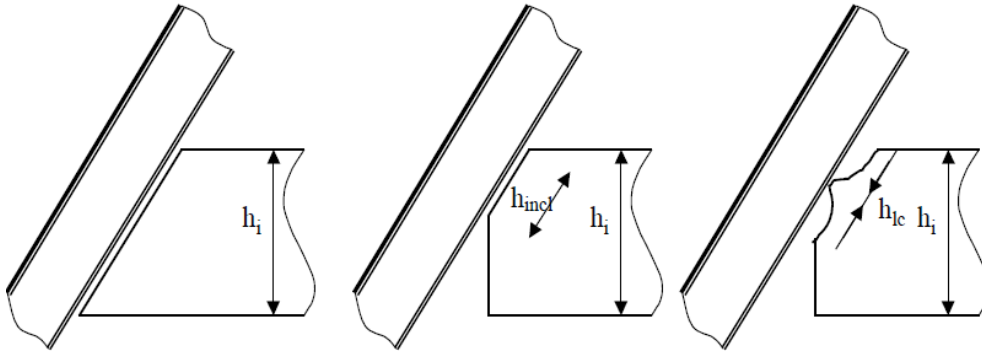


Figure 8-2, Different load height (Riska, Lecture Notes IX, ICE II, 2008)

This figure shows that the load height may vary with the same ice thickness. The pressure will then vary for the same ice thickness. Local ice actions are estimated using the ISO 19906 Standard (International, 2007).

8.2.1 Local actions from thin first-year ice

Considerable data from full scale measurement for level and rafted ice conditions have been collected to give representative values for local actions for first-year ice up to 1.5 m. These measurement shows the maximum load

Local actions effects can be estimated by applying a constant force uniformly over a local design area.

$$F_L = 3.72\sqrt{a_d w_L} \quad \text{for } a_d \geq 0.14$$

Equation 8-3

$$F_L = 10a_d w_L \quad \text{for } a_d \leq 0.14$$

Equation 8-4

These expressions are valid for $w_L / a_d \leq 10$ and $a_d \leq 0.4h_E$ is the characteristic ice thickness for ELIE. F_L is in[MN]. If the height of the local design area exceeds $0.4h_E$, full thickness local pressure equation may be used.

$$p_F = 2,35h^{-0.5} \quad \text{for } h > 0.35m$$

$$p_F = 4.0 \quad \text{for } h \leq 0.35m$$

Equation 8-5

p_F is the pressure in MPa and h is ice thickness in m.

In a deterministic design, the local pressure acting on the loaded area is

Analysis and design of the Sevan FPSO against abnormal ice actions

$$p_L = \gamma_L p_F, \quad \gamma_L = 2.5$$

Equation 8-6

Where γ_L reflects the concentration of the full-thickness pressure on the loaded area and p_F is determined by equation (4-5)

In multi-year ice and icebergs are capable to provide the confinement required to produce higher pressure for the same loaded area.

8.2.2 Massive ice features

Local pressure due to massive ice features, having a thickness of 1.5 m can be determined using empirical data found from indentation test in the Beaufort Sea and from measurement taken on the ice pressure panels of the Molikpaq structure in the same area.

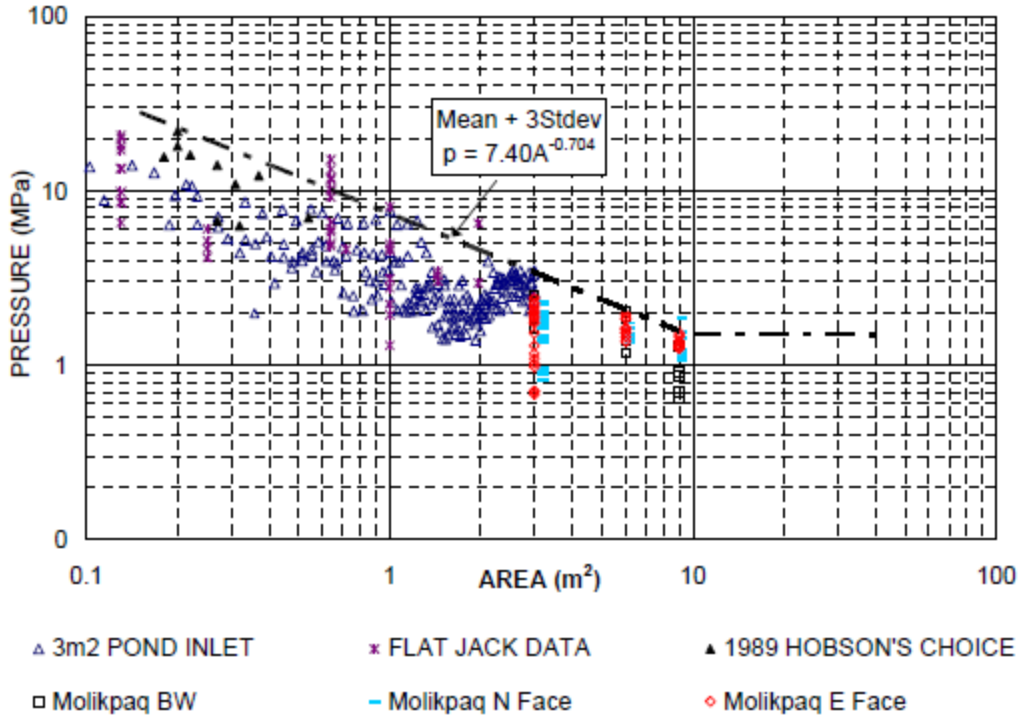


Figure 8-3, Ice pressure curve for massive ice features as function of load area Figure A.8-18(International, 2007)

Based on measurement data, the local pressure p_L [MPa] can be determined as

$$p_L = 7.40A^{-0.70} \quad \text{for } A \leq 10\text{m}^2$$

$$p_L = 1.48 \quad \text{for } A \geq 10\text{m}^2$$

Equation 8-7

Where A is the local design area. The pressure corresponds to the mean +3 standard deviations, corresponding to 99.7% percentile of the cumulative distribution. For global actions a constant pressure of 1.48 MPa is used.

8.3 Estimates of ice loads

The estimations of loads depend clearly on the load area. The definitions of the load area are not as clear as it should be.

8.3.1 Plate design

As the figure 8-1 shows, the loading height a_d for maximum actions effect is the length of the plate. The width w_l is equal with the stiffener spacing. This correspond plate design area of 1.7 m^2 for the Sevan FPU-Ice. With respect with the ice thickness of 3 m (DNV) calculations from the massive ice feature should be applied. The ice actions will then have a pressure of 5.11 MPa over the area of the plate.

8.3.2 Stiffener design

For stiffener design, the loading width is set to be four times the stiffener spacing. The load height for stiffeners design area is not précised stated. An estimation of the figure 8-1 may be a loading height of 0.8 of the plate height. This gives a loading area of 5.43 m^2 . With the same assumption for plate loading with a design ice thickness of 3 m, and pressure is taken from massive ice feature in equation 8-7. The ice action for stiffener design will be a pressure load of 2.26 MPa over an area of 5.43 m^2 .

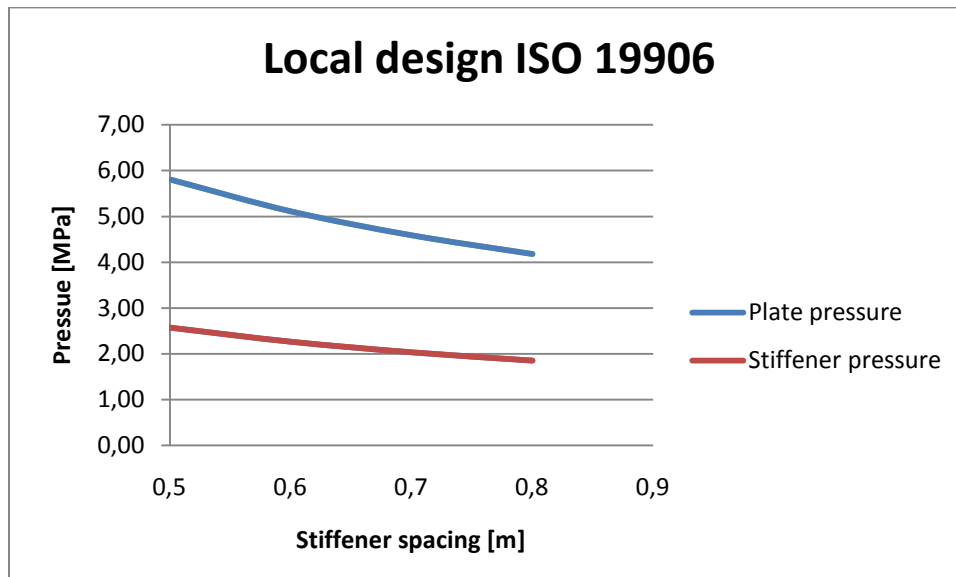


Figure 8-4, Local design pressure- stiffener spacing

When selecting a smaller stiffener spacing the pressure will increase due to decrease in area, however the net force will be the same. The estimates from the ISO 19906 coincide well with the estimation of the DNV requirement for POLAR and ICEBREAKING notation in pressure, but not in load area. The load area for ISO 19906 is large and may therefore be more conservative. The assumption may also be considered as conservative due to the way Sevan-FPU ice is design to managed ice. The ISO 19906 does not reflect on the structural shape and failure modes of ice actions. Flexural failure will result in significant lower ice action. Table 8-1 shows design loads for 5 structures built for massive ice feature. By comparing the design loads from these structures to the Sevan, one may find the design load to be in the right magnitude.

Structure	SSDC	CRI	Molikpaq	Taisiut	CIDS
Limiting Level Ice [m]	10	3	10	5.6	5.2
Ice Concentration	10/10	10/10	10/10	10/10	10/10
Design Local Ice Pressure [MPa]	8.3	2.8	3.0	4.1	6.2
Area for Local Pressure [m ²]	3.7	0.7	2.3	3.7	2.3
Design Ice load Global [MN]	900	436	640	560	640

Table 8-1, Design load on arctic structures, Table 4 (G.W.Timco, February 2009)

8.3.3 Impact pressures from glacial ice.

Estimation of impact pressure from glacial ice can be solved by a probabilistic model developed based on data from ship impacts with multi-year ice floes. Data were primarily from measurements of the Kigoriak ramming test on multi-year ice.

$$F(z) = \exp\left[-\mu \exp\left(\frac{-p}{\alpha}\right)\right], \quad \alpha = 1.25A^{-0.7}$$

Equation 8-8, Impact pressure from glacial ice

The cumulative probability distribution can be used for the local pressure p acting on an area A .

9 Global Loads

The determination of global ice actions should be based relevant full scale measurement, model experiments if they can be scaled reliably or established methods. ISO 19906 states that the following conditions should be considered;

- Quasi-static ice actions due to level ice; where inertial action effects within the structure can be neglected
- Dynamic actions due to level ice; where inertial actions effects within the structure are significant and a dynamic structure is required
- Quasi-static actions due to ice rubble and ice ridges; where inertial action effects within the structure can be neglected
- Impact from icebergs, ice island and large multi-year or first year features.
- Quasi-static actions, from features lodged against the structure, driven by met ocean actions
- Adfreeze actions effects including the frozen in condition
- Thermal action effects

These conditions shall be considered with limiting stress, limiting energy and limiting force mechanisms.

9.1 Global model test of the SEVAN FPU-ice

In spring 2008 the FPU-Ice was tested in the ice tank at HSVA (Oddgeir Dalane, 2009). The purpose of the test was to study the ice load level on the structure and the response in severe to extreme first-year ice conditions regarded as 100 year extreme ice conditions for eastern part of the Barents Sea. The buoy had a scale of 1:40 and test was executed in 4 different ice sheets. (Oddgeir Dalane, 2009)

- Test series 1000: Severe conditions-1.9 m thick level ice and 15m deep ridge
- Test series 2000: Extreme conditions, 1.9m level ice and 2m deep ridge
- Test series 3000: Successive ridges- Study of ice accumulations and ice floe transport
- Test series 4000: Successive ridges- Study of ice accumulations and ice floe transport – 6 m thick ice rubble field

9.1.1 Test set-up

The buoy was freely floating and moored on the false bottom, which was connected to a carriage. The carriage was moved with a constant velocity simulating incoming ice. When operating, the buoy will have 20-28 mooring lines depending on the global load level in ice. The mooring lines are grouped into 4 clusters each with 5-7 mooring lines. In the test the buoy was monitored in all ridged and rotational degree of freedom referred to as surge, sway, heave, roll, pitch, and yaw. Between the mooring lines and the structure a triaxial load cell was mounted measuring total mooring forces in the x-, y- and z- direction. The measurement from this load cell represent total mooring force on the structure, denoted as F_x , F_y and F_z . The total horizontal mooring force is;

$$F_{tot} = (F_x^2 + F_y^2)^{\frac{1}{2}}$$

Equation 9-1

Froude scaling was used to bring the model scale to full scale.

HSVA used fine-grained columnar type grown naturally from sodium chloride solution of salinity 7 ppt. The HSVA tested the Sevan FPU-ICE in several ice conditions such as level ice, ice ridges, ELIE/ALIE and managed ice for ice loads predictions. During test, 4 video cameras above and 2 cameras monitored ice behavior.

9.1.2 Test results

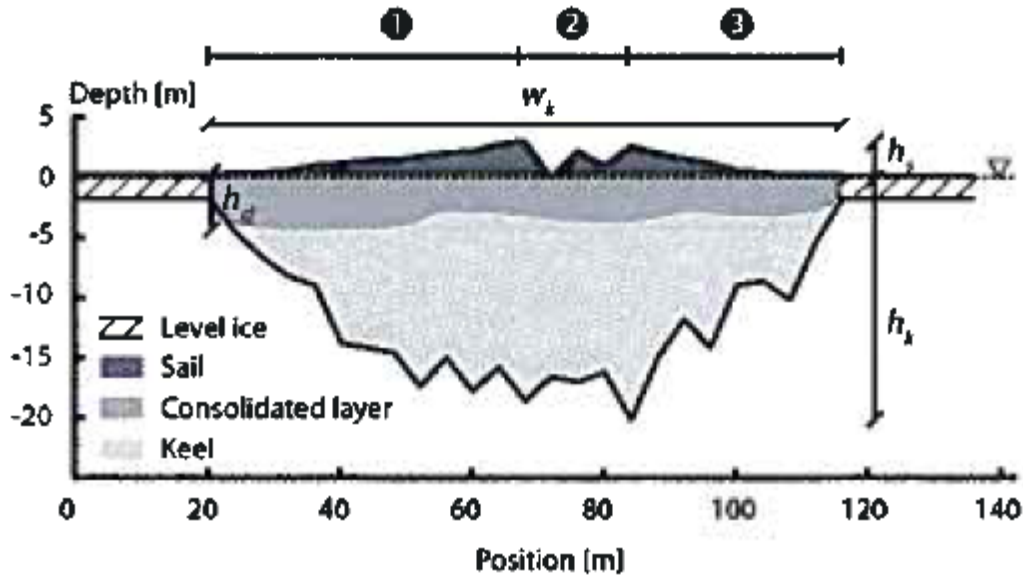


Figure 9-1, Ice Ridge (Oddgeir Dalane, 2009)

Ice ridges were in the test program embedded in level ice. The consolidated layer and the keel give the main contribution to the ridge action. The consolidated layer always failed in bending against the inclined side of the buoy. In part two of figure 9-1, two different behaviors of the consolidated layer was broken in bending by direct interaction with the buoy, or the buoy pushed rubble from the keel forwards, such that the rubble forced the consolidated layer upwards and thereby failing it in upwards bending. Rubble in the keel was packed together when the mooring forces were building up. After some time the buoy surged to its equilibrium position. The rubble was pushed forward inside a ridge, and pushed sideways near an end of a ridge. This made a saw tooth-like pattern in force. The floater cleared away most of the rubble from mooring lines and risers, however, single blocks of ice were observed in the deepest ridges.

The study showed that ice ridge forces are dependent on cross sectional area. With an increase in cross section area leads to an increase in forces. The ISO 19906 standard provides a method with dependency of ice ridge keel with no regards to ridge keel. The ISO 19906 may therefore give the same ice actions on two different ice ridges.

9.1.3 Managed ice

When operating in high infested ice water, assistance of icebreakers is essential. Severe ice ridges may not be broken by icebreakers. Icebreaker can break level ice upstream the ridges which reduces mooring

forces. One test series showed that mooring forces was reduced with over 50 %. This indicates that loads can be significant reduced by ice management. A report from Kulluk also states a significant reduction of forces in managed ice conditions.

9.1.4 Results

Test No	Description	Max F_x	Max Line Tension
1110/1130	2.0 m Level Ice	22.3 MN	4.6 MN
1100/1130	2.0 m Level Ice	30,8 MN	6.3 MN
1120	Non-conservative ice ULIE	51.6 MN	9.6 MN
2100	Conservative Ice condition ALIE	160.1 MN	27.4 MN
3100_1	Slightly conservative Ice conditions ULS/ALS	105 MN	18.3 MN
3100_2	Realistic Ice conditions Managed ice	65 MN	11,5

Table 9-1, Global load result from model test (Oddgeir Dalane, 2009)

The result of the model test showed that Sevan FPU-ice managed the ice in a downward bending. The significant part of the ice actions is on the conical part of the structure. No ice where submerged under the structure except minimal amounts for high-speed in level ice. The highest global loads are found in unmanaged ice ridges. The maximum peak force found for first-year ice ridges is 120 MN. For level ice the peak force is 20 MN

9.2 Global loading area

The Sevan FPU-ice is a conical shaped structure. The global load area depends on the global loading condition. Load area can be assumed to be half of the conical section with load height of 3 m. The loading area will then be 222.7 m², resulting in a global load intensity of 0.54 MPa.

10 Non linear finite element of ice actions

Ice is a complex material to model in finite element programs. A great number of geometric and material parameters and boundary conditions will affect the magnitude of ice actions. Also the application of external loading will influence the results.

Bjørnar Sand at the Norut Technology Ltd has made research on how to apply non linear element method to calculate ice forces on a conical shaped structure. The effects of material nonlinearities and friction between ice sheet and structure are taken into account. This chapter is a resume of parts of a PhD and a paper submitted to OMEA 2006, written by Bjørnar Sand (Sand, 2008) .

10.1 Ice in finite element program

The ice is model as a transversely isotropic or isotropic nonlinear material capable of cracking and crushing. Too be able to represent the behavior of ice cover over a broad range of strain, elastic, time-dependent creep and instantaneous, inelastic creep component of deformation must be considered. The most common model is often referred to the visco-plastic formulation. Ice is then interpreted on the basis of plasticity. The theory of plasticity represents a general mathematical framework for the description of ductile failure of material. These failure criterions have been applied to a wide material such as metals, polymers and concrete.

In general failure criterion can be defined in terms of components of the Cauchy stress tensor, σ_{ij} and interpreted as a hyper surface in the six-dimensional stress space spanned by σ_{ij} . The majority of failure criteria for ice have been limited to isotropic ice. These can be expressed in terms of various stress tensors.

10.2 Isotropic Failure Criterion

Reinicke and Remer introduced an elliptical surface yield surface for granular, isotropic ice. This failure surface describes an elliptic strength increase with increasing hydrostatic pressure. This is often referred to at the three-parameter failure criterion.

$$f(I_1, J_2, k_1, k_2, k_3) = k_1 J_2 + k_2 I_1 + k_3 (I_1)^2 = 0$$

Equation 10-1, Isotropic failure criterion

I_1 is the first stress invariant of the stress tensor σ_{ij} and J_2 is the second stress invariant of the deviatoric stress tensor s_{ij} . k_1, k_2 and k_3 are material parameters that must be determined experimentally.

10.3 Anisotropic Failure Criterion

Horrigemoe and Zeng have proposed a anisotropic failure criterion of elliptic type. This criterion is capable of predicting strengths in tension and in compression. It also accounts for the nonlinear effects of hydrostatic stress on multi axial strength of ice.

$$f(\sigma_{ij}, a_1 \dots a_{12}) = a_1 \sigma_x^2 + a_2 \sigma_y^2 + a_3 \sigma_z^2 + a_4 \sigma_x \sigma_y + a_5 \sigma_y \sigma_z + a_6 \sigma_x \sigma_z + a_7 \sigma_x + a_8 \sigma_y + a_9 \sigma_z + a_{10} \tau_{xy}^2 + a_{11} \tau_{yz}^2 + a_{12} \tau_{xz}^2 - 1 = 0$$

Equation 10-2, Anisotropic failure criterion

Where a_i ($i = 1, 2, \dots, 12$) are material constant which must be determined by twelve independent test. These tests are performed in tension, compression and shear test in respectively direction.

If the material is completely isotropic, the general criterion in equation 10-2 becomes identical to the three-parameter failure criterion in equation 10-1.

10.4 Transformation of state due to cracking and crushing

Ice exhibits two kinds of inelastic behavior under compression. The transition is defined in terms of the shape of stress-strain curve and behavior of material. At lower strain rates ($\dot{\epsilon} < \dot{\epsilon}_{D/B}$) the material is ductile and exhibits strain hardening, followed by strain softening. In higher stress rates ($\dot{\epsilon} > \dot{\epsilon}_{D/B}$), ice behaves in a brittle manner.

The transition between ductile and brittle behavior of ice is very important because it sets the conditions under which the compressive strength reaches a maximum. The strain rate $\dot{\epsilon}_{D/B}$ marks the transition between ductile and brittle is between $10^{-4} s^{-1}$ to $10^{-3} s^{-1}$ at temperatures range of $-40^\circ C$ to $-5^\circ C$. Because of the transition between ductile and brittle behavior of ice, the mechanical behavior can be approximated from the ductile or brittle end.

10.5 Modeling ice

To account for mechanics in both undamaged ice and damaged ice two separate constitutive models can be employed to simulate the transformation of state due to cracking or crushing of ice. The first model describes the behavior of unbroken ice and the second one describes the behavior of crushed or cracked ice. This can be done by modeling the ice with dual sets of elements which occupies the same volume by using coincident nodal points. The first set is the virgin elements and represents undamaged ice. The second set of elements represents the post-failure behavior of cracked or crushed ice. At the start of the analysis, the first set of element (virgin) is active and the damaged sets are deactivated. This can be achieved by multiplying the stiffness of the damaged elements by a severer reduction factor in the order of 10^{-6} . When the state of stress reaches the failure surface, i.e. $f = f(\sigma_{ij})$, failure is said to occur and the virgin elements are deactivated and the damaged elements are reactivated simultaneously.

10.6 Friction model

The most commonly used friction law is the Coulomb friction model. The sticking force limit the Coulomb friction model is a function of the friction coefficient and contact forces normal to the target surface.

10.7 Test analysis

Bjørnar Sand made an analysis on ice sheet interaction on a conical structure. The diameter of the conical structure in the waterline is 11.6 m, where three different values $\alpha = 45^\circ, 60^\circ, 75^\circ$ sloping angel.

The cone was modeled as a fixed and ridged structure. The ice sheet had a length of L and a width of $2L$. In numerical studies, L was set to be 45 m and the ice sheet had a thickness of 0.8m.

In case of granular, isotropic ice failure criterion in equation 10-2 was employed. To predict failure of transversely isotropic ice, the hyper-elliptic failure criterion was employed.

To verify the numerical results obtain during finite elements simulations, ice sheet forces were also calculating using the plastic limit analysis proposed by Ralston. Ralston’s model is based on the assumptions that the ice behaves in an elastic ideal-plastic manner and Johanson’s moment yield criterion. The moment yield criterion depends on the flexural strength σ_f of the ice sheet, which was set equal to 0.71 MPa. The comparisons between maximum horizontal forces obtain by finite element simulations and Ralston method as a function of the slope angel. The effect of ice structure friction was also included.

10.8 Ice ridges in finite element simulation

Ice actions from sea ice ridges may represent the worst ELIE and ALIE loading case when designing offshore structures in ice-infested areas. The common way to characterize ridges is based on the age of ridges, first year ridge or multiyear ridge. First year ridges are ridges accumulated by ice blocks of present year. Multiyear ridges are ridges that have survived for a number of summer seasons. The melt water produced during summer months drains into the ridge core and refreezes during the winter causing a solid mass of ice. Multi-year ridges will therefore be the worst loading scenario for ice ridges.

Ice ridges are found in various shapes and different consistence of various ice. There is therefore an interest to consider an idealized ice ridge model with a constant sail to keel ratio and geometry. In analysis of multi-year ridges an idealized multi-year ridge model with a constant sail to keel ratio and geometry was used.

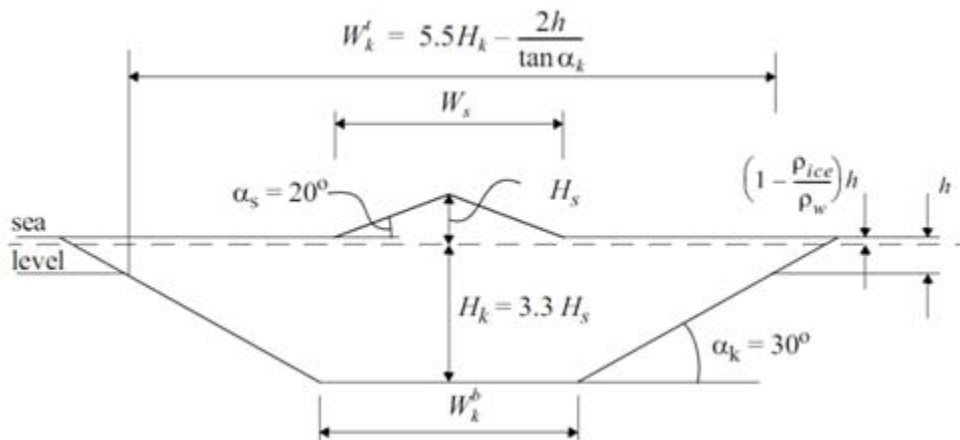


Figure 10-1, Idealized multi-year profile, Figure 2.7 (Sand, 2008)

The same element spatial discretization procedure for ice sheet was adopted for ice ridges as well. The effect of nonlinearities, strains, displacement and friction between ice and structure where taken into

account. Counter interaction forces were simulated with a contact algorithm that permitted surface to surface contact with coulomb friction sliding.

10.9 Ice ridges simulation results.

The multiyear ridges were embedded in an ice sheet similar to the ice sheet tested on the cone previous. The sail were set to 1.0 m. the ice within the ice sheet and ridge was assumed to be isotropic and the strength is constant through the thickness of the ice sheet and ridge. The ice ridge was moved into contact with the conical structure by applying a uniformly distributed load in the horizontal direction. The boundary conditions of this edge were such as to keep the ice sheet in a horizontal position. The remaining edges of the ice sheet and ridge were free.

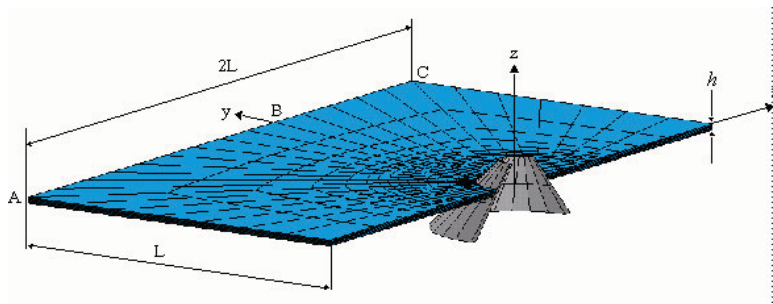


Figure 10-2, Geometry and element mesh of the ice sheet and upward bending cone

When applying the uniformly distributed load along the edge ABC, the ice ridge moves into the contact with the conical structure. Contact interaction between the ice sheet, ridge and the structure is described by a model which is based on finite sliding between a deformable body and a rigid body. Contact forces can be split into normal and tangential components. Tangential forces are due to friction that arises as the nodal points on the ice ridge meet the target surface of the structure and slides along it. The Coulomb friction model is employed and the sticking force limit of the Coulomb friction model is a function of the friction coefficient and the contact forces normal to the target surface.

To study the effect of various values of the friction coefficient between the ice and the conical structure, two different values of the friction coefficient were selected, i.e. $\mu = 0.0$ and 0.1 . The slope angle α of the cone was chosen in the range of 45° to 70° . There were two different reasons for the choice of this range, first, sloping angles below 45° are of little practical interests and, and second, for slope angles steeper than 70° , the ice failure mode is in the transition between bending failure and crushing failure. Typical force-displacement curves obtained by nonlinear finite element analysis are shown in the diagram below. In this diagram the horizontal force P_H and vertical ridge force P_V are plotted against the horizontal displacement at point B at the end of the ice sheet behind the ridge. In this example the cone angle was equal to 45° and the diagram also demonstrates the effect of the ice-structure friction.

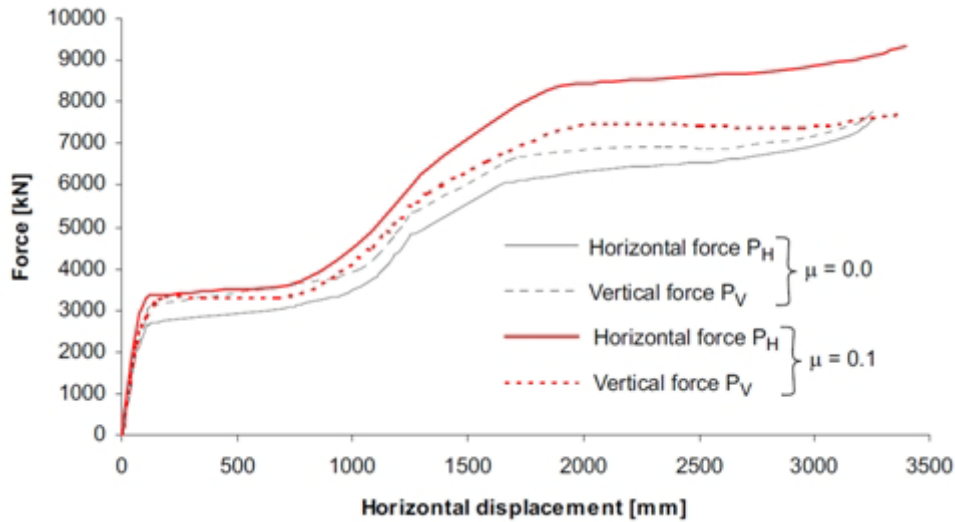


Figure 10-3, Force-displacement downward bending cone, Figure 6.61 (Sand, 2008)

Horizontal and vertical ice forces vs. displacement obtained by finite element simulations. It is assumed that the multi-year ice ridge is embedded in an ice sheet of thickness 0.8 m. with sail height equal to 1.0 m. The ice within the ice sheet and the ridge is assumed to be isotropic and the strength is constant through the thickness of the ice sheet and ridge. The elliptic failure surface for granular ice proposed by Reinicke and Remer was adopted to predict failure of solid isotropic ice. In this example a discrete, nonlinear spring model was applied to include the effect of buoyancy and gravity forces of ice sheet, while the iterative model for automatic calculation of buoyancy and gravity forces has been employed to include the weight and buoyancy forces of the multi-year ice ridge.

10.10 Discussion

The work performed by Bjørnar Sand is an indication that non-linear finite element simulation may be developed into a reliable tool for computing ice forces on offshore structures and realistic estimations ice failure modes and failure patterns. Non-linear finite element model of ice are capable to the ice properties by employing different failure criterion. This can be used in fine tuning structures in order of minimize the ice action for different loading cases. This method may also give reasonable estimation of ice actions for a specific structure and ice scenario. This method may also have result for ALIE actions when designing for iceberg and ice ridges. The ice crushing energy dissipated from impact may give more accurate estimation than numerical methods. The downside with this method is the modeling time and computational time in term of regards of cost benefits.

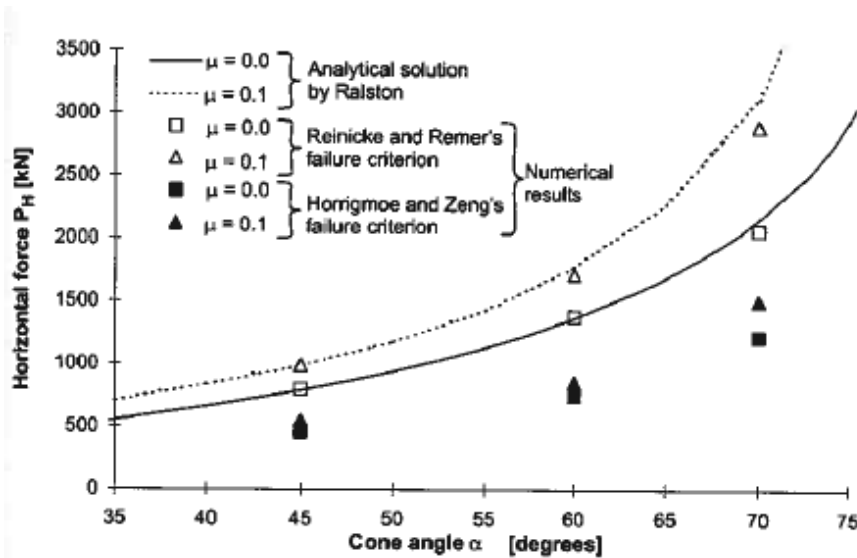


Figure 10-4, Cone angle effect on the Horizontal force, Figure 6.52 in (Sand, 2008)

The figure 10-6 describes how the cone angel affects on horizontal loads. As the cone angel increase the horizontal load increase significant. The result comes from a downward bending cone with a diameter of 9.04 m. The results may therefore only be used as an indication of the effect of cone angel.

Downward bending cone angel	Friction coefficient	Max Horizontal force [kN]	Max Vertical force [kN]
45	0.0	790	970
60	0.0	1365	970
75	0.0	2164	970
45	0.1	955	975
60	0.1	1715	978
75	0.1	3018	982

Table 10-1, Results from NFEA , Table 6.12 (Sand, 2008)

11 Methods for large displacement and plastic analysis

In this chapter, the theoretical calculation of local structure is addressed. Variance in structural layout may be of interest when comparing steel weight, building cost and structural capacity. The main focus is on the conical section and assumptions are made in order to calculate steel weight.

In conventional elastic linear model of design first yield is used as criterion for load carrying capacity of flexural members. This implies that the structure returns without plastic deformations. However steel has enormous strength reserves beyond first yield when considering plastic strength.

11.1 Strain hardening

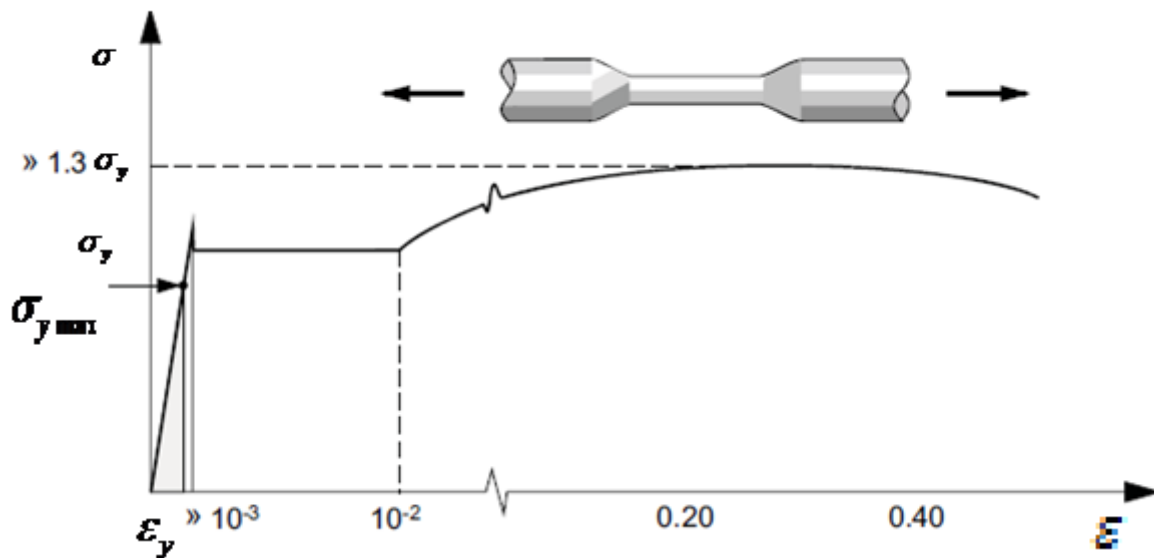


Figure 11-1, Stress-strain relationship, Figure 1.1 (Amdahl P. J., 2005)

The figure shows a stress strain relationship for mild steel. When the stress reaches the yield strength σ_y , the stress remains constant for increasing strain. For a strain of 10-20 times the yield strain ϵ_y , the flow stress increases caused strain hardening. The strain hardenings will attain maximum before decrease until fracture. This gives a tensile strength/yield strength ratio. This ratio varies within the different steel alloys.

11.2 Plastic moment and moment capacity

Plastic moment is calculated when the cross section have reached yield stress over the whole area. By comparing the plastic moment and the moment at first yield, shape factor α is determined.

Moment capacity of a stiffened panel may be calculated as for a beam. In most cases for plate stiffener, the plastic neutral axis will be within the plate.

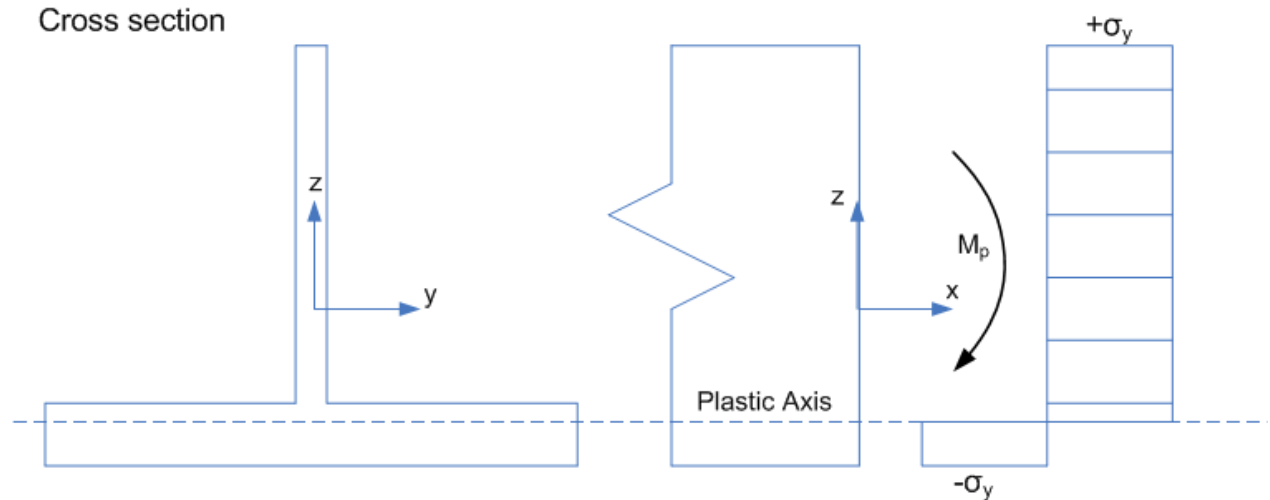


Figure 11-2, Cross section of a plate/stiffener

The neutral axis for fully plastic state is calculated such as the area of tension and compression is equal. For this particular stiffener y_p is located 10 mm below plate height.

The definition of plastic section modulus is determined by calculation the moment of the plastic neutral axis. The condition of pure bending moments yields

$$Z = \frac{M_p}{\sigma_y}$$

Equation 11-1

Where σ_y is the yield strength and M_p is the plastic moment. From figure (11-2)

$$M_p = P(y + y')$$

Equation 11-2

The force is then defined as;

$$P = \frac{\sigma_y A}{2}$$

The plastic section modulus is then expressed as

$$Z = \frac{P(y + y')}{\sigma_y} = \frac{A(y + y')}{2}$$

Equation 11-3

The elastic section modulus

Analysis and design of the Sevan FPSO against abnormal ice actions

$$W = \frac{I_{\text{elastisc state}}}{y_e}$$

Equation 11-4

The α is the shape factor, which represent resistance beyond first yield.

$$\alpha = \frac{P_c}{P_y} = \frac{M_p}{M_y} = \frac{Z}{W}$$

Equation 11-5

The α factor is calculated for six different stiffener arrangement in chapter 16.2.

11.3 Mechanism method for beams

Consider a simply supported beam axially under a concentrated load.

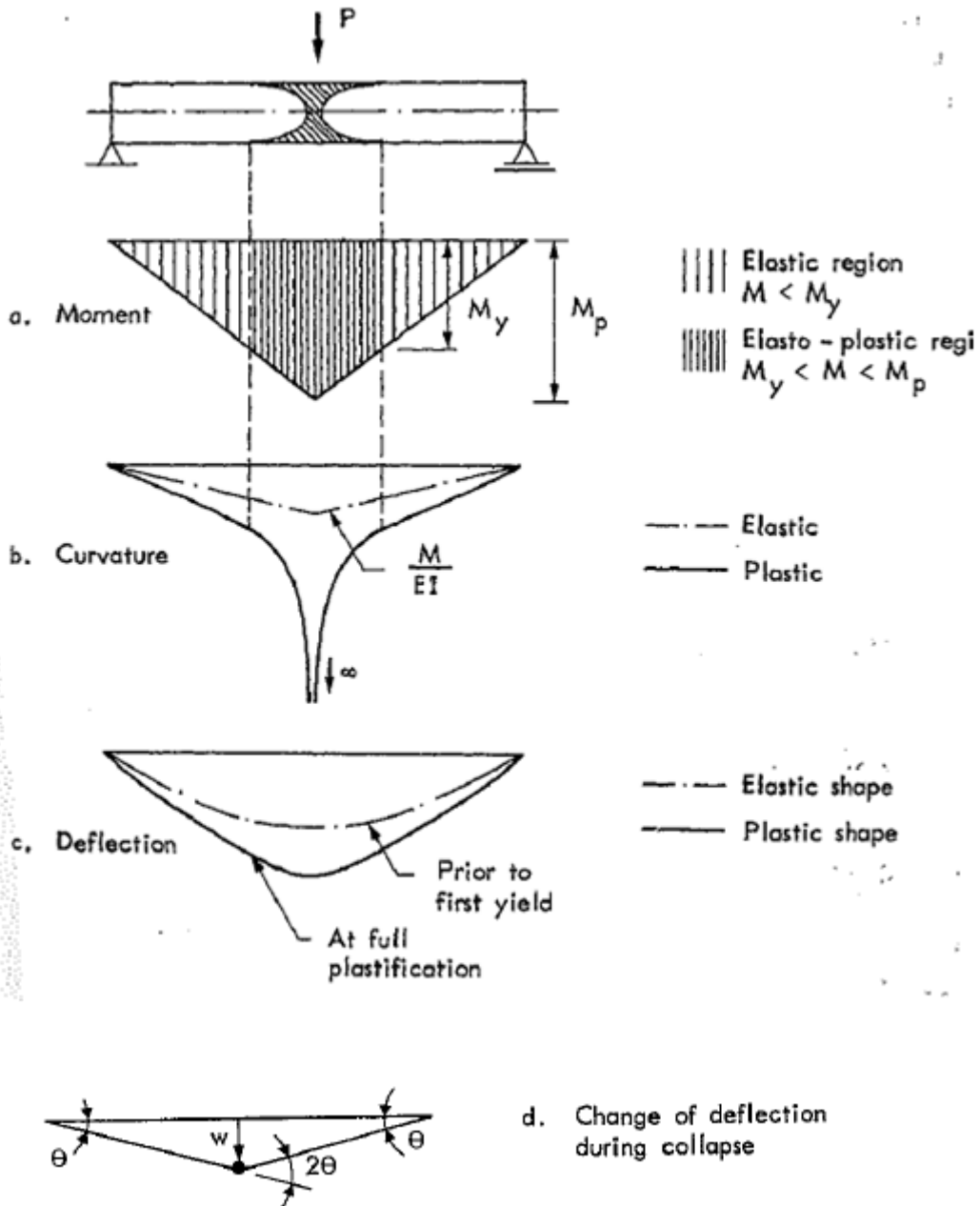


Figure 11-3, Elasto-plastic bending of beam, Figure 2.4 (Sørensen, 1985)

This is a statically determinate system and the moment curve is given in figure. The moment curve is unchanged even after plastication has occurred. The curvature in the cross section where plastication occurs goes towards infinity when the plastic section increases. It is seen that as full plastication develops the beam turns into a mechanism with a plastic hinge in the center. However, under constant load the plastic hinge can undergo any rotation.

Figure (11-3) indicates the change in deflection during plastic deformation and this curve represents the collapse mechanism. The load at which the formation of a plastic mechanism occurs is termed the plastic collapse load. The value of P_c can be determined by equating the magnitude of central bending moment to the fully plastic moment M_p .

$$\frac{P_c l}{4} = M_p \rightarrow P_c = \frac{4M_p}{l}$$

Equation 11-6

Analogous method for a fixed ended beam with uniform load gives

$$q_c = \frac{16M_p}{l^2}$$

Equation 11-7

11.4 Membrane forces to a beam

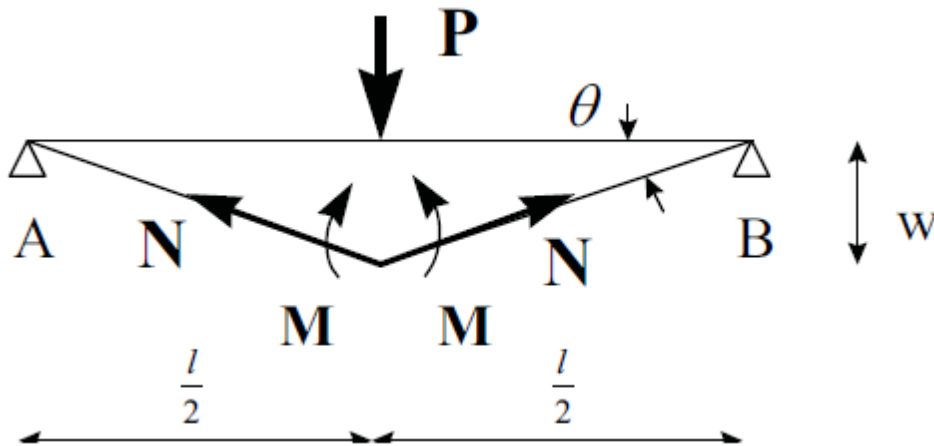


Figure 11-4, Simply supported-axially fixed beam, Figure 32 (Amdahl P. J., 2005)

As figure 11-4 shows, a beam has plastic collapse when midspan reaches fully plastic moment in equation 11-6. In the horizontal boundary condition at the end B is changed from free to fixed, will the collapse state be as figure 11-4. Due to fixity against inward displacement the beam elongates as soon as it undergoes finite displacement. θ and w represents now finite rotation and displacement.

Equilibrium considerations for figure 11-4 gives;

$$P = \frac{4M}{l} + \frac{4Nw}{l}$$

Equation 11-8

First term is the conventional bending term and the second represents contribution to the load-carrying from the membrane forces. The second term can be considered as a geometric stiffness which depends on the tensile axial force.

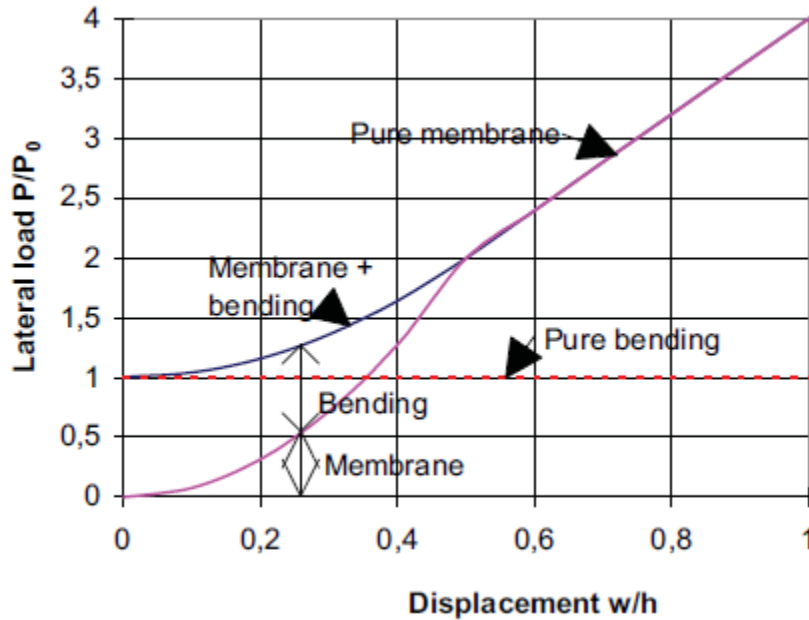


Figure 11-5, Load carrying capacity for rectangular beam at large deformations, Figure 35 (Amdahl P. J., 2005)

The figure 11-5 shows that if a beam can develop membrane forces, there is no unique collapse load. The capacity increases monotonously for increasing lateral displacement.

11.5 Plastic plate capacity

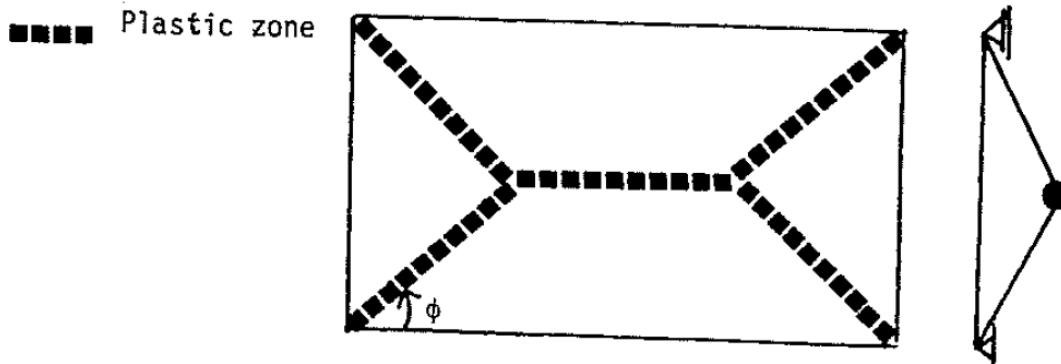


Figure 11-6, Plate, simply supported, Figure 3.1 (Sørense, 1985)

Figure 11-6 shows a plastic mechanism for a simply supported plate with no horizontal restrictions. Deformations of the plate are concentrated along the yield lines which correspond to the plastic hinge for beam. The plastic work is found by integration along the plastic zones.

For a continuous plate field, the boundaries may be assumed clamped and the collapse resistance in bending r_c is given by:

$$r_c = \frac{12f_y t^2}{l^2 \alpha^2}$$

Where f_y is the yield stress of the material, t is plate thickness and plate aspect factor is defined by

$$\alpha = \frac{s}{l} \left(\sqrt{3 + \left(\frac{s}{l}\right)^2} - \frac{s}{l} \right)$$

If the plate length is far greater than plate width, will the resistance be:

$$r_c = \frac{4f_y t^2}{s^2}$$

This is the same results as for the plastic resistance in bending for a plate strip with unit width.

12 IACS Rules for polar ship

The International Association of ship Classification Societies is in the process of issuing new unified rules for polar ships. These rules are based upon plastic analysis for plate, stiffeners and girders.

The IACS model for plate resistance is based on a yield line model for a plate subjected for patch loading. The yield lines are here located outside the patch load boundary. This is essentially the same as assuming the horizontal stiffener being located at the patch boundary and is non conservative. The non conservative is removed by introducing a simplification for collapse resistance.

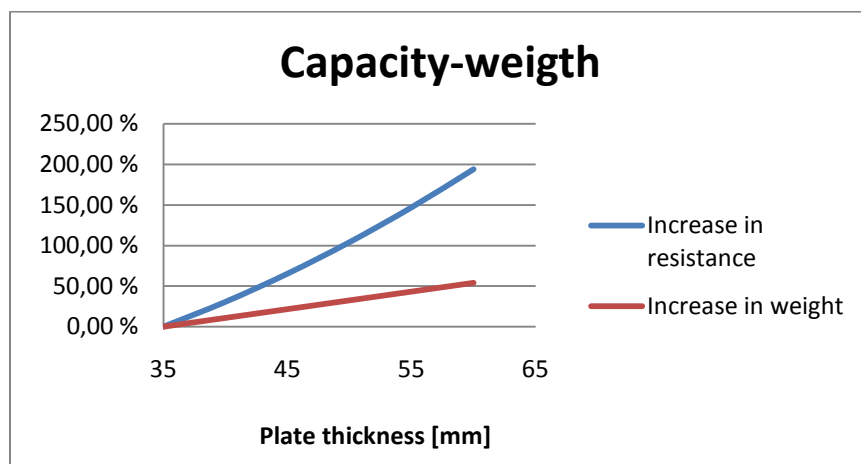
If the plate is loaded over the entire length is the resistance written as

$$r = \frac{4f_y t^2}{s^2} \left(1 + 0.5 \frac{s}{l} \right)^2$$

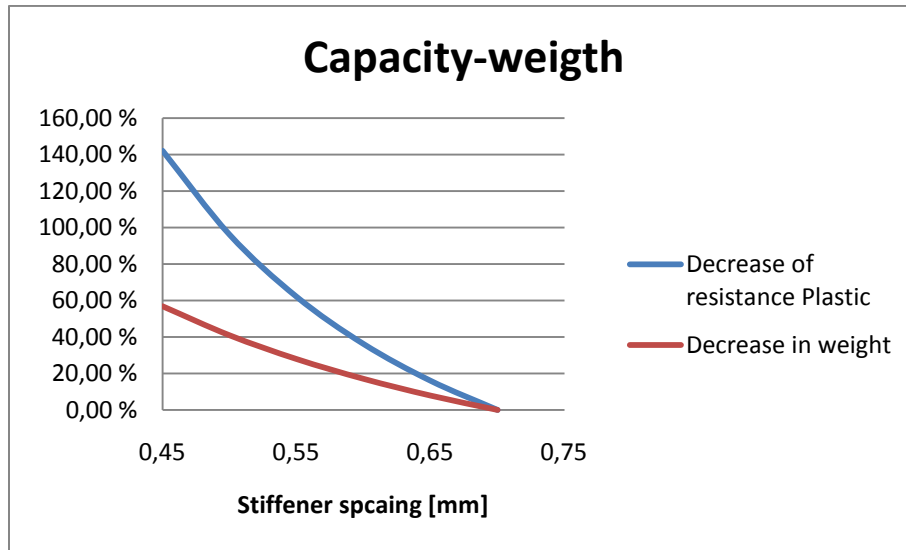
12.1 Comparing plastic resistance - weight

When selecting a structural configuration, several aspects are to be evaluated. Welding, steel weight, load capacity and access for painting/surveying. As stated earlier in the thesis, load capacity depends mainly on plate thickness and stiffener spacing. For a structure like Sevan FPU-ice both of these factors are essential due to the high load level. A plate with a thickness of 50 mm is relative for most steel cost a significant thick plate. An increase of plate thickness will lead to significant increase in cost, not only in increased steel but in welding, cutting and curvature bending. Welding a plate thickness of 50 mm requires advanced welding equipment and skilled personnel. A reduction in stiffener spacing makes access for inspections and painting and especially welding. The stiffener shape is a significant effect for stiffener with 600 mm spacing. A flat bar stiffener have for instance a lower bending moment capacity than a

For estimating the steel weight, several assumptions have been made. For simplification, only the conical icebreaking shaped is included in these estimations. The conical radius varies from 55.5 m at the top to 42.5 m in the bottom where the cylindrical shape starts. The conical section area is then of 6220 m². The assumption is that the increased number of stiffener at the conical top equals reduction in number of stiffener at the conical bottom. The stiffener calculation is therefore based on circumference of median radius of the conical part at 49.5 m. The steel weight is set to 7850 kg/m³. The stiffener profile used in the calculation is a flat bar with 600 mm web height.



12-1 Plate capacity-Weight



12-2

12.2 Welding cost

Figure 12-1 and 12-2 indicates how the steel weight and capacity increases and decreases in percent due to plate thickness and stiffener spacing. As mention previous, the decision of parameters is not only on steel weight but on production cost as well. Welding cost may contribute to a significant part of the production cost. A higher number of stiffener leads to a higher total length of welds. And an increase in plate thickness may lead to increased number of welding layers in the same joint and increased preparations before welding. The requirement welding quality is high for skin plates in the bow. Welding cost is one factor that needs to be investigated before deciding structural layout.

12.3 Strain level

The degree of plastic deformation or critical strain at fracture will show a significant scatter and depends upon factors as material toughness, presence of defects, strain rate and presence of strain concentrations. Simple plastic theory does not provide information on strains as such. Strains levels should therefore be assessed by means of adequate analytical models of strain distributions in plastic zoned or by non-linear finite element analysis with sufficiently detailed mesh in the plastic zones (Standards Norway, 2004)

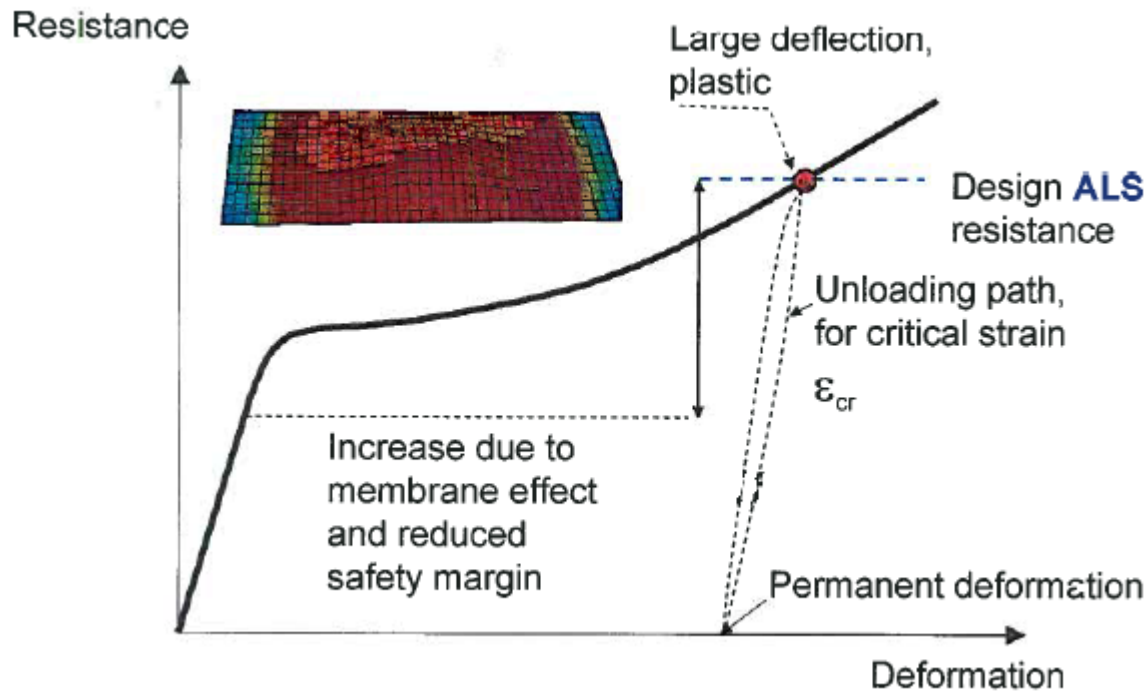


Figure 12-3, Resistance – deformation curve, (Amdahl P. j., 2003)

For structure that are designed so that yielding take place in the parent material, may the critical average strain in axially loaded plate material be used in conjunction with nonlinear finite element analysis or simple analysis:

$$\epsilon_{cr} = 0.02 + 0.65 \frac{t}{l}$$

Equation 12-1

Where t is plate thickness and l is the length of plastic zone (minimum $5t$). The allowable strain is then made independent on the mesh size /plate thickness ratio. However the maximum allowable strain is according to Norsok N004 15% for 355 steel.

NORSOK N004 proposed values for critical strain ϵ_{cr} with respect to different steel grades.

Steel grade	Critical strain	H
S 235	20%	0.0022
S 355	15%	0.0034
S 460	10%	0.0034

Table 12-1, Critical strain, Table A-3-4 (Standards Norway, 2004)

13 Collisions

Iceberg may cause a threat to all structures operating in arctic regions. Several different design philosophies may be applied depending on iceberg environment and the field conditions. On the Grand Banks, three oilfields have been developed with two different designs. The Hibernia used a gravity based structure (GBS) design for withstanding a one-million ton iceberg without damage. The Terra Nova and White Rose used a Floating Production and Storage Offloading (FPSO) design to shut down production and disconnect when a large iceberg threatens. The FPSO is only designed to withstand collisions with smaller icebergs. The FPSO solutions depend on iceberg surveillance and ice management systems.

Collision with iceberg and ice ridges is a scenario in ALIE study. Collision with iceberg can be analogous to ship collision. Collision with iceberg or ice ridges could cause reduction of structural strength and possible progressive structural failure. For a buoyant structure as the Sevan buoy can lead to flooding of one or several compartments, hence loss of buoyancy.

13.1 Design principles

With respect to distribution of strain energy dissipation there may be a distinction between

- Shared-energy design: Both structure and iceberg contribute to energy dissipation.
- Strength design: Structure is designed to withstand the collision with only minor deformations. The iceberg deforms instead and dissipates most of the energy.
- Ductility design: Structure suffers large plastic deformations and dissipates the most of the energy.

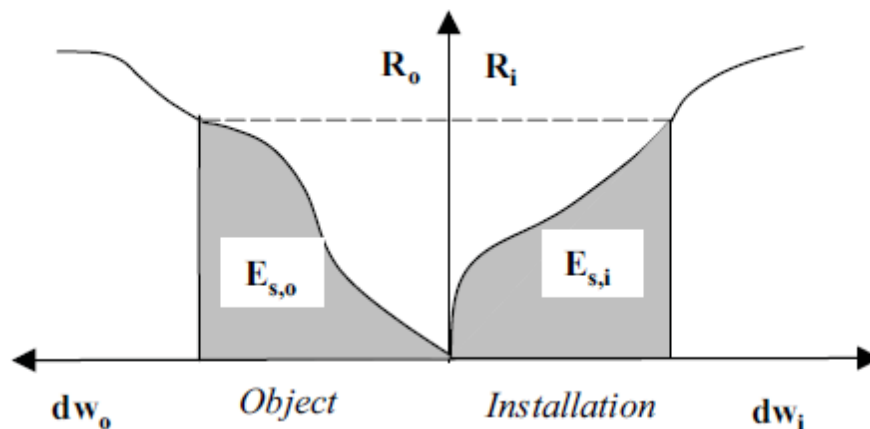


Figure 13-1, Impact design graph, Figure A.3-3 (Standards Norway, 2004)

In most cases ductility or shared-energy design is used. However, in the design of a FPSO for small iceberg strength design may be achievable due to the ice resistance reinforcement.

13.2 Analysis of collision

A fully integrated analysis is very demanding. It is therefore often found convenient to split the analysis into two uncoupled analyses.

13.2.1 Kinetic energy from iceberg

The kinetic energy of the colliding ice berg is calculated from

$$E_{kin} = \frac{1}{2}(m_1 + m_1^a)v_1^2$$

Equation 13-1

Where m_1 and m_1^a is respectively ice berg mass and iceberg added mass. v_1 is the speed of the ice berg.

Icebergs velocity and iceberg motion is a key issue with respect to the kinetic energy. Iceberg velocity should be calculated for extreme sea states related to the return period for ALIE.

13.2.2 Senario of collision

The SEVAN FPU-ICE is not design to encounter large iceberg. Their strategy is to use iceberg managed by towing iceberg in the extend possible. A typical iceberg size, capable to tow by offshore tugs is around 2-2.5 million tons. With a larger iceberg encountering, disconnecting of the buoy will be the action made.

The size and especially the speed of an iceberg will be a important factors.

13.2.3 Velocity and added mass

The impact velocity v_c is often taken as the sum of mead drift velocity and wave induced motion.

$$v_c = v_d + v_s$$

Where v_d is the drift velocity and v_s is the wave induced velocity. In the most severe load cases, wave induced storm surge motions of the iceberg will contribute in velocity. The surge velocity can according to Gus Cammaert in Maren Kristoffersen master thesis (Kristoffersen) for 1 000 and 10 000 tons iceberg reach a maximum velocity of around 5.3 ms^{-1} in a storm condition with a return period of 10^2 . Increased size of icebergs leads to decrease in the effect of wave induced surge forces, hence a lower kinetic energy.

McTaggart (Isaacson) have made a graph to determine added mass, where the added mass coefficient is made dimensionless with respect to displaced water. It is conservatively assumed that the wave drift forces are unaffected by the structure. With respect to the graph, an added mass coefficient in the order of 0.7 is conservative. The added mass for the structure is in the energy calculation below set to 40 % of

the total mass. Calculation with added mass coefficient of 0.7 may be considered as conservative

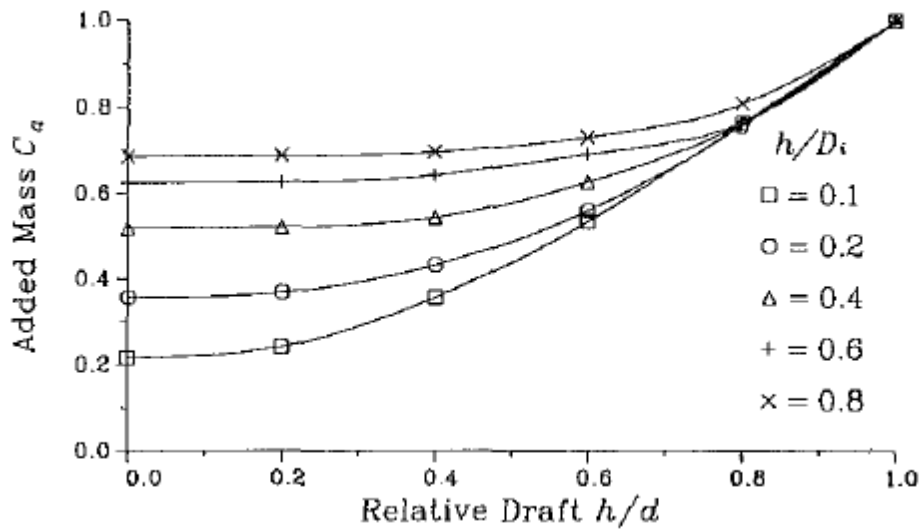


Figure 13-2, Added mass iceberg, Fig 3 (Isaacson)

13.2.4 Glancing

A scenario may be a collision where the iceberg glances the structure and continuing drifting after impact. The kinetic energy is then not entirely dissipated in the collision, hence a lower impact force.

13.2.5 Lateral collision

The worst case scenario is a central impact; the collision vector goes through the centre of gravity to the buoy. Using the principle of conservation of momentum the common velocity v_c of the buoy and iceberg at the end of impact period is

$$v_c = \frac{(m_1 + m_1^a)v_1}{(m_1 + m_1^a + m_2 + m_2^a)}$$

Equation 13-2

Where m_2 and m_2^a is respectively mass and added mass of the buoy.

The calculation is based on the assumption that the inertia forces predominate hydrodynamic and mooring resistance. And that the elastic strain energy in a magnitude is so small that it may be considered neglected. The energy dissipated as strain energy can be estimated by:

$$E_s = \frac{1}{2}(m_1 + m_1^a)v_1^2 \frac{1}{1 + \frac{m_1 + m_1^a}{m_2 + m_2^a}}$$

Equation 13-3

The equation 13-3 also shows that if the mass of the structure, is significant larger than the ice mass, the strain energy dissipated as strain energy equals the kinetic energy of the iceberg. The effect of velocity after impact is therefore valid for when the iceberg mass is in the vicinity of the structural mass. An impact of an iceberg with a mass near the structure contains such a large kinetic energy, that a design against impact is not realistic for a steel structure.

Iceberg	50	1 000,00	10 000,00	50 000,00	100 000,00	1 000 000,00	[tonn]
Iceberg density	0,9	0,90	0,90	0,90	0,90	0,90	[tonn/m ³]
Volume	55,56	1 111	11 111	55 556	111 111	1 111 111	[m ³]
Diameter	4,73	12,85	27,69	47,34	59,65	128,50	[m]
Mean drift velocity	0,30	0,30	0,30	0,30	0,30	0,30	[m/s]
Max surge velocity	5,30	5,30	5,30	6,30	4,50	2,00	[m/s]
Velocity	5,60	5,60	5,60	6,60	4,80	2,30	[m/s]
Added mass	0,70	0,70	0,70	0,70	0,70	0,70	[factor]
Effective mass	85,00	1 700,00	17 000,00	85 000,00	170 000,00	1 700 000,00	[ton]
Kinetic energy	1,33	26,66	266,56	1 851,30	1 958 400,00	4 496 500,00	[MJ]
Mass ratio	0,00	0,01	0,10	0,51	1,03	10,25	-
Strain energy	1,33	26,39	241,77	1 223,92	967 011,76	399 614,98	[MJ]

13-1, Iceberg calculations

13.3 Structure-ice collision model

A structure –ice collision model have been developed by Robert Brown (Daley, 1999). A simple model is made by assuming is normal force act through the centre of gravity of the structure and ice. The structure is considerably more massive than the ice in order of 10 times. The solution is made by equating kinetic energy and crushing energy.

The force is related to the pressure. The pressure area is assumed to be of the form of

$$P(A) = P_0 A^{ex}$$

Equation 13-4

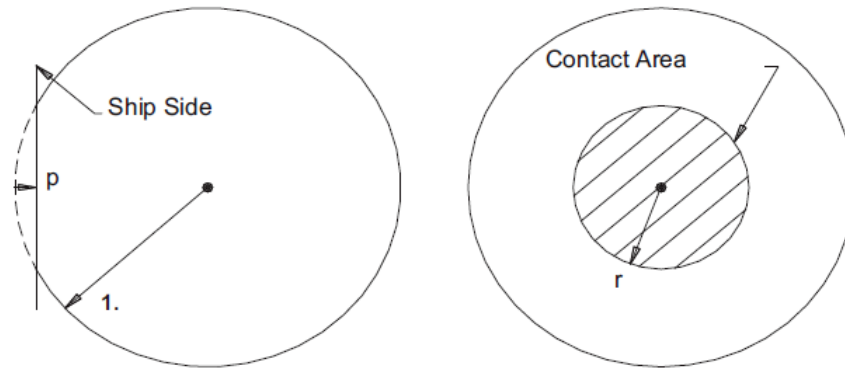


Figure 13-3, Shape of contact area, Figure 4 (Daley, 1999)

Where ex is the assumed area exponent, $P(A)$ is the average pressure over the contact area A and P_0 is the average pressure over 1 m^2 . The force is given as

$$F = PA \rightarrow F = P_0 A^{ex} A \rightarrow F = P_0 A^{(ex+1)}$$

Equation 13-5

The contact area of a sphere (iceberg) striking a flat plate plane would be circular with radius, the contact area would be:

$$A = \pi r^2$$

Equation 13-6

Using basic geometry, the value of r can be written:

$$r = \sqrt{2Rp - p^2} \rightarrow r^2 = 2Rp - p^2$$

Equation 13-7

$$A = \pi(2Rp - p^2)$$

Equation 13-8

R is the radius of the iceberg and p is the amount of penetration.

The crushing energy is

$$E_{crush} = \int F dp$$

Equation 13-9

$$E_{crush} = \frac{P_0}{(2 + ex)(2\pi R)^{(1+ex)} p^{(2+ex)}}$$

Equation 13-10

The kinetic energy is:

$$E_{kinetic} = \frac{1}{2}(M_e + A)V_n^2$$

Equation 13-11

By equation the kinetic energy and crushing energy and solve for p ,

$$p = \frac{P_0}{(2 + ex)(2\pi R)^{(1+ex)} V_n^{2+ex}}$$

Equation 13-12

By substituting equation 13-10 and equation 13-11 and collecting the terms given an expression of the force

$$F_n = P_0^{\frac{1}{2+ex}} [\pi(2 + ex)R M_e]^{mex} V_n^{2mex}$$

Equation 13-13

Where $mex = (1 + ex) / (2 + ex)$

A sensitivity analysis for the area exponent with values between 0 and -0.7 have been carried out with the result that small collisions show little dependence on the factor.

Iceberg Size	500	1 000.00	10 000.00	50 000.00	Tonn
Velocity	500.00	1 000.00	10 000.00	50 000.00	ms ⁻¹
Kinetic energy	13.33	26.66	266.56	979.2	MJ
Strain energy	13.28	26.46	248.378	716.76	MJ
Max force	141.46	195.61	574.00	1 093.34	MN
Max penetration	1.64	2.37	8.06	15.54	m
Area of impact	44.00	77.91	496.95	1 552.81	m ²
Max force/Area	3.22	2.51	1.16	0.70	MPa

13-2, Table of Structure-ice collision calculation

The calculations above, does not considering the steel resistance capacity in terms of different structural layouts. The calculation and the structure-ice collision may therefore be inaccurate.

13.4 Discussion

Iceberg may as stated earlier, be of many sizes and shapes. The establishment of the ALIE design load depends on iceberg size and impact velocity. The maximum impact speed depends on the sea condition.

These variables may vary from one location to another. K, Eik and T, Gudmestad (Gudmestad) wrote in a draft for the Cold Region Science and Technology, that a maximum impact load for corresponding to a 10 000 year event was 85 MJ for a concept without any iceberg management capabilities. An alternative system with iceberg detection and disconnection capabilities including disconnect correspond 1.8 MJ. A ALIE load of 1.8MJ is in my opinion a very small load.

A design check for ALIE may be performing by analyses the capacity of the structure by non linear finite element method. A load is transferred as pressure until a certain critical plastic strain. The work dissipated in plastic strain before fracture can be calculated. An important factor is that not all of the kinetic energy of the iceberg has to absorb as strain energy. A part of the kinetic energy is dissipated crushing of ice. An analysis where a model of iceberg impacting a structure may also be conducted.

14 Finite element method

The finite is a numerical method to approximate solutions of partial differential equations. The method is used to solve complex problems in structural mechanics. In the FEM method, the structural system is discretized into elements connected with nodes. Elements may have physical properties such as thickness, density, Young's module, shear modules and Poisson's ratio.

The finite element method is based on three principles.

- Equilibrium, express by stresses
- Kinematic compatibility, expressed by strains
- Stress-strain relations

In finite element methods analysis it is assumed that the response of the structure is elastic to the applied loads.

Elastic deformation implies that the structure will recover immediately after unloading. The stresses and strains are usually proportional, meaning that linear theory is applicable in accordance with Hooke's law.

$$\sigma = E\varepsilon$$

Equation 14-1

The theory about non linear finite elements method collected from Torgeir Moan book TMR4190 (Moan, Finite Element Modeling and Analysis of Marine Structures, 2003) and the ABAQUS theory manual (Simulia).

14.1 Shell elements

Most finite elements programs provide the user a wide range of choices as to the element types to be used. For a stiffened panel like the local model of SEVAN FPU-ice, general shell elements are most appropriate- Shell elements gives a combination of membrane and bending stresses in the element. Shell elements have a thickness requirement. The thickness should not be less than 1/10 of the element dimension. Solid elements may be a better choice for very thick plates to better capture the shear strain. However solid elements require significant higher resources in computer time.

Shell elements ABAQUS/Standard provides shell elements in three categories.

- General purpose
- Thin plate
- Thick plate

14.2 General purpose elements

The general purpose shell ABAQUS's element provides robust and accurate solutions in all loading conditions for thin and thick shell problems. Thickness change as a function of in plane deformations is allowed in their element formulation. These elements do not suffer from transverse shear locking, nor do they have any unconstrained hourglass mode. (Simulia)

14.3 Thin plate theory

Thin plate theory is based on the assumptions;

- the stress σ_z is negligible
- the deformation accords with Kirchhoff-Navier's hypothesis.

The Kirchhoff's theory implies no shear deformations in a plane normal to the plate plane, i.e. the transverse shear stresses $\gamma_{xz} = \gamma_{yz} = 0$

14.4 Thick plate theory

Thick plate theory is on linear theory and plane stress. The thick plate differs from thin plate by accounting for transverse shear deformations. Thick plate presents therefore a better approximation of the shear forces and corresponding forces which is important for thick plated. Thick plate elements only require C^0 -continuity to be conformed and are hence easier to formulate than elements based on Kirchhoff's theory.

Irregular meshes of S8R elements converge very poorly because of severe transverse shear locking; therefore, this element is recommended for use in regular mesh geometries for thick shell applications.

15 Non linear theory

When the stress reaches the yield stress the material behaves plastic. Once the plastic deformations begin, only a small increase in stress causes large deformations. At plastic deformations, linear theory is not longer valid; hence non linear theory has to be employed.

Non linear theory is then based on nonlinear stress-strain relationships due to nonlinear effects. These effects can be caused by:

- Geometry
- Material
- Boundary condition

15.1 Geometrical nonlinearity

Geometrical nonlinearity may be illustrated by a two bar system

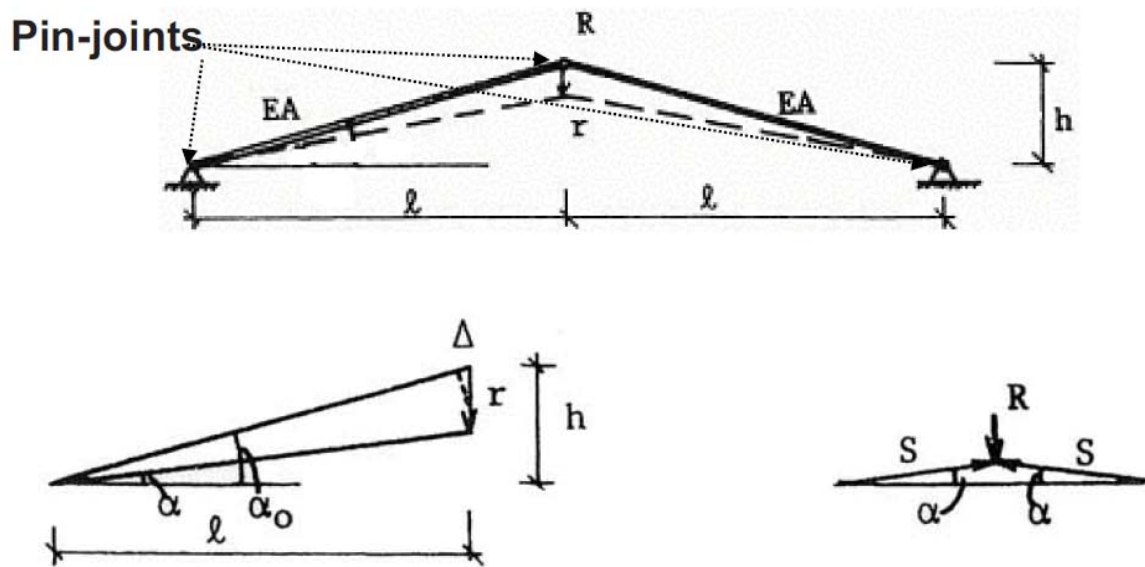


Figure 15-1, Deformations and displacement (Moan)

The strain ε is given as $\varepsilon = 1 - \frac{\cos \alpha_0}{\cos \alpha}$, hence the equilibrium can be written as

$$R = 2S \sin \alpha = 2EA \sin \alpha \left(1 - \frac{\cos \alpha_0}{\cos \alpha} \right)$$

Equation 15-1

Equation 15-1 may with some mathematic and geometric formulation be modify to

$$R = 2EA \left(\frac{h}{r} - 1 \right) \left(\frac{1}{\sqrt{l^2 + (h-r)^2}} \right) \left(\frac{1}{l^2 + h^2} \right) r$$

Equation 15-2

$$R = K(r)r$$

Equation 15-3

This shows that the stiffness is a function of the displacement, hence a nonlinear relationship between the force and displacement.

15.2 Non linear material

When the stress causes the material to deform plastic, the linear relationship from hooks law between stress and deformation is no longer valid. Plastic deformation can impair the utility of the structure by causing permanent deflections and residual stresses to remain after unloading.

The plasticity may be taken into account by defining a material curve model. The model is an elastic power-hardening relationship, where the stress is assumed to be proportional to strain to a power after reaching yield strength

$$\sigma = E\varepsilon, \quad (\sigma \leq \sigma_0)$$

$$\sigma = K\varepsilon^n \quad (\sigma \geq \sigma_0)$$

Equation 15-4

Ramberg-Osgood model is also a model used in nonlinear material problems. The model regards elastic and plastic strain separately before being summed.

$$\varepsilon = \frac{\sigma}{E} + \alpha \frac{\sigma_0}{E} \left(\frac{\sigma}{\sigma_0} \right)^n$$

Equation 15-5

Where α are material factor and n a hardening exponent for the plastic term.

15.3 Solution methods

The method to solve nonlinear can be solved by incremental, iterative or a combination of the two methods. These are often considered standard methods for Finite element programs. An alternative approach for solving non linearity is direct integration method. In this project thesis this approach will not be discussed.

15.3.1 Incremental method, Euler-Cauchy

Euler-Cauchy provides a solution of the non linear problem by a stepwise application of external loading. For each step the displacement increment, Δr is determined by $K(r)dr = dR$. The total displacement is obtained by adding displacement increments.

$$\Delta R_{m+1} = R_{m+1} - R_m$$

$$\Delta r_{m+1} = K(r_m)^{-1} \Delta R_{m+1}$$

$$r_{m+1} = r_m + \Delta r_{m+1}$$

Equation 15-6

Initial condition $r_0 = 0$

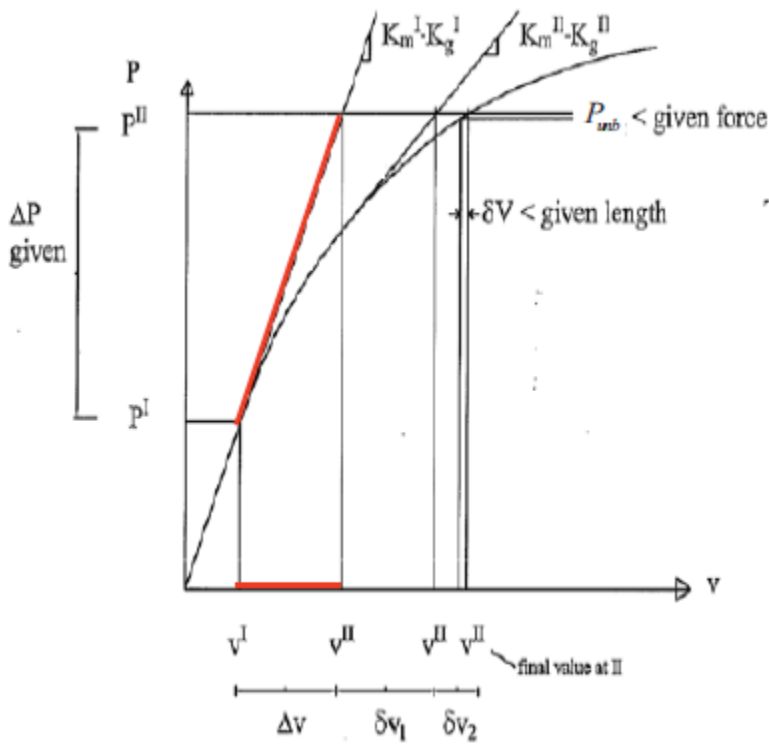


Figure 15-2, Incremental, Euler-Cauchy (Moan)

15.3.2 Newton-Raphson method

Newton-Raphson is the most frequently used iterative method for solving non-linear structural problems

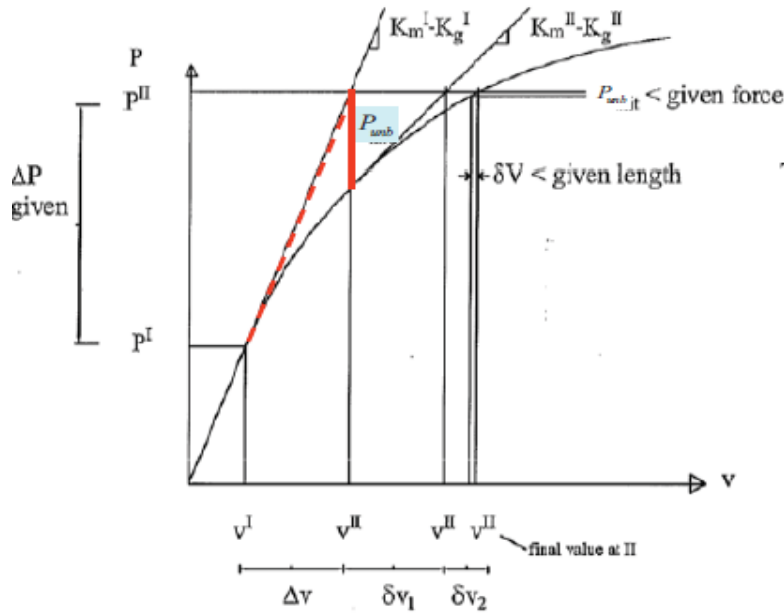


Figure 15-3, Newton Raphson (Moan)

$$r_{n+1} - r_n = \Delta r_{n+1} = K_I^{-1}(r_n)(R - R_{int})$$

Equation 15-7

This method requires that that K_I is established and that Δr_{n+1} is solved from $R - R_{int} = K_{I(n)} \Delta r_{n+1}$ in each iterative step. Updating the K_I for each step is time-consuming, the modified Newton-Raphson method is a method that updates the K_I less frequently, hence reduce the computation time.

15.4 Combined methods

Combined methods of incremental and iterative are most commonly applied in non linear analysis. The external load is applied in increments and in then in equilibrium is achieved by iteration in each increment. Load incremental methods experience difficulties when the tangent stiffness becomes zero(limiting point). A solutions used, is to use increment of displacement.

15.4.1 Arc-length method

Arc length method is a technique to pass the limiting point. In the Arc length method, the load factor at each iteration is modified so that the solutions follow an indentified patch until convergence is reached. The Arc-length method introduces an extra variable, involving both the displacement and load. The increment in the load displacement space is described by a displacements vector Δr and an increment parameter, such that $\Delta R = \Delta \lambda R_{ref}$. The Arc-length method will have some problem with convergence near failure point. This can be solved by reduced increments. The advantages of the Arc length method is that the method describes the behavior after reaching limiting point or bifurcation point

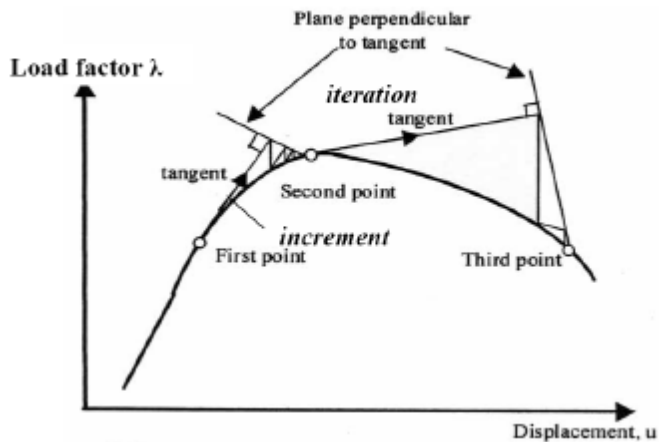


Figure 15-4, Arc length method (Moan)

15.5 Direct integration methods

The procedure discussed is method for directly solving the nonlinear equations based on an incrementation and iterations of loads or displacement. These methods are considered as standards methods in ABAQUS.

An alternative approach is to use so-called finite difference methods for direct integration of the dynamic equation of motion to solve the static problem. Nonlinear structural effects makes K a function of r , $K(r)$ and the load R is increased artificially or a function of time. A finite method difference are explicit if the displacements at a new time step $t + \Delta t$, can be obtained by the displacement, velocities and accelerations of previous time step.

$$M\dot{r}(t) + C\dot{r}(t) + Kr(t) = R(t)$$

15-8

15.5.1 ABAQUS/Explicit

The explicit dynamic analysis procedure in ABAQUS is based upon the implementation of an explicit central integration rule together with use of diagonal or lumped element mass matrices. The equations of motion for the body are integrated using the explicit central difference integration rule

$$\dot{u}^{(i+\frac{1}{2})} = \dot{u}^{(i-\frac{1}{2})} + \frac{\Delta t^{(i+1)} + \Delta t^{(i)}}{2} \ddot{u}^{(i)}$$

$$u^{(i+1)} = u^{(i)} + \Delta t^{(i+1)} \dot{u}^{(i+\frac{1}{2})}$$

15-9

Where \dot{u} is velocity and \ddot{u} is acceleration. The superscript $^{(i)}$ refers to the increment number. The central difference integration operator is explicit in that the kinematic state can be advanced using known

values of values of $\dot{u}^{(i-\frac{1}{2})}$ and $\ddot{u}^{(i)}$ from the previous increment. The explicit integration rule is quite simple but does not provide the c

The computational efficiency of the explicit procedure is high compared to implicit because the use of diagonal element mass matrices because the inversion of the mass matrix that is used in the computation for the accelerations at the beginning of the increment is triaxial

$$u^{(i)} = M^{-1} \cdot (F^{(i)} - I^{(i)})$$

Where M is the diagonal lumped mass matrix, F is the applied load vector, and I is the internal force vector. The explicit procedure requires no iterations and no tangent stiffness matrix.

The central difference operator is not self-starting because the value of the mean velocity $\dot{u}^{(-\frac{1}{2})}$ need to be defined.

An explicit analysis is often used for impact analyses where two models interact with each other.

15.6 Numerical integration

Number of integration points strongly effects on the computational time, and methods that give highest exactness for a certain number of points are preferred

The ABAQUS provides two methods of calculating the cross-sectional behavior of a shell, Simpson's rule and Gauss quadrature. The user can specify the number of section points through the thickness of each layer and the integration method as described below. The default integration method is Simpson's rule with five points for a homogeneous section and Simpson's rule with three points in each layer for a composite section.

The three-point Simpson's rule and the two-point Gauss quadrature are exact for linear problems. The default number of section points should be sufficient for nonlinear applications (such as predicting the response of an elastic-plastic shell up to limit load). For more severe thermal shock cases or for more complex nonlinear calculations involving strain reversals, more section points may be required; normally no more than nine section points (using Simpson's rule) are required. Gaussian integration normally requires no more than five section points.

Gauss quadrature provides greater accuracy than Simpson's rule when the same number of section points is used. Therefore, to obtain comparable levels of accuracy, Gauss quadrature requires fewer section points than Simpson's rule does and, thus, requires less computational time and storage space.

15.6.1 Full integration

Full integration is a quadrature rule adequate to present integrals of all terms in the element stiffness matrix if the element is not distorted.

15.6.2 Reduced integration

Reduced integration may be applied shell element in ABAQUS. A reduced integration uses a (lower-order) integration to form the element stiffness. The mass matrix and distributed loadings are still

integrated exactly. Reduced integration usually provides more accurate results with element that are not distorted or loaded in in-plane bending. Reduced integration has also the advantage of significantly reduces computational running time, especially in three dimensions.

When applying reduced integration with first-order linear elements like the S4R, hourglass control is required. ABAQUS provides automatically hourglass control. The second-order reduced-integration elements like S8R generally do not have the same difficulty and are recommended in cases when the solution is expected to be smooth. First-order elements are recommended when large strains or very high strain gradients are expected.

15.7 Imperfections

Derivations from ideal geometrical form of a structural element are categorized as geometric imperfection. From their effect on structural behavior, the geometric imperfections are divided into two classes;

- Variations in cross-sectional data
- Out of straightness

As far as structural strength is concerned the ultimate load is relatively little influence by normal derivations in cross-sections. The out of straightness is far more important for ultimate strength.

The response of some structures depends strongly on the imperfections in the original geometry. Particularly if the buckling modes interact after buckling occurs. A model in a Finite Element Program will initially be by perfect geometry. There is therefore in interest of introduce geometric imperfection.

A geometric imperfection is generally introduced in a model for a post buckling load-displacement analysis. Imperfections in a Finite elements program are usually introduced be perturbations in the geometry. ABAQUS for instance offers three ways to define an imperfection.

- A linear superposition of buckling Eigen modes.
- From the displacements of a static analysis.
- Specifying the node number and imperfections values directly.

The finite element program will algorithm based on perturbed coordinates.

15.8 Fracture

Usually the equivalent plastic strain has formed the foundation for evaluating fracture in metal structures. Structures subjected to analysis are with large mesh caused computing time. Fracture problems are on the other hand very local and will therefore require some failure criterion implemented in Finite element code to obtain reliable results. There are many fractures models. The models can generally be divided into four groups:

- Empirical models
- Void growth models
- Continuum damage mechanics
- Porosity based material models

The different models give each failure criteria for different loading. A combination of several functions may therefore be utilized to give a good prediction.

15.9 Implementing in fracture FEM

There are several ways to implement fracture in Finite Element Method programs. The failure criterion has to establish before running analysis.

15.10 Ductile fracture

Ductile fracture criteria is a criteria used in finite element software. Ductile fracture consists of both stress and strain state. Empirically these criteria expressed as

$$D_{cr} = \int_{\varepsilon_{eq}^{th}}^{\varepsilon_{eq}^f} f \left(\frac{\sigma_H}{\sigma_{eq}} \right) d\varepsilon_{eq}$$

Equation 15-10

Where:

ε_{eq}^{th} = threshold strain

ε_{eq}^f = Effective fracture strain

$\frac{\sigma_H}{\sigma_{eq}}$ = Hydrostatic stress-equivalent stress ratio, called triaxiality

The damage starts when the threshold strain is reached. After accumulating damage up to the critical value D_{cr} fracture occurs.

These are some methods to simulate fracture when a failure criterion is reached.

- Remeshing – A new mesh is built around the propagating crack front
- Stress/ stiffness reduction – The stress or stiffness is removed over several steps when the element has reached the failure criteria
- Node release – Every adjacent element have completely independent nodes and are constrained to move together. When a critical value of fracture is reached, the constraints are removed
- Element kill operation – When an element has reached the critical value of the failure criteria, the whole element is removed

ABAQUS have build in element deletion where the element is no longer capable to carry stress. The element stiffness is then equal to zero. A common fracture parameter in commercial finite element

software is equivalent plastic strain ε_{cr} . When an element has exceeded the critical strain value, the element is either removed or elements ties are released in order to simulate fracture.

16 Modell

The model is made be structural drawings and input from Sevan.

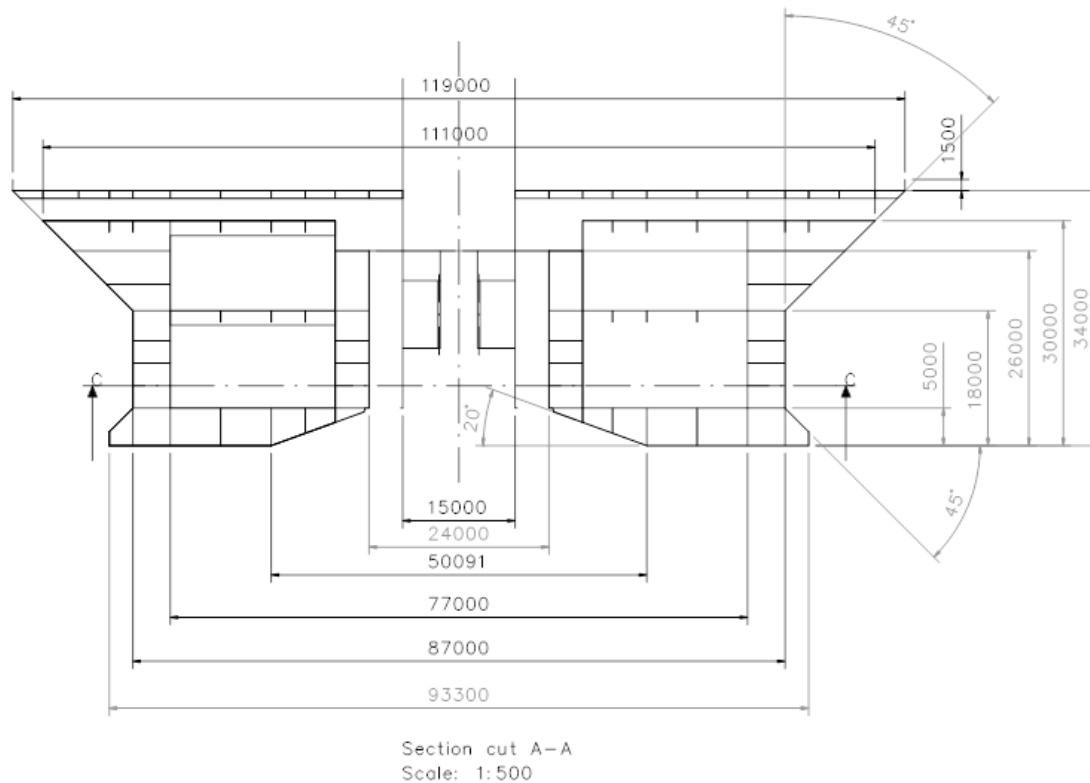


Figure 16-1, Cross section cut

The plate radius of the model is set to be 51.5 m, which is the ice draft waterline radius. For modeling simplifications, the radius was hold constant. The conical section is therefore as cylindrical sections. The important factor is the stiffener distance. This is considered to be constant, and therefore the number of stiffener increases as the radius increase. The model is an outcut in the middle between the vertical stringers. The first analysis for ultimate strength showed resulting in large displacement for (buckling) for the deck. In the ultimate strength analysis, the deck thickness is increased to 30 mm to avoid numerical problems due to the excessive stresses in the deck.

16.1 Modell 1

- Plate thickness 50 mm
- Stiffener flat bar 600 mm x 30 mm
- Stiffener spacing 600 mm
- Ring girder 3000 mm x 40 mm 400 mm x 40 mm flens

- Yield strength 355 MPa

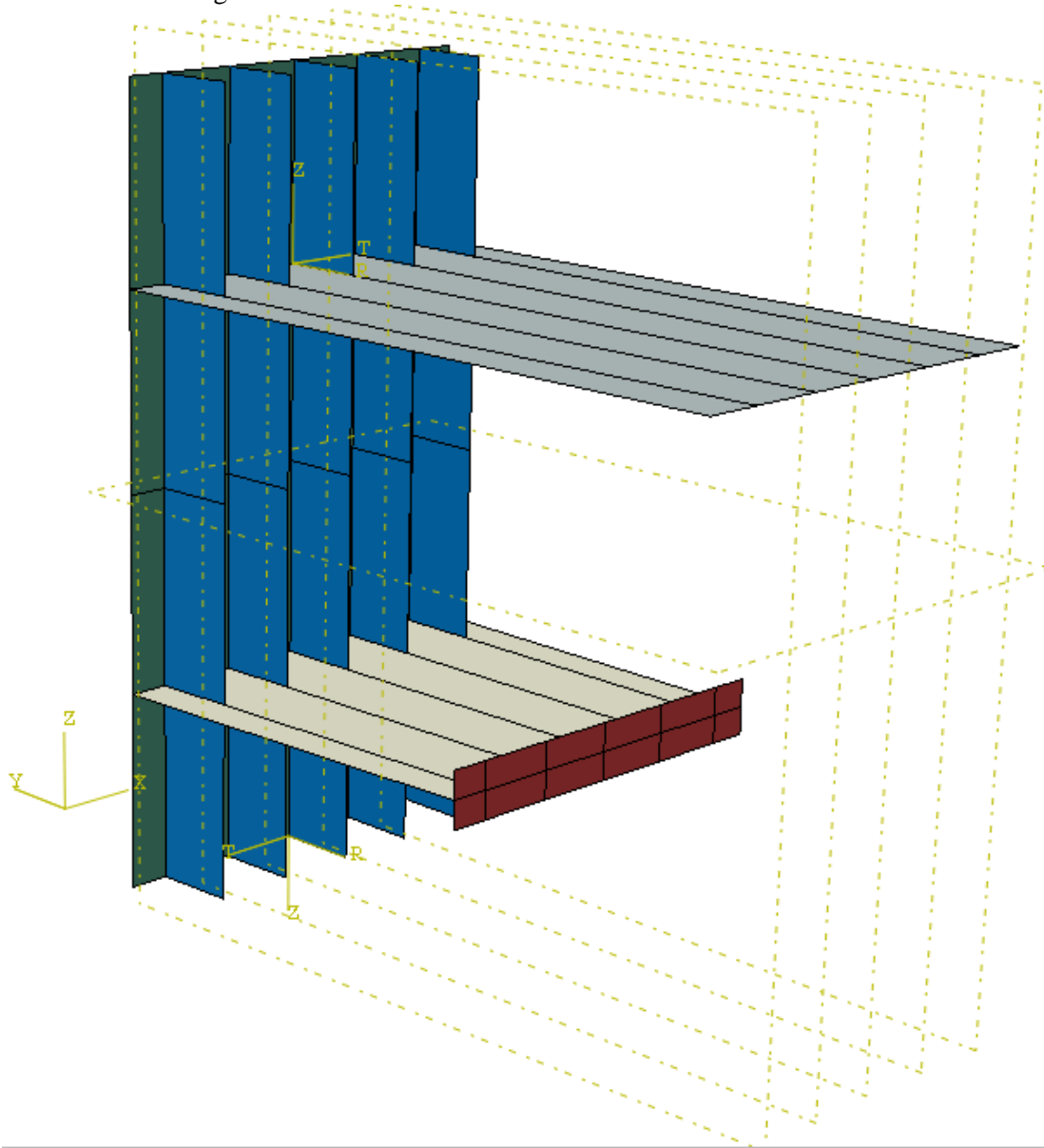


Figure 16-2, Finite Element model 1

16.2 Various models

The first structural layout input from Sevan present in autumn 2009 was a plate thickness of 50 mm and stiffener spacing at 0.6m. The stiffener arrangement was however different from the layout given in January. The stiffener presented was a 750 mm high T-bar. The variance in the models is therefore in different stiffener layout. As the first model was analyzed, the first yield stresses in the stiffener were caused by bending moment at the stiffener midpoint. Six different models of stiffener profile is made and analyzed.

Model	Stiffener height[mm]	Stiffener type	Flange[mm]	α factor
1	600x30	Flat	0	1.59
2	500x30	T-bar	100x30	1.96
3	550x30	L-bar	50x30	2.11
4	500x30	L-bar	100x30	1.96
5	600x30	L-bar	50x30	2.05
6	600x30	T-bar	100x30	2.05

Table 16-1

The shape factor refers to chapter 11.2 and is an indicator of plastic strength after first yield stress.

16.3 Material

The material used in the analysis is type EH 36 Carbon steel with excess yield strength of 355 MPa. The steel properties include strain hardening. The Young modulus is set to 204 00 MPa. The same material properties are used as found in a Marintek report. (F.Klæbo, 2006)

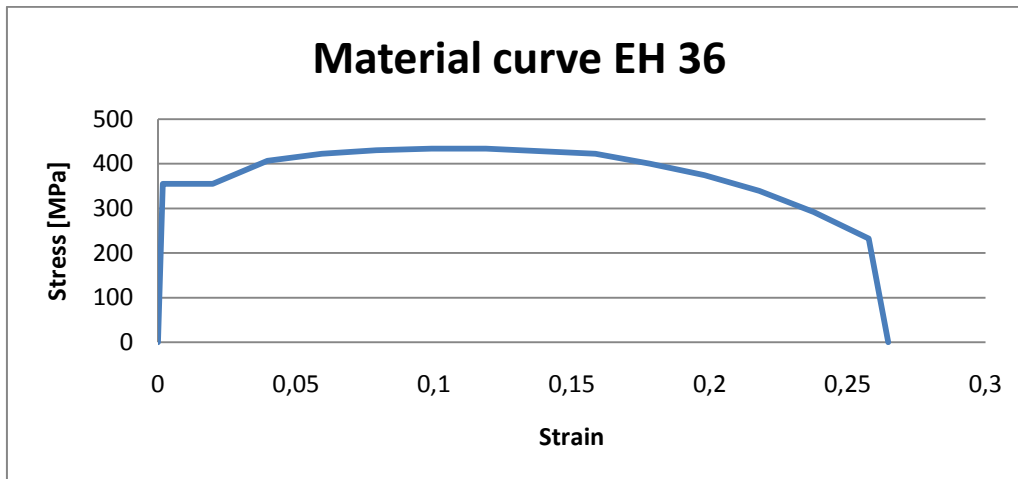


Figure 16-3, Material curve EH 36 steel

17 ABAQUS Analysis

The analysis is run by ABAQUS 6.9-2. The focus is made on several load cases to ensure the classification requirement but also to find the ultimate capacity before collapse.

17.1 Abaqus parameters

17.1.1 Step

A general static step is applied to loads by increment. In the general step, the method of solving the equation and solutions technique is chosen. The method of solving is set to direct and the solutions technique is full Newton. ABAQUS reduced automatically the increment size and use an adequate number of iteration to obtain convergence. The increment size is set to 0.1 and with a minimum of 1.0^{-8} .

17.1.2 Elements applied

The elements applied for analysis is rectangular shell elements. Quadratic elements are mainly more cost efficient than triangular elements. Triangular elements are used for structure with complex geometry to avoid badly distorted elements which leads to inaccurate results. To avoid badly distorted elements in the model, a partition using datum sys have been applied on the ring stiffener and deck. The distorted elements are on the parts where the accuracy is not important due to low stresses, however a distorted mesh will increase CPU time due to convergence rates are slower.

ABAQUS provide two elements for rectangular shell elements, S4 and S8. These elements provide robust and accurate solutions in all loading conditions for thick and thin shell problems. S4 is used for thin shell and S8 for thick shell.

17.1.3 S4R

The S4R is a 4-node, quadrilateral stress/displacement shell element, with reduced integration with five d.o.f in each node. The membrane kinematics of S4 is based on an assumed-strain formulation that provides accurate solutions for in-plane bending behavior. S4R are recommended by the ABAQUS Analysis Users Manual for when large strains or very high strain gradients are expected.

17.1.4 SR8

The S8R is an 8-node, quadrilateral stress/displacement shell element, with reduced integration with five d.o.f in each node. In the model, the S8R elements have been applied to the stiffener due to the shear forces. Shell behavior of shear stresses can be described with shear flexible shell theory and analyzed accurately with second order thick shell elements like S8R. Irregular mesh of S8R elements converge very poorly because of severe transverse shear locking in distorted elements.

17.1.5 Mesh

When using finite element programs it is always important to have in mind that the result are numerical values that may not be correct due to boundary conditions, modeling errors and material properties. A finer mesh will generally give better results. Lower order elements require more elements to represent a curved surface. Higher order elements and finer mesh will on the other hand require higher resources on disks place, memory and CPU.

A convergence test is a way to check the mesh. The test may be done on displacement or stresses. Stresses generally converge more slowly, so it may not be sufficient to only examine the displacement convergence. The convergence test was executed by onset of a load of 10 MPa over a two plate field. Mesh sizes varies between 100 mm to 20 mm and a load displacement curve.

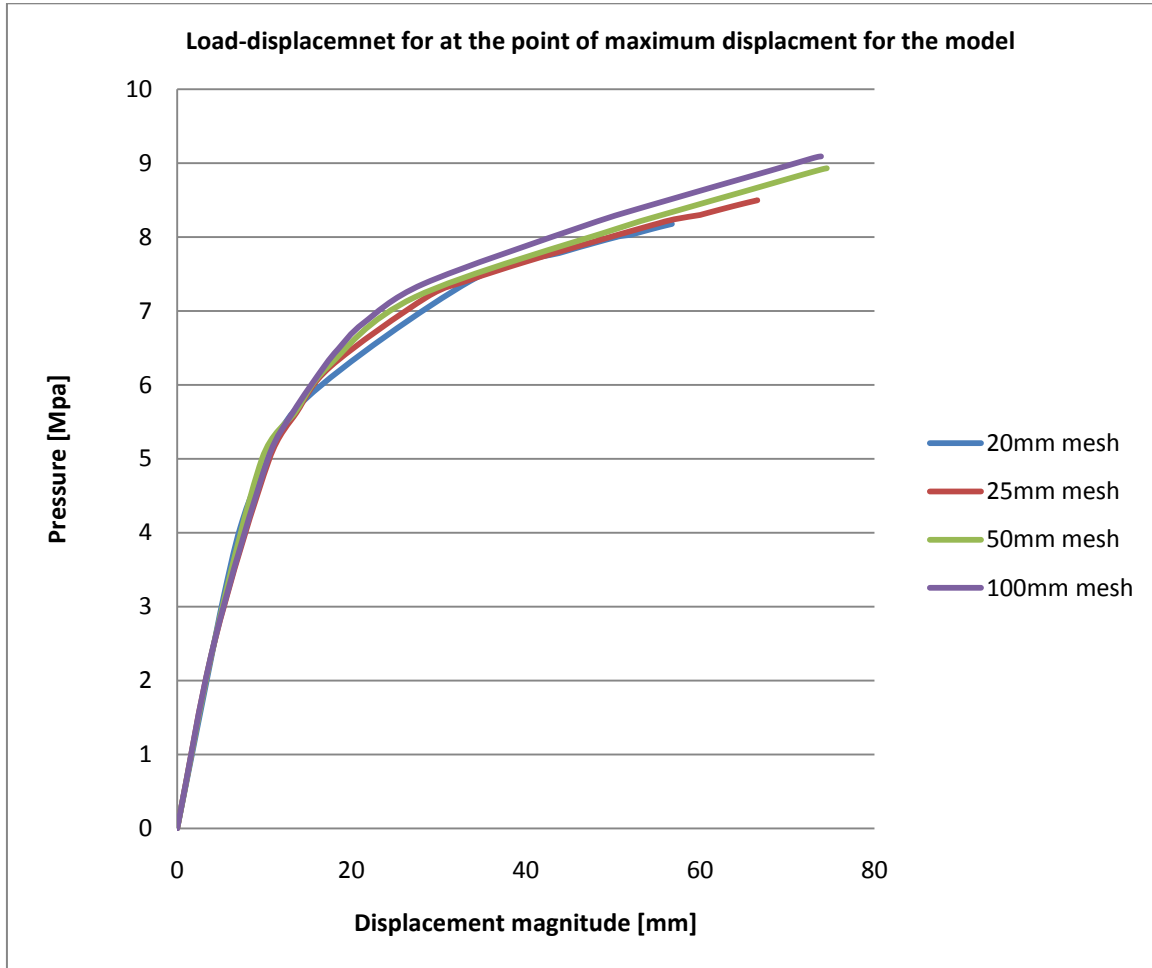


Figure 17-1, Load-Displacement curve, Converges test

As seen in figure 17-1 there is quite a difference in the capacity when using 100 mm and 20 mm elements size. The analysis is stop on 8.17 MPa for a 20 mm element mesh and at a 9.092 MPa for a 100 mm element mesh. The difference in accuracy between 25 and 20 mm element mesh is as expected, very small. The mesh size should also be determined with respect of structural dimension. In the model where the stiffener has a flange of 100 mm, and a stiffener height of 500 mm, an element size of 25mm would be the most appropriate. A mesh size of 25 mm results in 103138 elements.

17.2 S8R

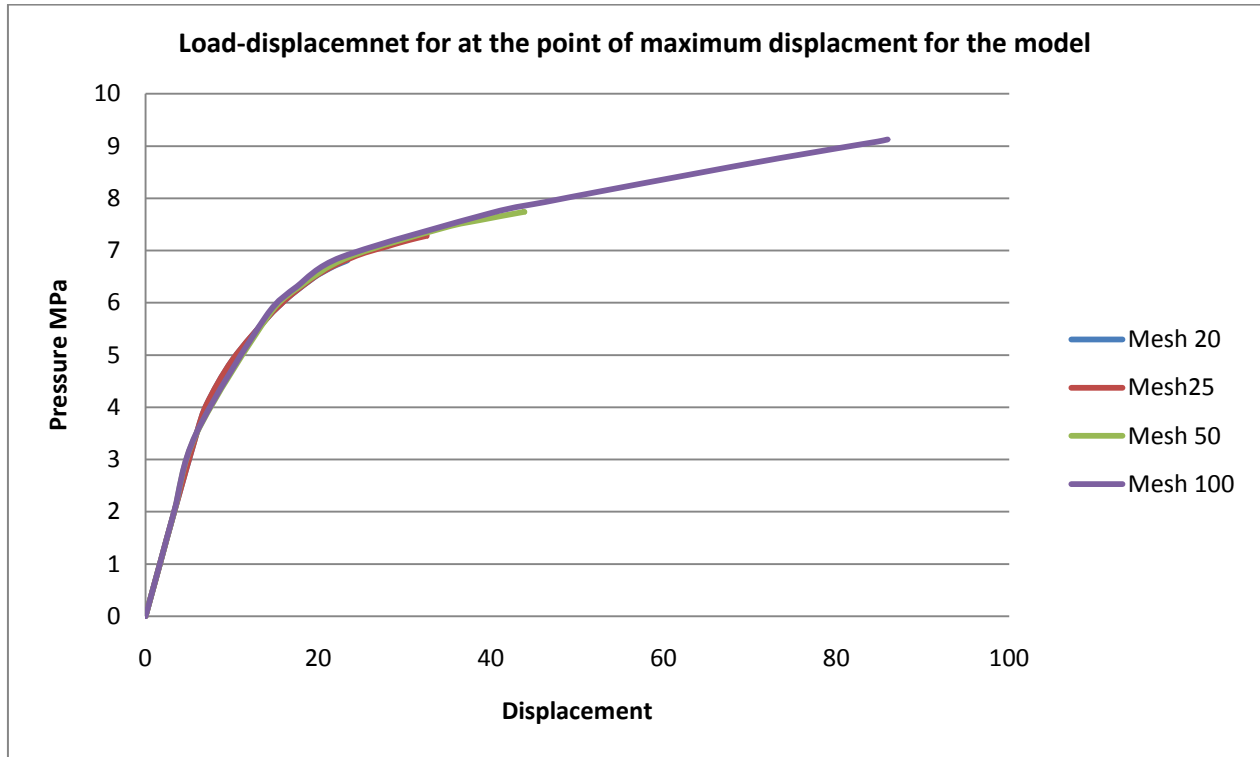


Figure 17-2, Load-Displacement curve, Converges test S8R

The convergence test for the SR8 convergence shows a good convergence. The ABAQUS manual recommend use of S4R elements for analysis with large stain.

17.2.1 Boundary conditions

Boundary conditions of local structural parts are essential to get an accurate result. The effects of the surrounding structure can be simulated by using approximate displacement and for boundary conditions. The most accurate solutions for boundary conditions will be to model Use of symmetry is often used if the structure and loading are symmetrical about the plane.

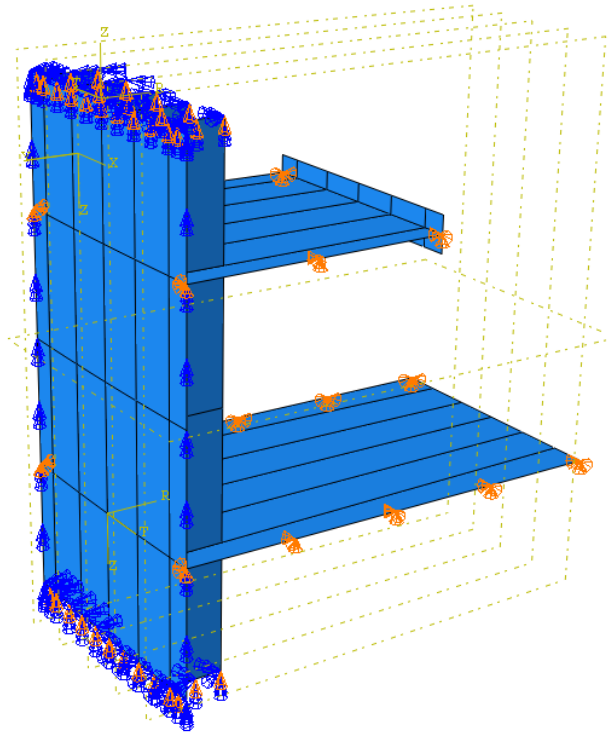


Figure 17-3, Boundary conditions

The boundary conditions in this made using a cylindrical datum system where R is radial direction; T is tangential direction and Z vertical direction. For boundary conditions, these are referred to respectively as U1, U2 and U3. The rotation degree of freedom is U4, U5 and U6.

The main concern for the boundary condition is how the pressure forces are dissipated. The forces from the load will go from: Plate → Stiffener → Ring stiffener/Deck. The Ring stiffener and Deck is therefore restrained from translation in U1, U2, and U3.

On the horizontal plane at the top and bottom, Stiffener and plate edge is constrained from U3, U4, U5 and U6. Plates are along the vertical plane constrained against rotation along the vertical axis i.e. U6.

Analysis and design of the Sevan FPSO against abnormal ice actions

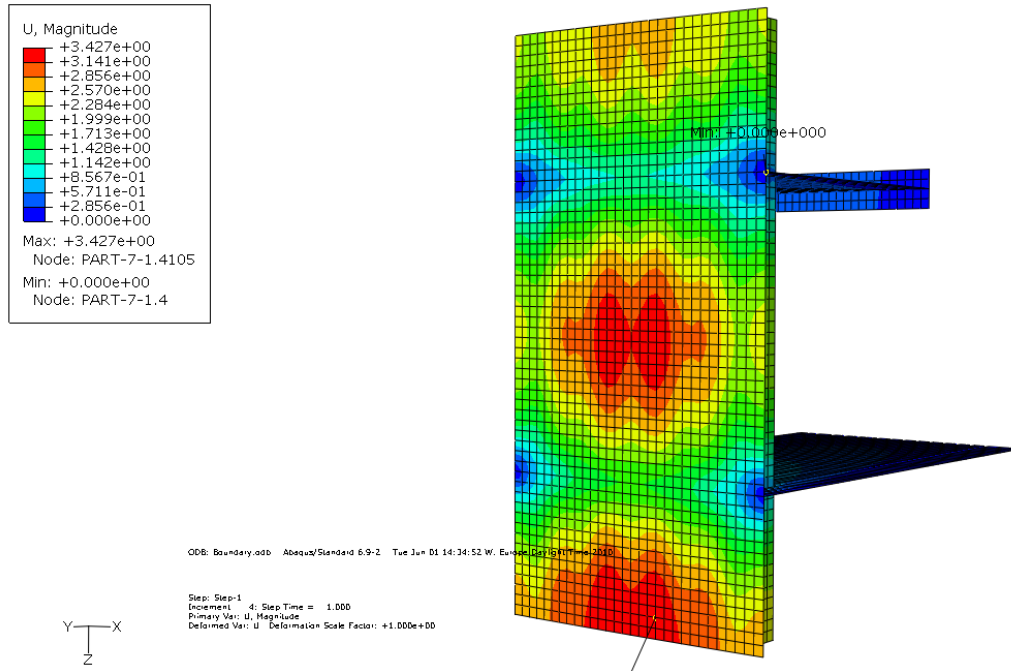


Figure 17-4, Displacement of model

Figure 17-3 shows the magnitude of displacement when loaded with a 2 MPa pressure load on the whole surface. As the figure shows, there is a false stiffness where the ring stiffener and deck. The stiffness of the ring stiffener is higher due to increased thickness, hence a larger false stiffness. The displacement will therefore not be symmetric. The model will therefore have a higher accuracy in the middle of the model.

Another and probably better boundary condition for the ring stiffener and deck would be to have springs connected to ground. The ridged body translation is assumed to uniform dissipated over the length of the ring stiffener and deck. Several attempts have been made without any results.

The same boundary conditions are used on the all of the models.

When reducing the mesh size, the reaction forces at where the plate is constrained in the ring stiffener and deck will increase significant.

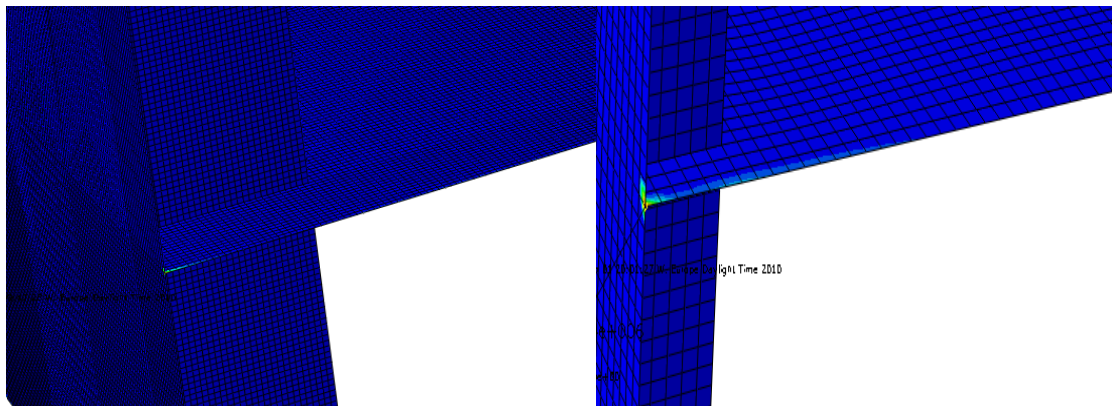


Figure 17-5, Different in horizontal force

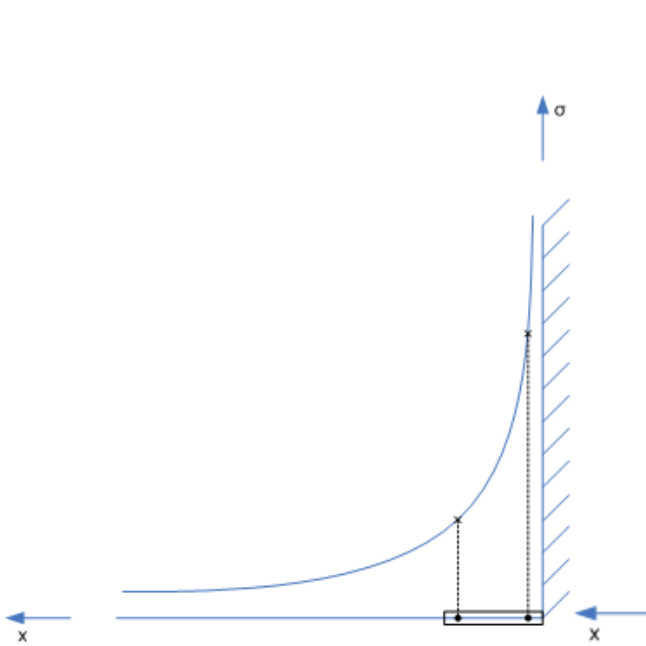


Figure 17-6, Stress small element

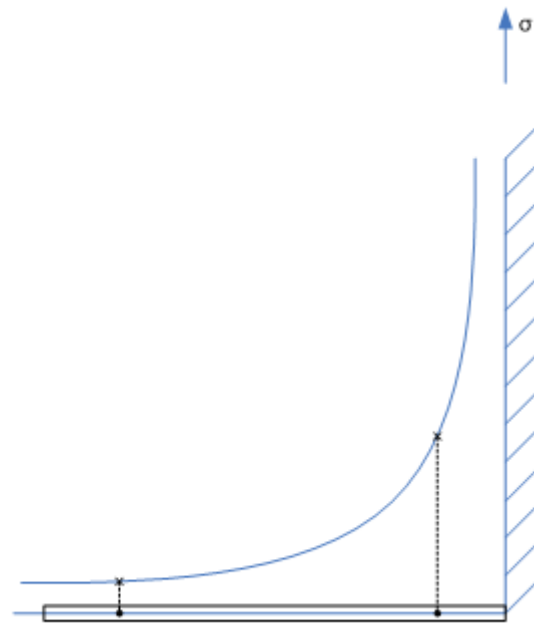


Figure 17-7, Stress large elements

17.3 Load conditions

Ice loading is not the easiest to apply on a structure. Ice is a material that does not generally fail simultaneously at one single pressure. As state in chapter 8.1, studies made on pressure panels show that a force may reach 4 MN, resulting in pressure gradients at 40 MPa. However the pressure consists over a very small area. Numerical ice load situations may occur and typically the load will have high intensity in a limited area and decreasing intensity with increasing contact area.

17.3.1.1 Load case 1

ISO 19906 Massive ice pressure ELIE found in chapter 8.1.

5.11 MPa over a plate

Analysis and design of the Sevan FPSO against abnormal ice actions

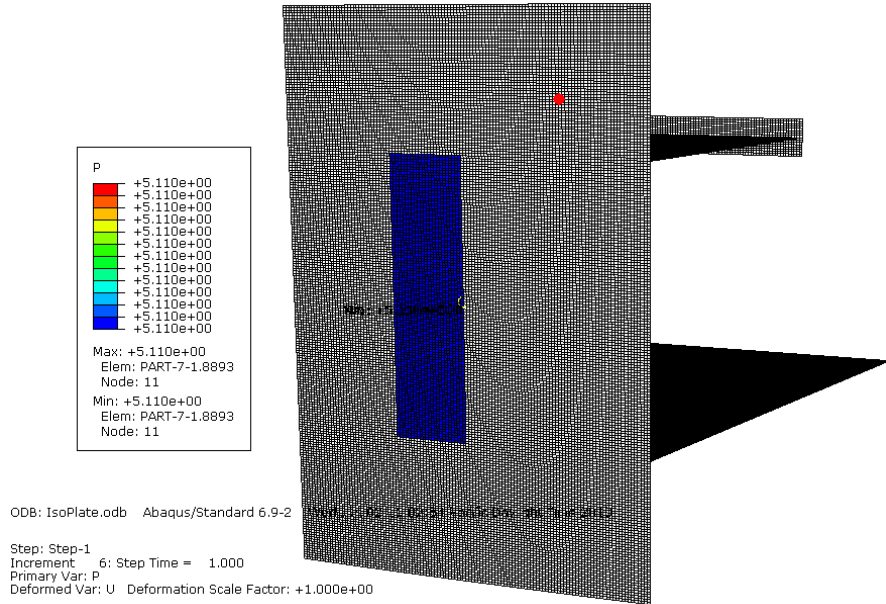


Figure 17-8, Pressure load ISO plate

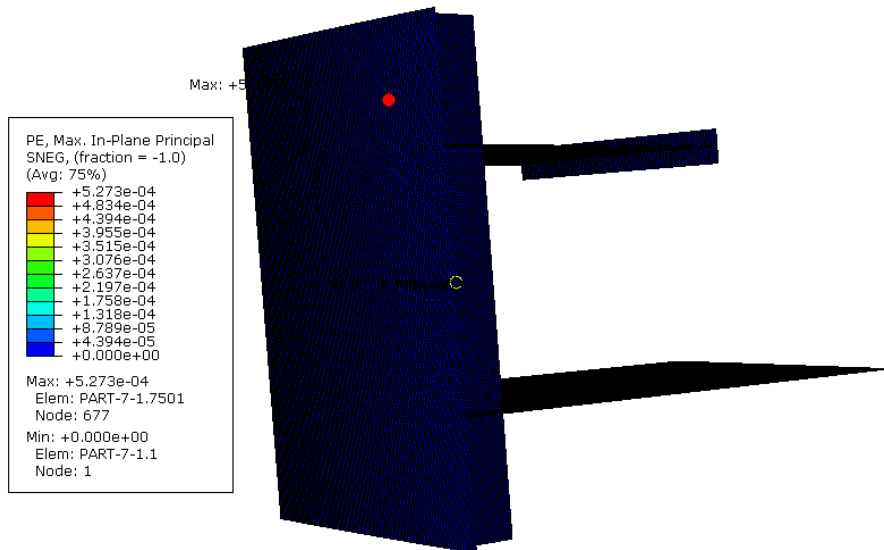


Figure 17-9, Plastic strain

The result of the analysis is the maximum Von Mises Stress (343MPa) occurred at the midpoint of the stiffener. No plastic strain occurred.

17.3.1.2 Load case 2 ISO 19906 Massive ice pressure ELIE Stiffener

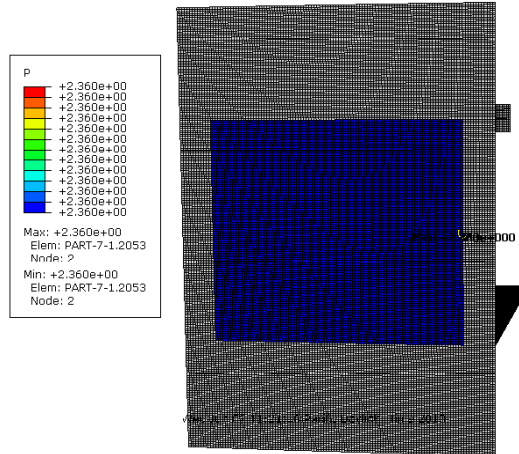


Figure 17-10, Pressure load ISO stiffener

For stiffener design, the loading width is set to be four times the stiffener spacing. The load height for stiffeners design area is not clear stated. An estimation of the figure may be 0.8 of the plate length. This gives a loading area of 5.43m^2 . With ice thickness of 3 m, and pressure is taken from massive ice feature estimates a pressure load of 2.26 MPa For the stiffener test, 100% of the plate height is use.

The result of the analysis is the maximum Von Mises Stress (315MPa) occurred at the midpoint of the stiffener. No plastic strain occurred.

17.3.2 Load case 3

As mention in chapter 8.3, the ELIE load for a plate is the whole plate.

Loading of a plate may vary. Studies have showed that peak loads of 40 MPa have been observer for a very small area. Patch loading may be applied with different load intensities. As the area, increase the pressure loads decrease. One way to ensure that the entire curve is covered is to divide the loading area in several pressure zones with different intensity. For the high intensity field, the load area is set by quadratic areas using the stiffener spacing as dimension. Pressure is then:

$$P^{high} = 7.4(A^{high})^{-0.7}$$

Equation 17-1

Where $A^{high} = 0.6 \cdot 0.6 = 0,36\text{m}^2$

The medium intensity field is a set to be

$$A^{medium} = (0.6 \cdot (2.828 - 0.6)) + A^{high} = 1.7\text{m}^2$$

Equation 17-2

Pressure for the medium intensity is then

$$P^{medium} = 7.4(A^{medium})^{-0.7}$$

Equation 17-3

17-4

The low intensity filed is using

$$A^{low} = (2 \cdot 0.6 \cdot 2.828) + A^{medium}$$

Equation 17-5

Pressure for the low area can then be written as

$$P^{low} = 7.4(A^{low})^{-0.7}$$

Equation 17-6

Pressure zone	Area [m ²]	Pressure [MPa]	Force [MN]
High	0.36	15.13	5.45
Medium	1.70	5.11	8.67
Low	5.09	2.37	12.06
Sum	5.09		26.18

Table 17-1, Pressure zones

The result in force that is twice as large using loading areas of 5.09 m in the equation 17-1 and may therefore be considered as conservative.

In load case 4, finding the ultimate strength is the target for the six different stiffener options. All six models are applied the load level at 180% of the load fund in chapter 17.2.2

Load	100%	120%	140%	160%	180%
High [MPa]	15,13	18,2	21,2	24,2	27,2
Medium [MPa]	5,11	6,1	7,2	8,2	9,2
Low [MPa]	2,37	2,8	3,3	3,8	4,3

17.3.2.1 Force displacement

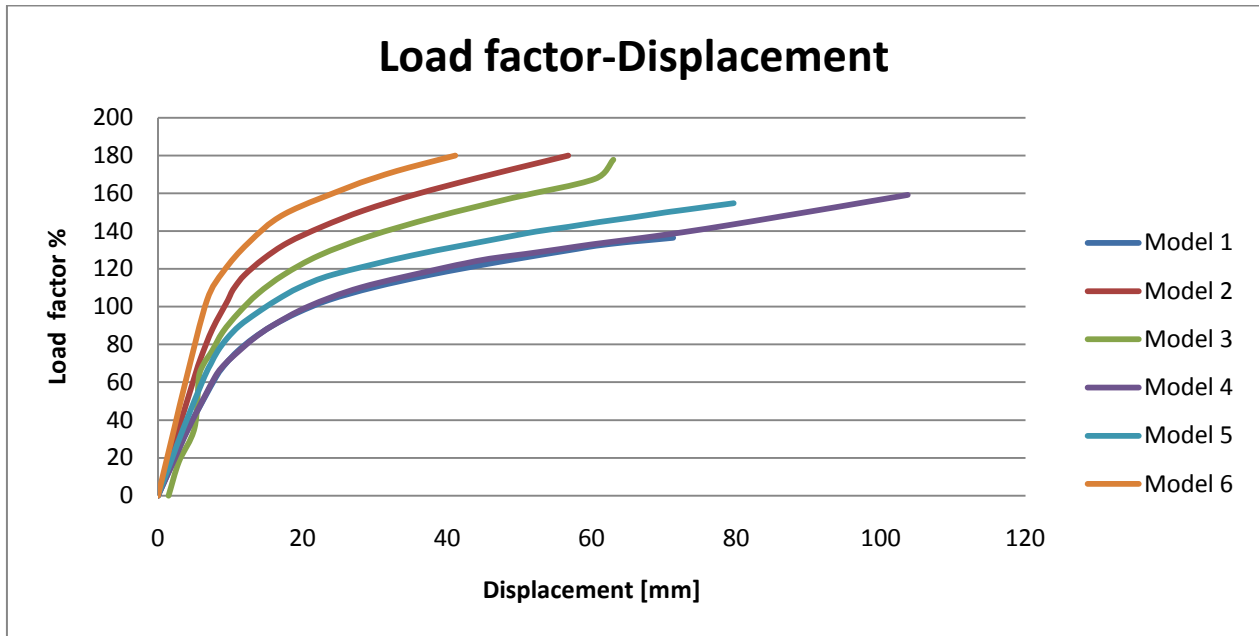


Figure 17-11

17.3.2.2 Plastic strain

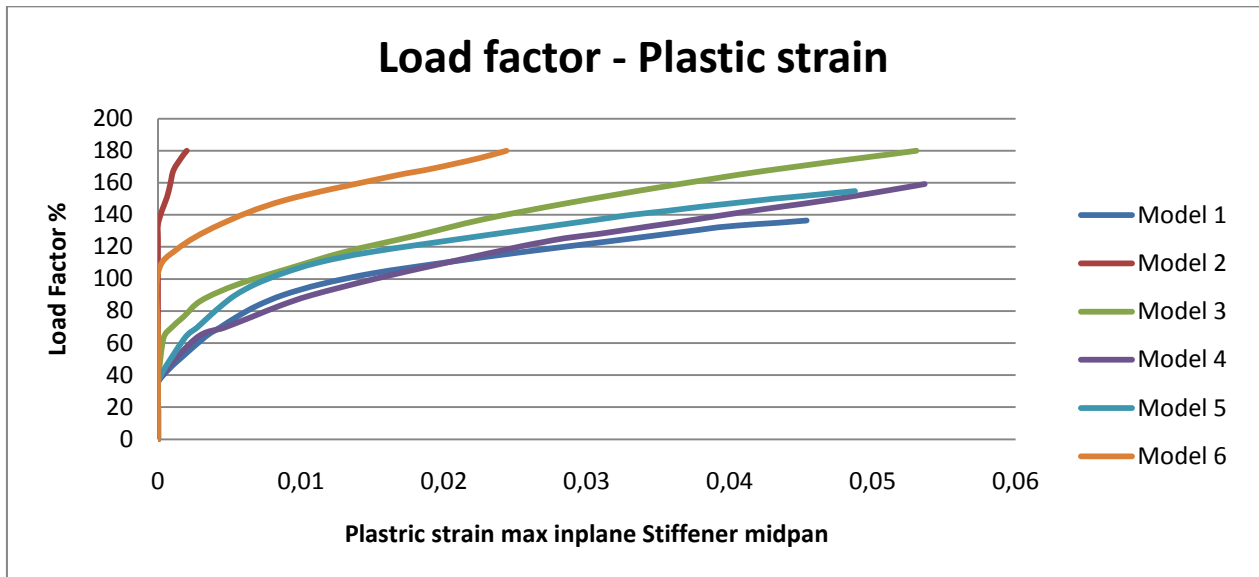


Figure 17-12

17.3.2.3 Equivalent plastic strain in uniaxial compression

As steel have a significant lower material strength in compression, The PEEQ is chosen as critical strain.

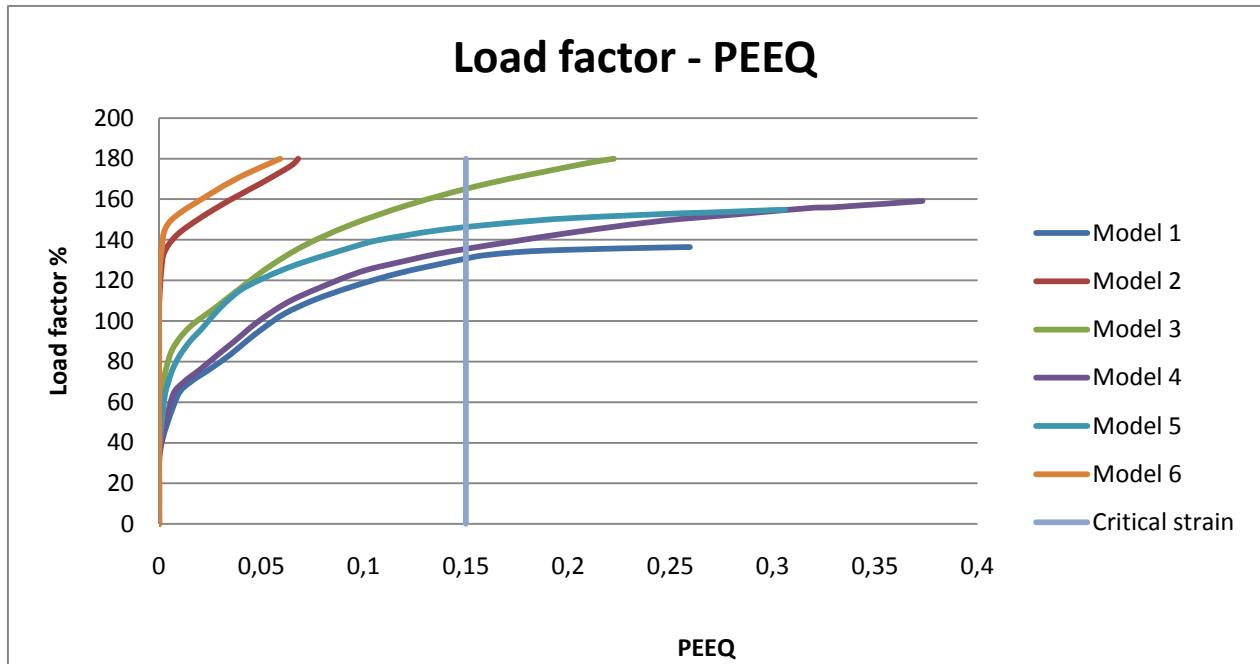


Figure 17-13, P

The different between model 2 and model 6 and the other models are significant. Model 2 and 6 represents the two models with T-bar stiffener of 100 mm flange. Interesting is that the PEEQ max for the two models with T bar stiffener is not on the same place as for the other stiffener.

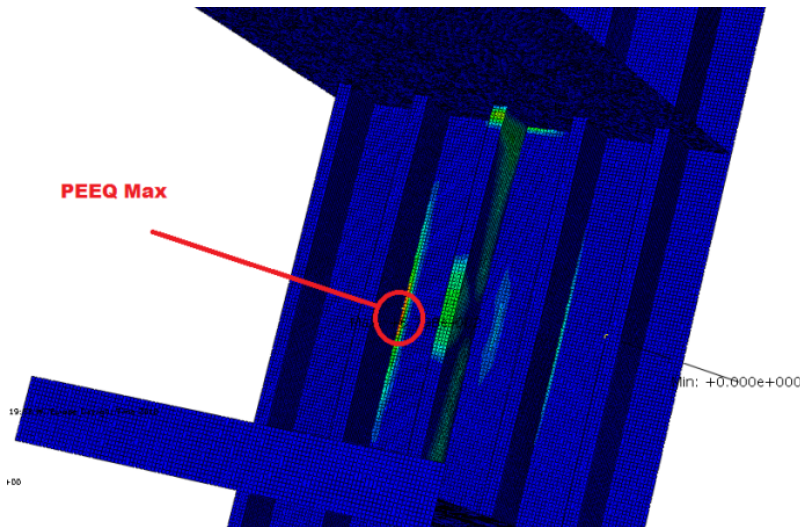


Figure 17-14, Maximum PEEQ stress model 2 and 6

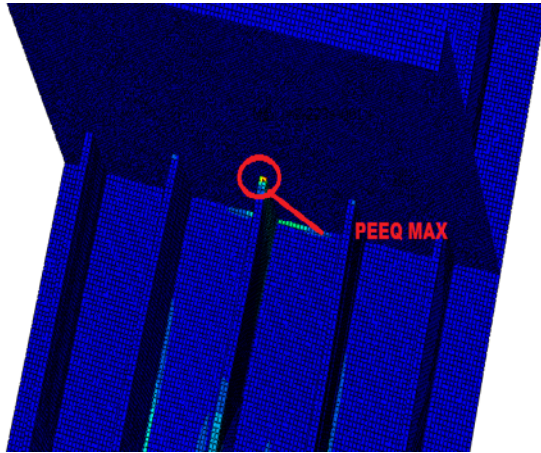


Figure 17-15, Maximum PEEQ stress

17.4 Plastic strain energy dissipated

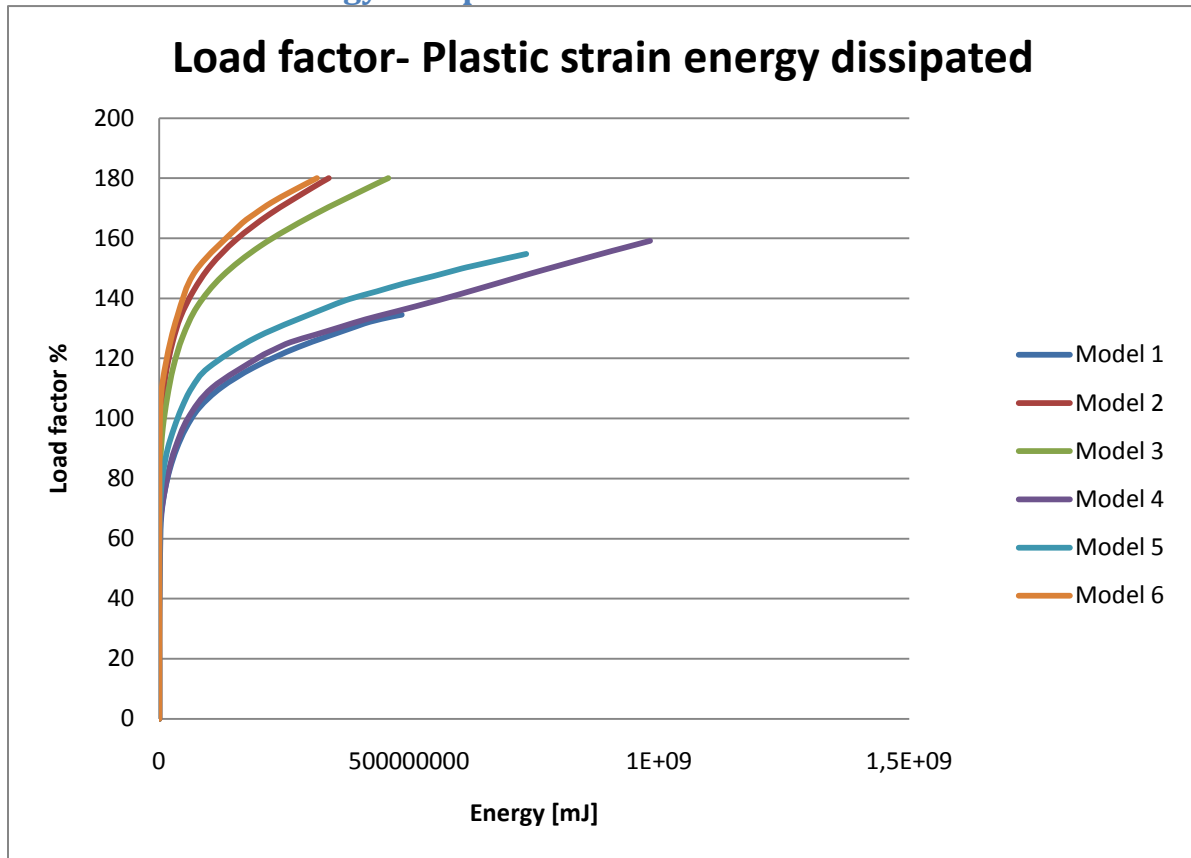


Figure 17-16

There result for dissipated energy is not as expected. The energy dissipated in plastic strain is large for model 4 and model 5 despite the load factor is higher for the other models. The expected results are on the other hand opposite. When looking on the Von Mises Stress (appendices), stresses are more even distributed over the model.

17.5 External Energy for the whole model

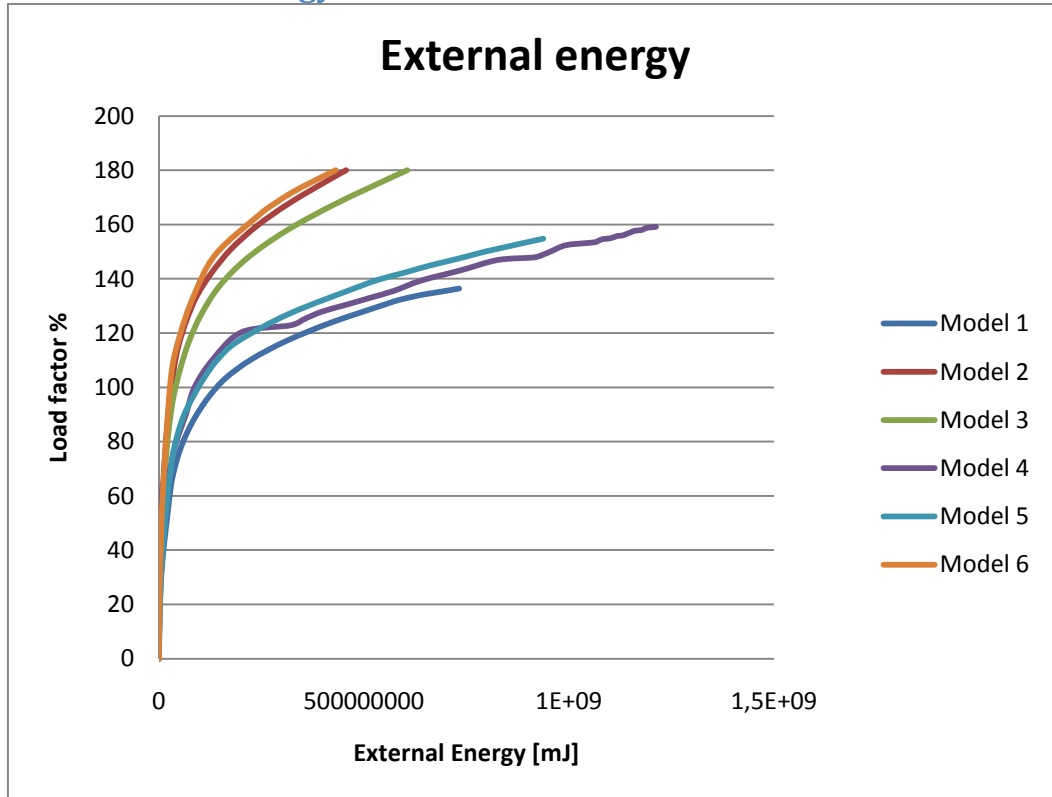


Figure 17-17

The figure 17-17 shows the external energy for the whole model. The graph for model 4 is remarkable uneven and long. The result for the external energy should be investigated further to get an explanation why the external energy for model 4 and 5 is of this magnitude.

17.5.1.1 Conclusion

The conclusion for the analyses perform is that the fracture load for the plate – stiffener model is not set. The models were made with intension of making them as similar to each other so the comparing of the models would be easier. As showed in the plots, the stiffener design with a T-bar stiffener was significant stronger and the maximum plastic strain was not on the same location as for the other models. An explanation of why the analysis for the other stiffener analysis diverge and aborted should be investigated.

18 Conclusion and recommendations for further work

The ELIE design load for the Sevan FPU-ice is 5.11 MPa over an area of a whole plate. For stiffener design, the ELEI load is 2.27 MPa for an area consisting of 80% of the plate height times four stiffener spacing.

The NLFEA analyses perform may not be as good as expected. The variance in the analysis for relative similar model is a clear indication that the result needs to be investigated further. A more comprehensive analysis would be recommended with more realistic boundary condition. A larger model will probably give easier and more accurate boundary conditions. ALIE events may include severe damage and the structural integrity of the damaged structure should be verified by a global analysis. In the finite element analysis buckling of the stiffener is a subject that has to be more thoroughly checked.

Choosing a structural layout depends mainly on resistance and cost. The cost varies on steel weight and production cost. The production cost may vary from one yard to another due to different building techniques. Feasible building techniques in terms of welding and prefabrication should be looked in to for establish building cost for different structural layout.

Collision with iceberg is a subject that may be investigated with regards to analysis and prediction. For a prediction point of view, the site location is essential to establish the properties of potential iceberg impact. Added mass and impact speed due to storm wave is factors that need a deeper investigation for establishing kinetic energy at impact.

Impact of large iceberg requires large models. A large model may cause large inaccuracy in modeling, so experience in modeling may be a significant advantage. An impact analyses of an iceberg colliding with the structure is using explicit method may also be recommended for further works. The work made, is made with regards to the conical section. At an impact of an ALIE iceberg, the ice feature will not only impact the conical section, but also the circular section. A structural analysis of the cylindrical shaped section may therefore be of interest.

Bibliografi

- Amdahl, P. j. (2003). *Design of plates and stiffeners against ice actions, Arctic Offshore Eng, DNV.*
- Amdahl, P. J. (2005). *TMR4205 Buckling and Ultimate Strength of Marine structure.*
- Daley, R. B. (1999). *Computer Simulation of transverse Ship-ice Collisions.* Memorial University of Newfoundland.
- DNV. (2009). Rules for Classifications of Ship. DNV.
- F.Klæbo, J. A. (2006). *Strength anlysis of floating platform exposed to ice loads.*
- G.W.Timco, R. (February 2009). *Overview of Historical Canadian Beaufort Sea.* NRC Canadian Hydraulics Centre.
- G.W.Timeco, K. (2006). How well can we predict ice loads. *Proceedings 18th International Symposium on Ice, IAHR'06*, (ss. Vol. 1, pp167-174, Sapporo, Japan, 2006). Sapporo, Japan.
- Gudmestad, K. E. Iceberg management and impact on design of offshore structures.
- Internastional. (2007). *ISO/CD 19906.*
- Isaacson, K. A. (u.d.). PROBABILISTIC EVALUATION OF DESIGN ICEBERG COLLISION. *Journal of Cold Regions Engineering, Vol. 4, No. 2, June, 1990 .*
- Kristoffersen, M. *Master thesis: Design of Floating Drilling and Production Units in Artic areas.*
- Ltd., B. &. (July 2000). *Full Scale Experience with Kulluk.* The National Research Council of Canada.
- M.E Johnston, K. I. (1998). Localized pressures during ice–structure interaction: relevance to design criteria. *Cold Regions Science and Technology*, (ss. 105-117).
- Moan, T. (2003). *Finite Elemnet Modeling and Analysis of Marine Structures.* Trondheim.
- Moan, T. *Lecture TMR4305.*
- Moan, T. *TMR4190 Finite Element Method.*
- Norway, S. *N-003.*
- Oddgeir Dalane, V. A. (2009). A MORED ARCTIC FLOATER IN FIRST YEAR ICE RIDGES. *OMAE2009-79945*, (s. 9). Honolulu, Hawaii.
- R.M.W.Frederking, D. a. (1992). Local contact pressures in ship/ice and structure/ice interactions. *Cold Region Science and Technology* (ss. 169-185). Amsterdam: Elsevier Science Publishers B.V.
- Riska, K. (2008). *Lecture Notes IX, ICE II.*
- S.Løset, K. O. (2006). *Actions from ice on actic offshore and costal structure.*

Analysis and design of the Sevan FPSO against abnormal ice actions

Sand, B. (2008). *Nonlinear finite element simulations of ice forces on offshore structure*. Luleå.

Simulia. *Abaqus Theory Manual*.

Standards Norway. (2004). *N-004*.

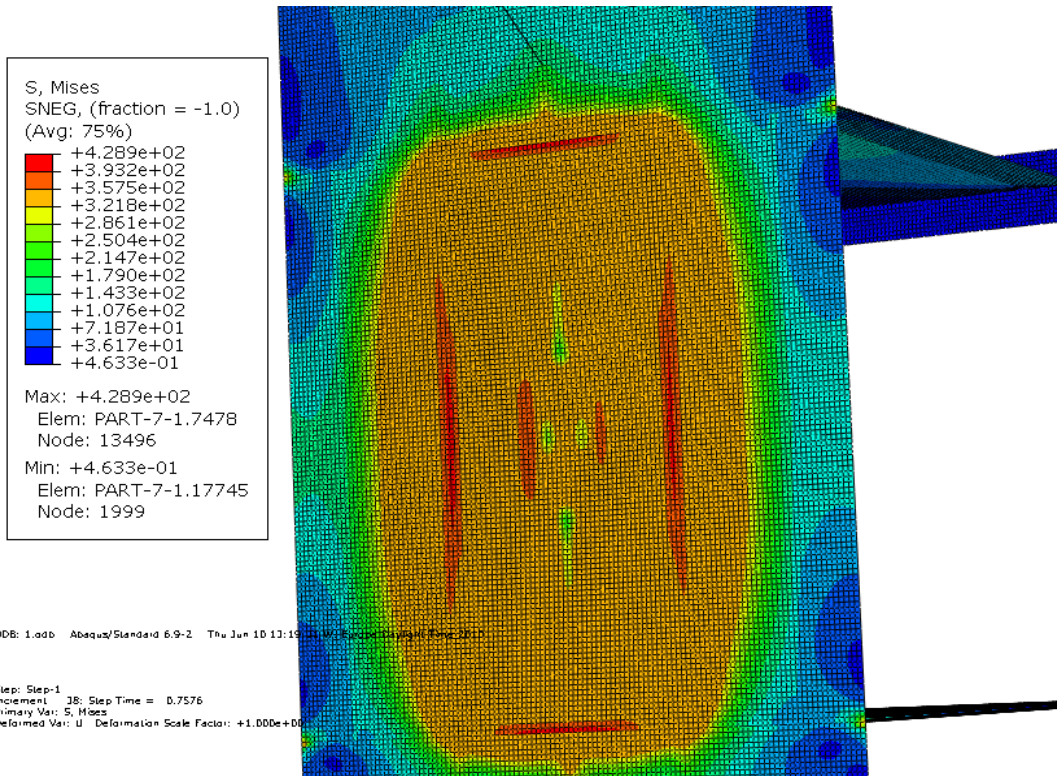
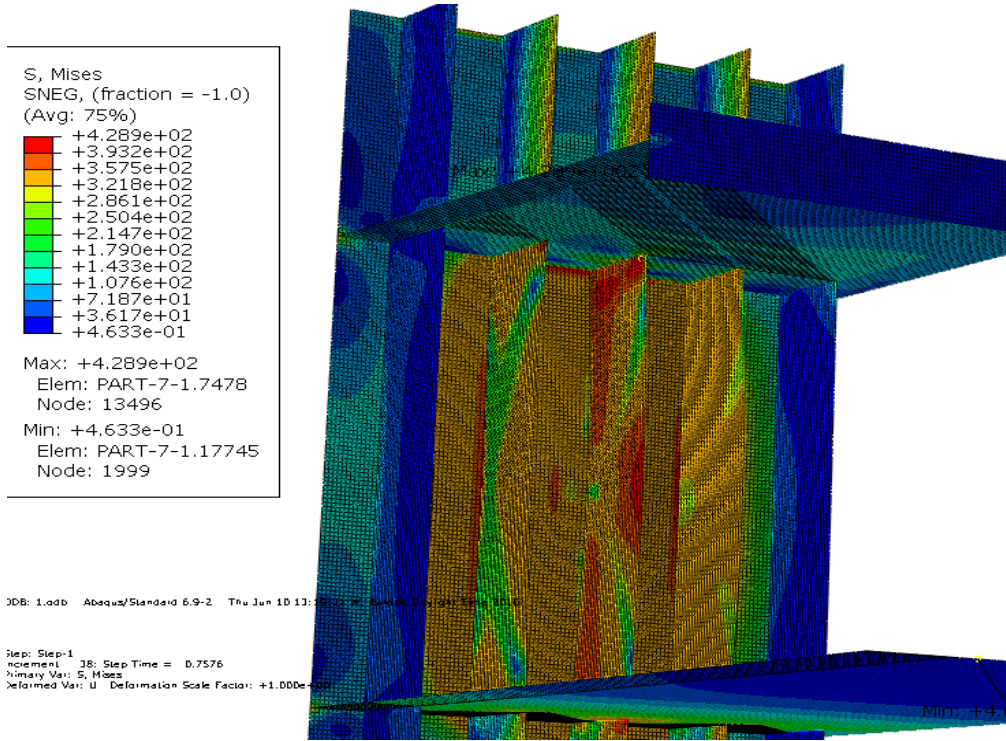
Søreide, T. H. (1985). *Ultimate Load Analysis of Marine Structure*. Tapir.

www.athropolis.com. (found 2010)

Analysis and design of the Sevan FPSO against abnormal ice actions

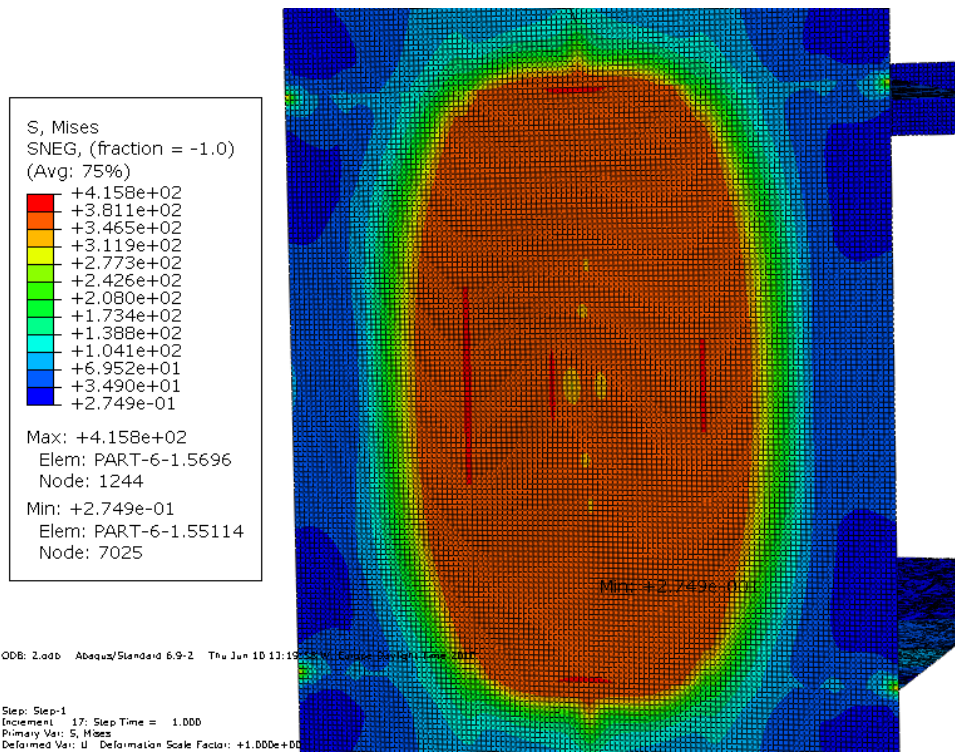
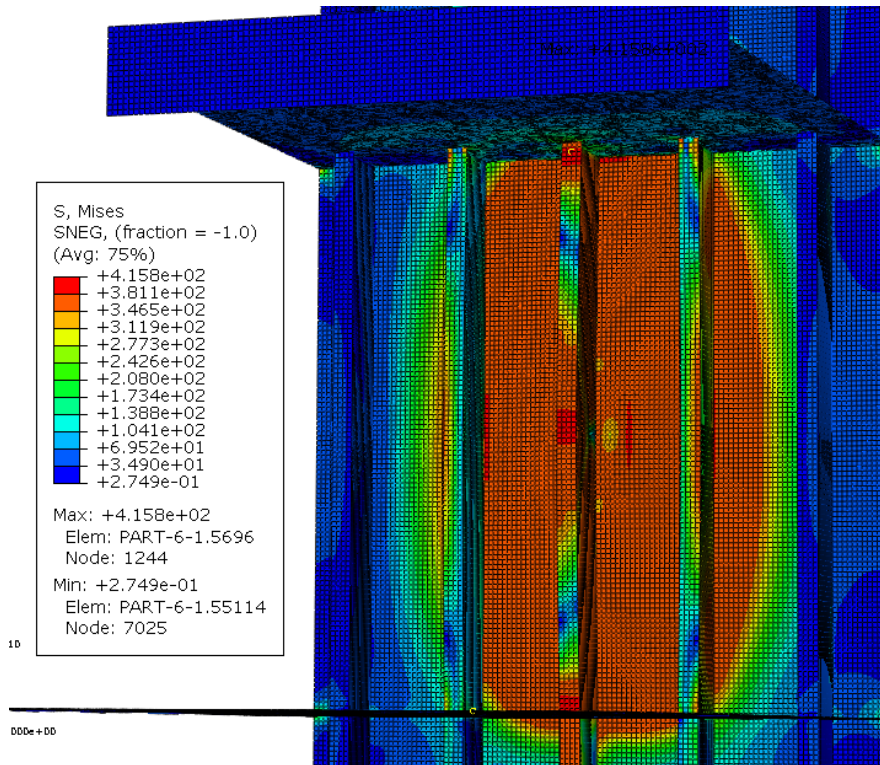
Appendices

Model 1: Von Mises Stress



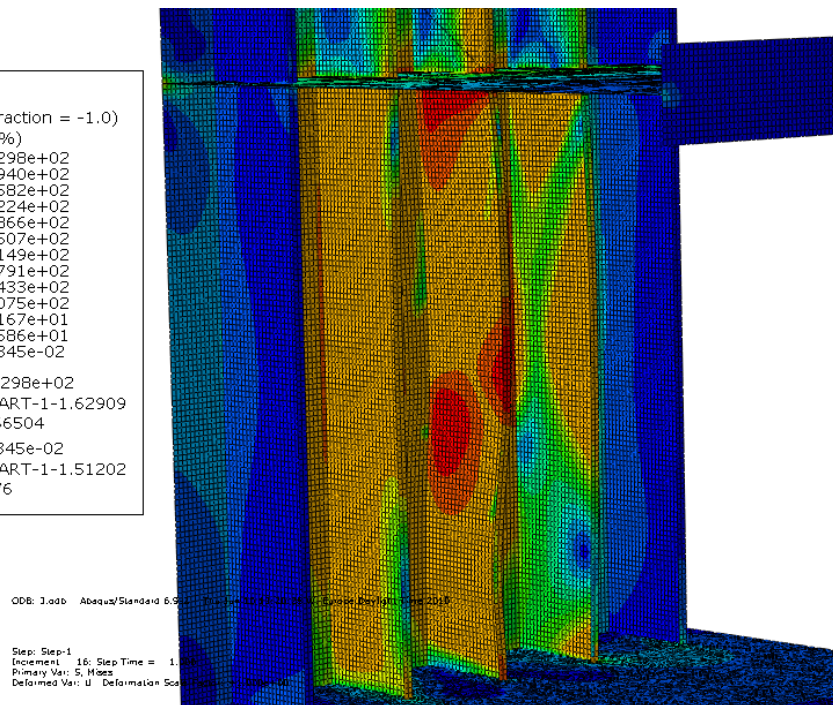
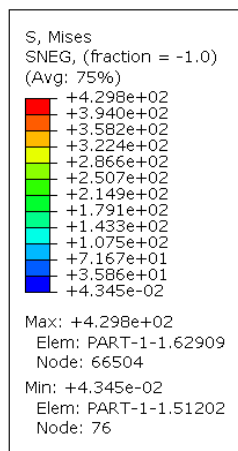
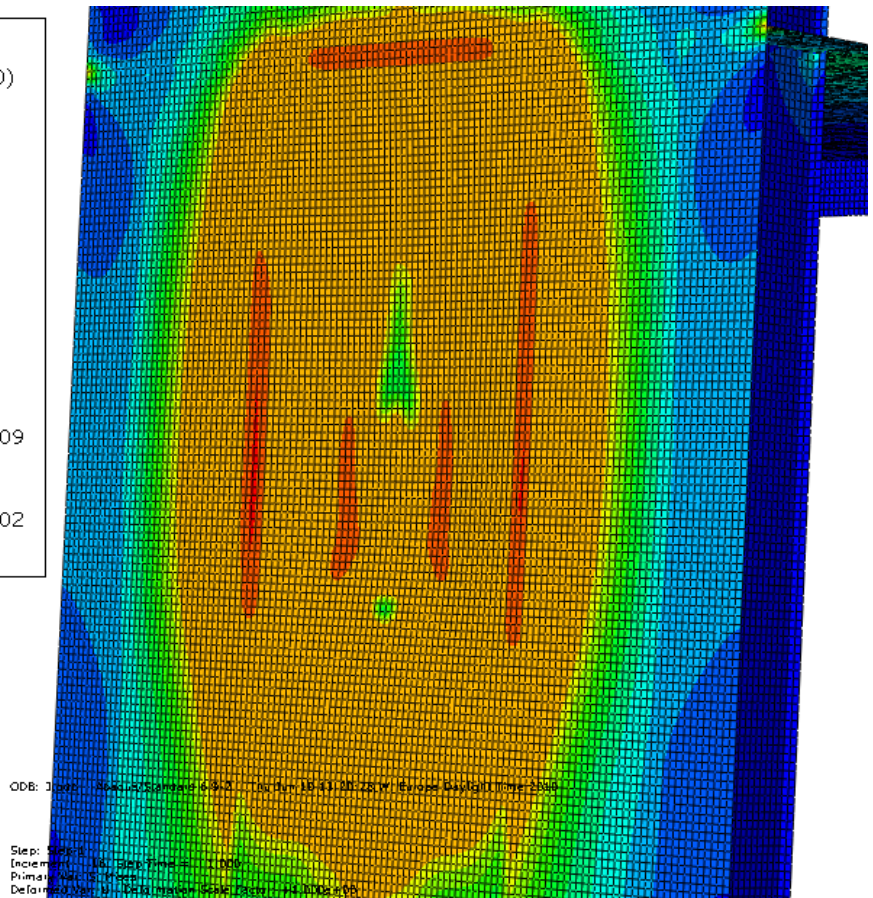
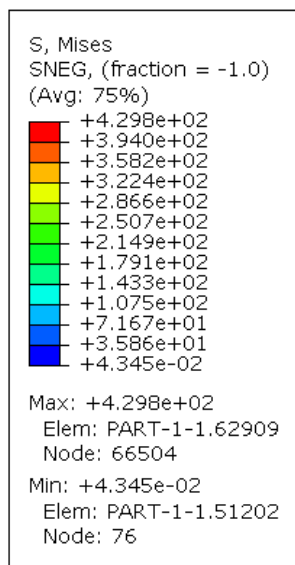
Analysis and design of the Sevan FPSO against abnormal ice actions

Model 2: Von Mises Stress

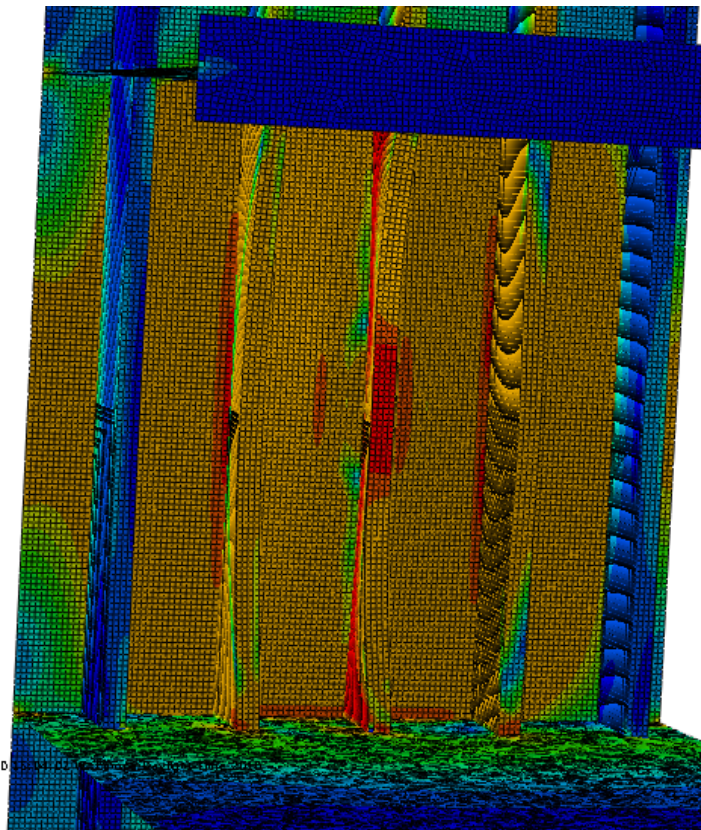
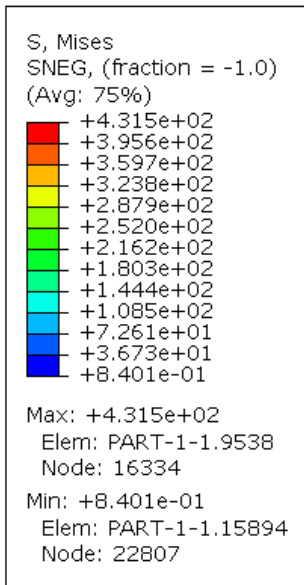


Analysis and design of the Sevan FPSO against abnormal ice actions

Model 3: Von Mises Stress

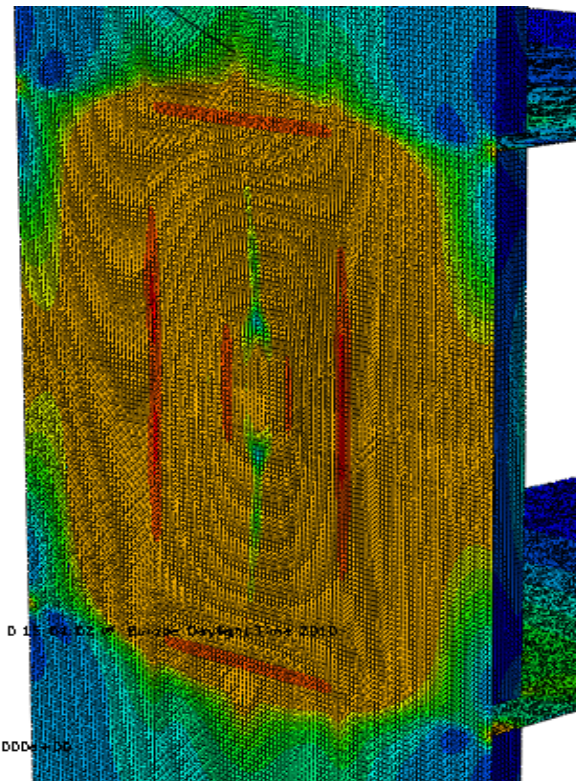
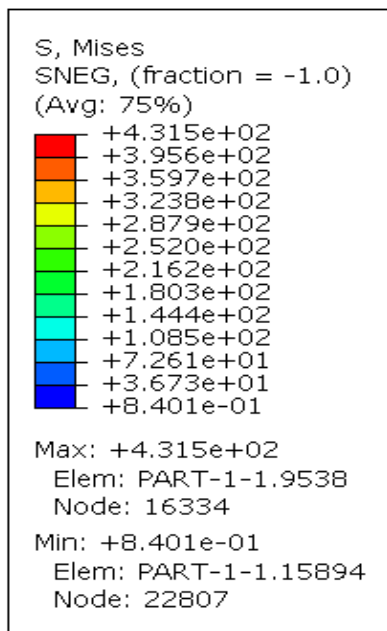


Model 4: Von Mises Stress



ODB: 4.odb Abaqus/Standard 6.9-2 Thu Jun 10 10:30:02 AM 2010

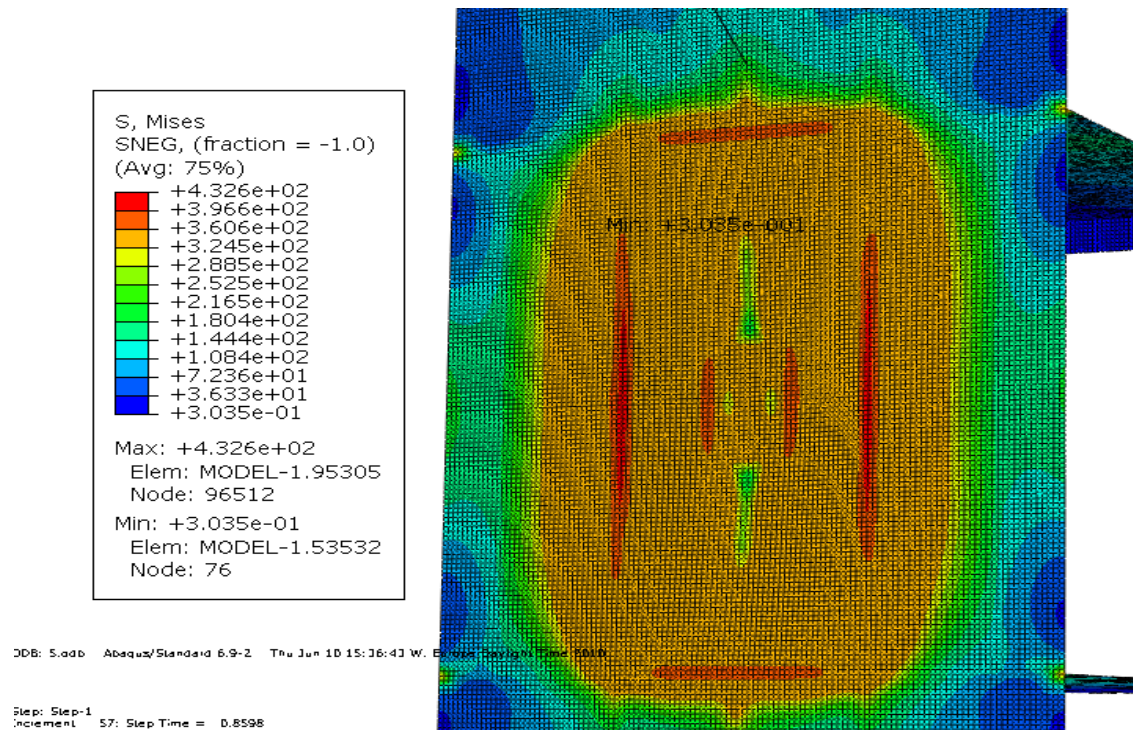
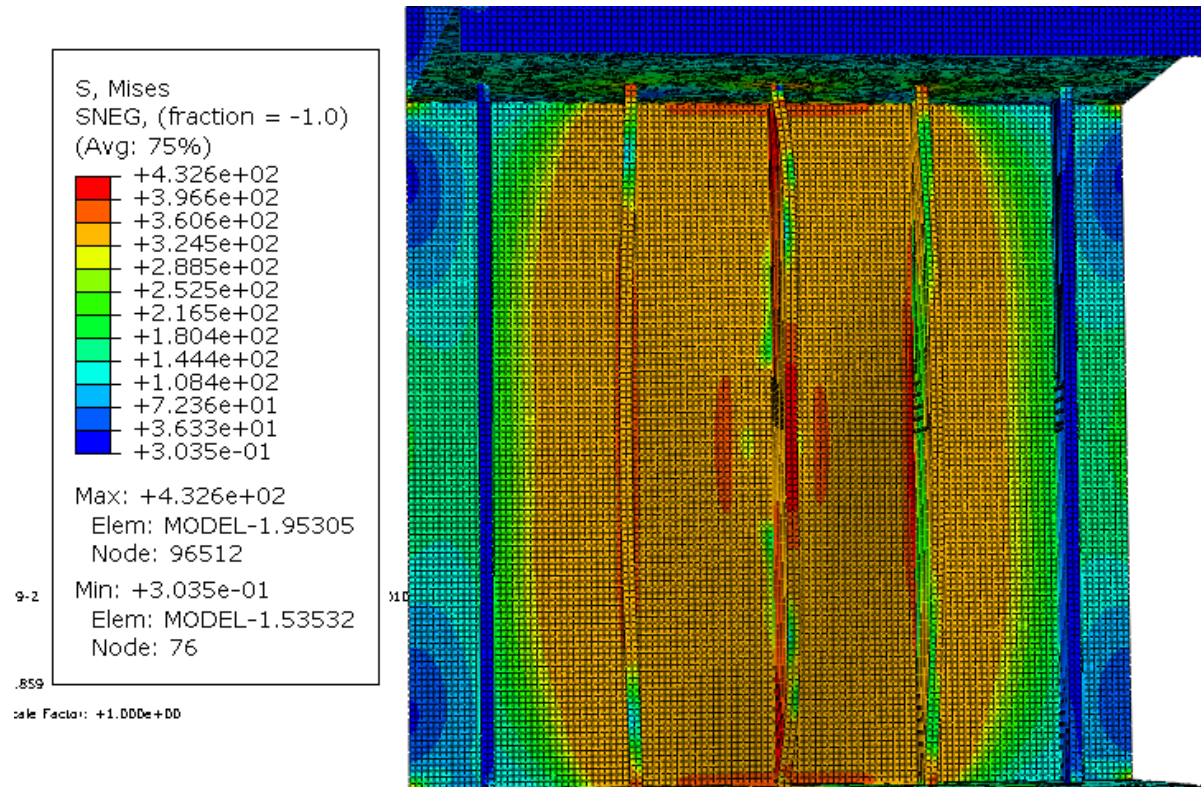
Page: 10 of 1



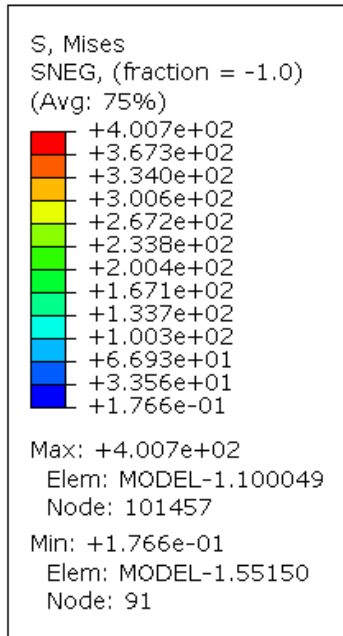
ODB: 4.odb Abaqus/Standard 6.9-2 Thu Jun 10 10:30:02 AM 2010

Step: Step-1
Increment: 62; Step Time = 0.8843
Primary Var: S, Mises
Deformed Var: U Deformation Scale Factor: +1.000e+00

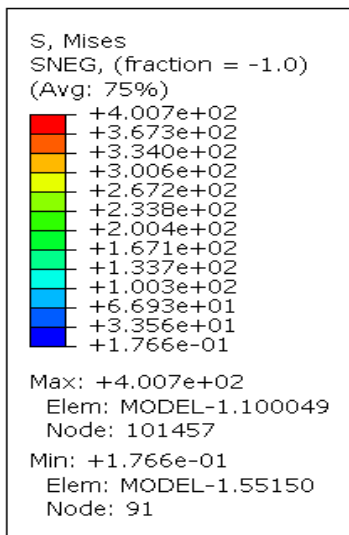
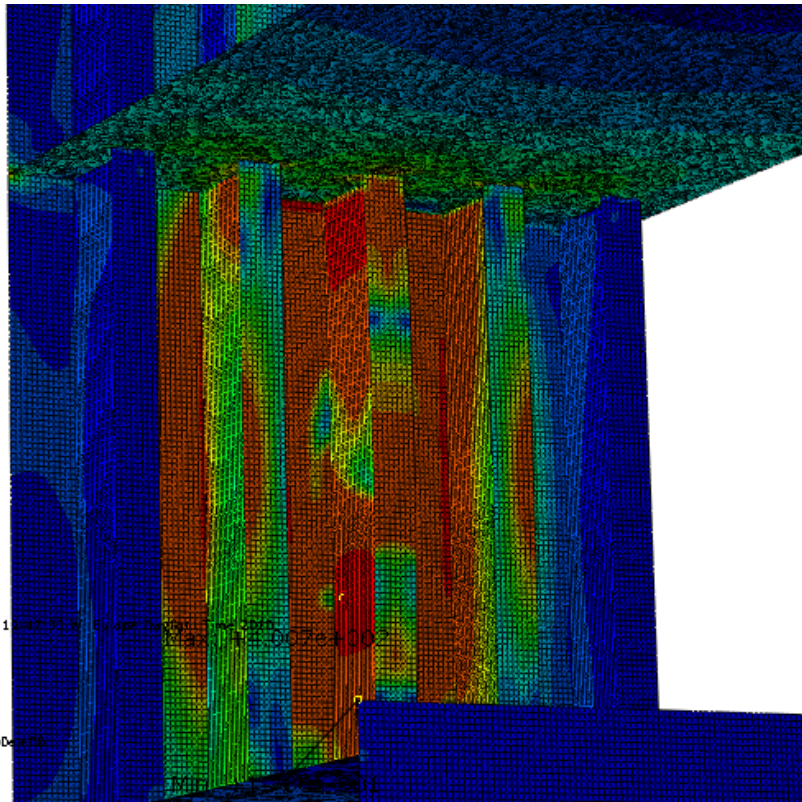
Model 5: Von Mises Stress



Model 6: Von Mises

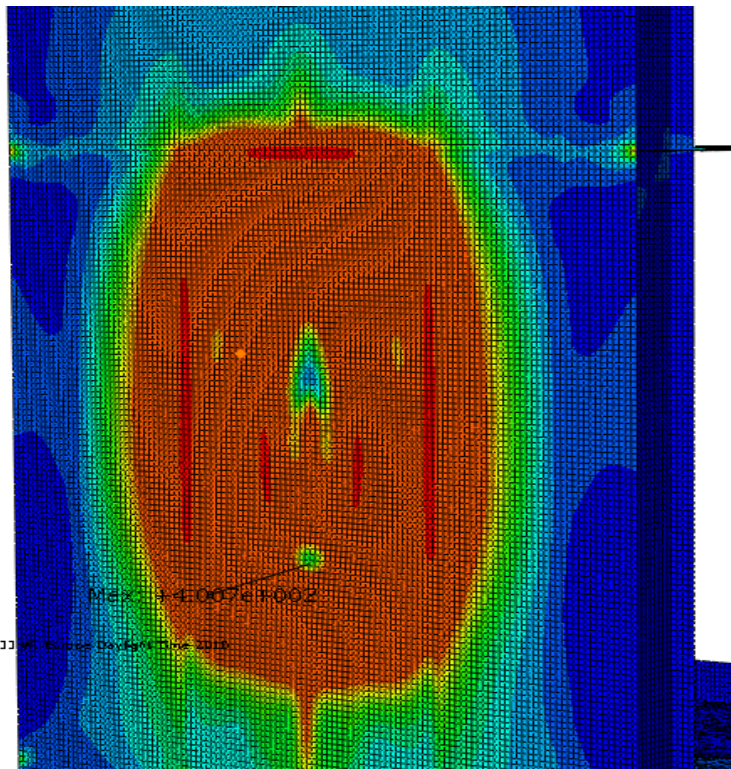


Step: Step-1
Increment 12: Step Time = 1.000
Primary Var: S, Mises
Deformed Var: U Deformation Scale Factor: +1.000e+00



ODB: 6.odb Abaqus/Standard 6.9-2 Thu Jun 10 11:47:33 AM Europe/Dublin Time 2010

Step: Step-1
Increment 12: Step Time = 1.000
Primary Var: S, Mises
Deformed Var: U Deformation Scale Factor: +1.000e+00



Analysis and design of the Sevan FPSO against abnormal ice actions

Weight-resistance calculation

Radius top	55.5 m						
Radius Low	43.5 m						
Height	16 m						
Dr	12 m						
Length of surface conical	20 m						
Ice Breaking Conical surface area	6220 m ²						
Number of stiffener	428.3	462.5	502.4	549.5	606.0	675.2	-
Stiffener weight	171151.5	184808.8	200742.4	219572.9	242169.5	269787.7	Tonn
Total weight	173593.0	187250.3	203183.9	222014.4	244611.0	272229.2	Tonn
Resistance	5.3	6.2	7.3	8.6	10.4	12.9	MPa
DNV resistance	10.2	11.0	11.9	13.0	14.3	15.9	tonn
Decrease of resistance Plastic	0.0	0.2	0.4	0.6	1.0	1.4	-
Decrease in weight	0.0	0.1	0.2	0.3	0.4	0.6	-
DNV resistance	15.9	14.3	13.0	11.9	11.0	10.2	tonn
Plastic resistance	12.9	10.4	8.6	7.3	6.2	5.3	MPa

Plastic capacity calculations

Stiffener number	1	2	3	4	5	6	
Plate thickness	50.0	50.0	50.0	50.0	50.0	50.0	mm
Stiffener distance	600.0	600.0	600.0	600.0	600.0	600.0	mm
Web height	600.0	500.0	550.0	500.0	600.0	600.0	mm
Web Thickness	30.0	30.0	30.0	30.0	30.0	30.0	mm
Flange width	0.0	100.0	50.0	100.0	50.0	50.0	mm
Flange thickness	0.0	30.0	30.0	30.0	30.0	30.0	mm
Elastic height	146.9	144.7	146.6	144.7	162.6	162.6	mm
Inertia moment	1.45E+07	1.64E+09	1.72E+09	1.64E+09	2.13E+09	2.13E+09	mm ³
Plastic height	40.0	40.0	40.0	40.0	41.3	41.3	mm
Alfa factor	1.6	2.0	2.1	2.0	2.0	2.0	-